Direct and Highly Regioselective and Enantioselective Allylation of β-Diketones

Wesley A. Chalifoux, Samuel K. Reznik, and James L. Leighton*

Department of Chemistry, Columbia University, New York, NY, 10027

Supplementary Methods

General Information. β-Diketones were purchased from commercial sources or synthesized using a known procedure.[31] All reactions were carried out under an atmosphere of nitrogen in flame or oven-dried glassware with magnetic stirring unless otherwise indicated. Degassed solvents were purified by passage through an activated alumina column. Anhydrous chloroform was purchased from Aldrich. Thin-layer chromatography (TLC) was carried out on glass backed silica gel XHL TLC plates (250 μm) from Sorbent Technologies; visualization by UV light, phosphomolybdic acid (PMA) stain or potassium permanganate ($KMnO_4$) stain. Gas chromatographic analyses were performed on a Hewlett-Packard 6890 Series Gas Chromatograph equipped with a capillary split-splitless inlet and flame ionization detector with electronic pneumatics control using either a Supelco β-Dex 120 (30 m x 0.25 mm) or Supelco β-Dex 325 (30 m x 0.25 mm) capillary GLC column. HPLC analysis was carried out on an Agilent 1200 Series using either a Chiralpak AD-H (250 × 4.5 mm ID) column or Chiralcel OD (250 × 4.5 mm ID) column. ^{1}H NMR spectra were recorded on a Bruker DPX-300 (300 MHz), Bruker DRX-300 (300 MHz), Bruker AVIII nano bay-400 (400 MHz), or a Bruker AVIII single bay-400 (400 MHz) spectrometer and are reported in ppm from $CDCl_3$ internal standard (7.26 ppm). Data are reported as follows: (bs= broad singlet, s = singlet, d = doublet, t = triplet, q = quartet, quin = quintet, sep = septet, m = multiplet, dd = doublet of doublets, ddd = doublet of doublet of doublets, dddd = doublet of doublet of doublet of doublets; coupling constant(s) in Hz; integration). Proton decoupled ^{13}C NMR spectra were recorded on a Bruker DRX-300 (300 MHz) or a Bruker AVIII single bay-400 (400 MHz) spectrometer and are reported in ppm from $CDCl_3$ internal standard (77.0 ppm). Infrared spectra were recorded on a Nicolet Avatar 370DTGS FT-IR. Optical rotations were recorded on a Jasco DIP-1000 digital polarimeter. (APCI)-MS was conducted on a JMS-LCmate LCMS (JEOL).

General procedure 1: Allylation and crotylation with *E*-crotylsilane

To a solution of β-diketone (1.0 equiv) in anhydrous $CHCl_3$ (0.05-0.10 M) was added (*S*,*S*)-allylsilane **3**[32] (1.2 equiv) or (*S*,*S*)-*E*-crotylsilane **20**[33] (1.3 equiv) and the resulting mixture was allowed to stir at 23 °C until the reaction was deemed complete by ^{1}H NMR spectroscopy. The reaction mixture was cooled to –40 °C, TBAF (4.0-4.5 equiv, 1M in THF) was added, and the mixture was stirred at –40 °C for 1 h. Saturated NH_4Cl was added, the mixture warmed to

[31] Heller, S.; Natarajan, S. R. *Org. Lett.* **2006**, *8*, 2675.
[32] Kubota, K.; Leighton, J. L. *Angew. Chem. Int. Ed.* **2003**, *42*, 946.
[33] Hackman, B. M.; Lombardi, P. J.; Leighton, J. L. *Org. Lett.* **2004**, *6*, 4375.

ambient temperature, and extracted with CH_2Cl_2. The organic phases were combined, washed with H_2O, brine, and dried over $MgSO_4$. The mixture was filtered, concentrated in vacuo, and the crude product purified by column chromatography (silica gel).

General procedure 2: Crotylation using *Z*-crotylsilane

To a solution of (*S*,*S*)-*Z*-crotylsilane **21**[32] (1.3 equiv) in anhydrous $CHCl_3$ (0.05-0.1 M) was added AgOTf (1.3 equiv) and the resulting mixture was allowed to stir at 23 °C for 20-30 min to allow the silyl triflate to form. To this mixture was added β-diketone (1.0 equiv) and the reaction was stirred at 23 °C for 40-70 h. The reaction mixture was cooled to –40 °C and TBAF (4.5 equiv, 1M in THF) was added and the mixture was stirred at –40 °C for 1 h. Saturated NH_4Cl was added, the mixture warmed to ambient temperature, and extracted with CH_2Cl_2. The organic phases were combined, washed with H_2O, brine and dried over $MgSO_4$. The mixture was filtered, concentrated in vacuo and the crude product purified by column chromatography (silica gel).

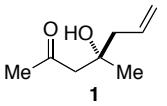

1

Compound 1: This reaction was performed according to general procedure 1 (9.99 mmol of acetylacetone in $CHCl_3$ at 23 °C for 1 h). Purification by flash chromatography (gradient 10%-50% Et_2O/pentane) afforded **1** (1.03 g, 72% yield) as a pale yellow liquid. The enantiomeric excess of **1** was determined to be 89% by chiral GC (see GC trace below). $[\alpha]_D = -5.5°$ (c 4.7, CH_2Cl_2); R_f = 0.38 (30% Et_2O/pentane); ^1H NMR (400 MHz, $CDCl_3$) δ 5.81 (dddd, *J* = 17.5 Hz, 10.2 Hz, 7.4 Hz, 7.4 Hz, 1H), 5.11-5.01 (m, 2H), 3.80 (bs, 1H), 2.64 (d, *J* = 17.2 Hz, 1H), 2.52 (d, *J* = 17.2 Hz, 1H), 2.32-2.20 (m, 2H), 2.15 (s, 3H), 1.20 (s, 3H); ^{13}C NMR (100 MHz, $CDCl_3$) δ 210.9, 134.0, 118.3, 71.3, 51.7, 46.6, 31.8, 26.9; IR (neat) 3459, 3077, 2977, 2932, 1702, 1641 cm^{-1}; APCI LRMS *m/z* 143.04 ($[M+H]^+$, 20), 125.04 ($[M–OH]^+$, 100).

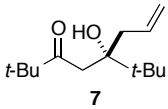

7

Compound 7: This reaction was performed according to general procedure 1 (0.21 mmol of 2,2,6,6-tetramethylhepta-3,5-dione in $CHCl_3$ at 23 °C for 18 h). Purification by flash chromatography (5% EtOAc/hexanes) afforded **7** (40 mg, 83% yield) as a colorless oil. The enantiomeric excess of **7** was determined to be 87% by chiral GC (see GC trace below). $[\alpha]_D$ = +36.0° (c 1.6, CH_2Cl_2); R_f = 0.45 (5% EtOAc/hexanes); ^1H NMR (300 MHz, $CDCl_3$) δ 5.90 (dddd, *J* = 16.5 Hz, 10.5 Hz, 8.6 Hz, 6.0 Hz, 1H), 5.28 (s, 1H), 5.05-4.95 (m, 2H), 2.76 (d, *J* = 18.1 Hz, 1H), 2.64 (d, *J* = 18.1 Hz, 1H), 2.52 (dddd, *J* = 14.3 Hz, 6.0 Hz, 1.6 Hz, 1.6 Hz, 1H), 2.21 (dd, *J* = 14.3 Hz, 8.6 Hz, 1H), 1.15 (s, 9H), 0.95 (s, 9H); ^{13}C NMR (75 MHz, $CDCl_3$) δ 220.6, 136.3, 117.1, 77.6, 45.4, 41.7, 39.0, 37.4, 26.7, 25.7; IR (cast film) 3439, 3075, 2964, 2876, 1688, 1638 cm^{-1}; APCI LRMS *m/z* 227.38 ($[M+H]^+$, 25), 209.35 ($[M–OH]^+$, 100).

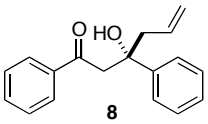

8

Compound 8: This reaction was performed according to general procedure 1 (0.24 mmol of 1,3-diphenyl-1,3-propanedione in $CHCl_3$ at 23 °C for 13 h). Purification by flash chromatography (10% EtOAc/hexanes) afforded **8** (51 mg, 80% yield) as a off-white solid. The enantiomeric excess of **8** was determined to be 96% by chiral HPLC (see HPLC trace below). $[\alpha]_D$ = +83.7° (c 3.5, CH_2Cl_2); R_f = 0.36 (1:6 EtOAc/hexanes); ^1H NMR (400 MHz, $CDCl_3$) δ 7.92-7.87 (m, 2H), 7.61-7.54 (m,

1H), 7.48-7.41 (m, 4H), 7.34-7.27 (m, 2H), 7.23-7.17 (m, 1H), 5.81-5.68 (m, 1H), 5.12-5.05 (m, 2H), 4.85 (s, 1H), 3.84 (d, J = 17.4 Hz, 1H), 3.33 (d, J = 17.4 Hz, 1H), 2.71-2.57 (m, 2H); ^{13}C NMR (100 MHz, $CDCl_3$) δ 201.5, 146.0, 137.1, 133.7, 133.6, 128.7, 128.2, 128.1, 126.7, 124.9, 118.4, 75.4, 48.1, 46.6; IR (cast film) 3480, 3063, 3027, 2978, 2904, 1669, 1597, 1448, 1215 cm^{-1}; APCI LRMS *m/z* 249.22 ([M–OH]$^+$, 100).

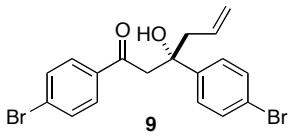

9

Compound 9: This reaction was performed according to general procedure 1 (0.23 mmol of bis(*p*-bromobenzoyl)methane in $CHCl_3$ at 23 °C for 19 h) Purification by flash chromatography (15% EtOAc/hexanes) afforded **9** (64 mg, 68% yield) as a pale yellow solid. The enantiomeric excess of **9** was determined to be 95% by chiral HPLC (see HPLC trace below). $[\alpha]_D$ = +106.9° (c 3.2, CH_2Cl_2); R_f = 0.28 (15% EtOAc/hexanes); ^{1}H NMR (400 MHz, $CDCl_3$) δ 7.76-7.71 (m, 2H), 7.62-7.57 (m, 2H), 7.44-7.39 (m, 2H), 7.31-7.27 (m, 2H), 5.70 (dddd, J = 17.9 Hz, 10.4 Hz, 7.4 Hz, 7.4 Hz, 1H), 5.12-5.03 (m, 2H), 4.68 (s, 1H), 3.73 (d, J = 17.4 Hz, 1H), 3.27 (d, J = 17.4 Hz, 1H), 2.65-2.52 (m, 2H); ^{13}C NMR (100 MHz, $CDCl_3$) δ 200.1, 145.0, 135.6, 132.9, 132.1, 131.3, 129.6, 129.2, 126.8, 120.9, 119.0, 75.2, 47.9, 46.5; IR (cast film) 3483, 3074, 2976, 2905, 1672, 1585 cm^{-1}; APCI LRMS *m/z* 406.77 ([M–OH]$^+$, 75), 224.91 ([M–C_8H_6BrO]$^+$, 25), 147.05 ([M–$C_8H_6Br_2O$]$^+$, 100).

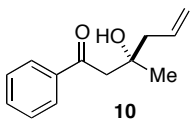

10

Compound 10: This reaction was performed according to general procedure 1 (0.16 mmol of benzoylacetone and in $CHCl_3$ at 23 °C for 21 h). Purification by flash chromatography (1:4 EtOAc/hexanes) afforded **10** (26 mg, 81% yield) as an orange oil consisting of a mixture of regioisomers. The regioselectivity was determined by ^{1}H NMR to be 19:1. The enantiomeric excess of **10** was determined to be 97% by chiral HPLC (see HPLC trace below). $[\alpha]_D$ = –19.7° (c 1.9, CH_2Cl_2); R_f = 0.42 (1:4 EtOAc/hexanes); ^{1}H NMR (400 MHz, $CDCl_3$) δ 7.97-7.91 (m, 2H), 7.62-7.56 (m, 1H), 7.51-7.44 (m, 2H), 5.89 (dddd, J = 17.6 Hz, 10.2 Hz, 7.4 Hz, 7.4 Hz, 1H), 5.13-5.03 (m, 2H), 4.18 (s, 1H), 3.17 (d, J = 17.2 Hz, 1H), 3.07 (d, J = 17.2 Hz, 1H), 2.45-2.33 (m, 2H), 1.31 (s, 3H); ^{13}C NMR (100 MHz, $CDCl_3$) δ 201.9, 137.3, 134.1, 133.6, 128.7, 128.1, 118.4, 71.8, 46.8, 46.5, 27.2; IR (cast film) 3478, 3072, 2976, 2931, 1670, 1597, 1580, 1214 cm^{-1}; APCI LRMS *m/z* 205.23 ([M+H]$^+$, 100), 187.19 ([M–OH]$^+$, 95).

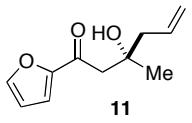

11

Compound 11: This reaction was performed according to general procedure 1 (0.51 mmol of furoylacetone and in $CHCl_3$ at 23 °C for 24 h). Purification by flash chromatography (gradient 25%-50% EtOAc/hexanes) afforded **11** (68 mg, 68% yield) as a yellow oil. The regioselectivity was determined by ^{1}H NMR to be >20:1. The enantiomeric excess of **11** was determined to be 95% by chiral HPLC (see HPLC trace below). $[\alpha]_D$ = –23.4° (c 3.6, CH_2Cl_2); R_f = 0.28 (1:2 EtOAc/hexanes); ^{1}H NMR (300 MHz, $CDCl_3$) δ 7.60 (dd, J = 1.7 Hz, 0.7 Hz, 1H), 7.23 (dd, J = 3.6 Hz, 0.6 Hz, 1H), 6.56 (dd, J = 3.6 Hz, 1.7 Hz, 1H), 5.88 (dddd, J = 17.6 Hz, 10.3 Hz, 7.4 Hz, 7.4 Hz, 1H), 5.14-5.02 (m, 2H), 3.88 (s, 1H), 3.03 (d, J = 16.4 Hz, 1H), 2.94 (d, J = 16.4 Hz, 1H), 2.43-2.29 (m, 2H), 1.29 (s, 3H); ^{13}C NMR (100 MHz, $CDCl_3$) δ 190.1, 152.9, 147.0, 133.9, 118.5, 118.0, 112.5, 71.9, 46.8, 46.6, 27.1; IR (cast film) 3478, 3132, 3076, 2976, 2931, 1660, 1567, 1468 cm^{-1}; APCI LRMS *m/z* 195.57 ([M+H]$^+$, 100), 177.58 ([M–OH]$^+$, 50).

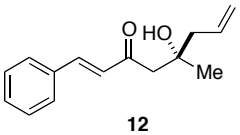

12

Compound 12: This reaction was performed according to general procedure 1 (0.35 mmol of (*E*)-6-phenylhex-5-ene-2,4-dione in $CHCl_3$ at 23 °C for 16 h). Purification by flash chromatography (1:4 EtOAc/hexanes) afforded **12** (60 mg, 75% yield) as an orange oil. The regioselectivity was determined by ^{1}H NMR of the crude product mixture to be > 20:1. The enantiomeric excess of **12** was determined to be 97% by chiral HPLC (see HPLC trace below). $[\alpha]_D = -22.6°$ (c 4.1, CH_2Cl_2); R_f = 0.28 (1:4 EtOAc/hexanes); ^{1}H NMR (400 MHz, $CDCl_3$) δ 7.60-7.53 (m, 3H), 7.44-7.37 (m, 3H), 6.73 (d, *J* = 16.2 Hz, 1H), 5.89 (dddd, *J* = 17.5 Hz, 10.2 Hz, 7.4 Hz, 7.4 Hz, 1H), 5.15-5.05 (m, 2H), 4.09 (s, 1H), 2.88 (d, *J* = 16.7 Hz, 1H), 2.77 (d, *J* = 16.6 Hz, 1H), 2.42-2.28 (m, 2H), 1.28 (s, 3H); ^{13}C NMR (75 MHz, $CDCl_3$) δ 201.7, 143.7, 134.1, 134.1, 130.9, 129.0, 128.5, 126.8, 118.4, 71.8, 48.9, 46.8, 27.1; IR (cast film) 3463, 3074, 2975, 2930, 1677, 1640, 1605, 1576 cm^{-1}; APCI LRMS *m/z* 231.19 ([M+H]$^+$, 70), 213.17 ([M–OH]$^+$, 10), 147.13 ([M–C_5H_8O+H]$^+$, 100).

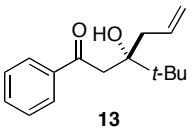

13

Compound 13: This reaction was performed according to general procedure 1 (0.33 mmol of 4,4-dimethyl-1-phenylpenta-1,3-dione in $CHCl_3$ at 23 °C for 16 h). Purification by flash chromatography (5% EtOAc/hexanes) afforded **13** (64 mg, 79% yield) as a pale orange oil. The regioselectivity was determined by ^{1}H NMR of the crude product mixture to be 16:1. The enantiomeric excess of **13** was determined to be 98% by chiral HPLC (see HPLC trace below). $[\alpha]_D = +26.7°$ (c 2.5, CH_2Cl_2); R_f = 0.34 (5% EtOAc/hexanes); ^{1}H NMR (400 MHz, $CDCl_3$) δ 7.95-7.90 (m, 2H), 7.61-7.55 (m, 1H), 7.50-7.44 (m, 2H), 5.92 (dddd, *J* = 16.8 Hz, 10.2 Hz, 8.8 Hz, 5.9 Hz, 1H), 5.27 (s, 1H), 4.99-4.90 (m, 2H), 3.19 (d, *J* = 16.8 Hz, 1H), 3.07 (d, *J* = 16.8 Hz, 1H), 2.58 (dddd, *J* = 14.1 Hz, 5.9 Hz, 1.4 Hz, 1.4 Hz, 1H), 2.31 (dd, *J* = 14.1 Hz, 8.8 Hz, 1H), 1.01 (s, 9H); ^{13}C NMR (100 MHz, $CDCl_3$) δ 204.2, 137.7, 136.1, 133.5, 128.7, 128.1, 117.8, 78.6, 41.7, 39.3, 39.0, 25.8; IR (cast film) 3432, 3073, 2958, 2876, 1665, 1597, 1209 cm^{-1}; APCI LRMS *m/z* 247.34 ([M+H]$^+$, 80), 229.36 ([M–OH]$^+$, 100).

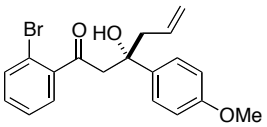

14

Compound 14: This reaction was performed according to general procedure 1 (0.19 mmol of 1-(1-bromophenyl)-3-(4-methoxyphenyl)-1,3-propanedione in $CHCl_3$ at 23 °C for 21 h). Purification by flash chromatography (1:4 EtOAc/hexanes) afforded **14** (56 mg, 80% yield) as a pale yellow oil. The regioselectivity was determined by ^{1}H NMR analysis of the crude product mixture to be 18:1 (see HMBC spectrum below). The enantiomeric excess of **14** was determined to be 94% by chiral HPLC (see HPLC trace below). $[\alpha]_D = +34.9°$ (c 3.7, CH_2Cl_2); R_f = 0.34 (25% EtOAc/hexanes); ^{1}H NMR (400 MHz, $CDCl_3$) δ 7.60-7.53 (m, 1H), 7.34-7.22 (m, 4H), 7.09-7.02 (m, 1H), 6.86-6.79 (m, 2H), 5.78-5.66 (m, 1H), 5.11-5.03 (m, 2H), 4.41 (s, 1H), 3.79 (s, 3H), 3.69 (d, *J* = 16.9 Hz, 1H), 3.37 (d, *J* = 16.9 Hz, 1H), 2.67-2.53 (m, 2H); ^{13}C NMR (100 MHz, $CDCl_3$) δ 205.6, 158.4, 141.6, 137.6, 133.6, 133.4, 131.9, 128.7, 127.4, 126.3, 118.6, 118.5, 113.5, 75.6, 55.2, 51.8, 48.0; IR (cast film) 3498, 3073, 3004, 2933, 2835, 1687, 1610, 1586, 1512, 1250 cm^{-1}; APCI LRMS *m/z* 357.07 ([M–OH]$^+$, 30), 177.21 ([M–C_8H_6BrO]$^+$, 100).

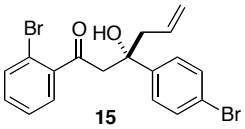

15

Compound 15: This reaction was performed according to general procedure 1 (0.17 mmol of 1-(1-bromophenyl)-3-(4-bromophenyl)-1,3-propanedione in $CHCl_3$ at 23 °C for 16 h). Purification by flash

chromatography (1:5 EtOAc/hexanes) afforded **15** (55 mg, 77% yield) as an orange oil. The regioselectivity was determined by ^{1}H NMR of the crude product mixture to be > 20:1 (see HMBC spectrum below). The enantiomeric excess of **15** was determined to be 92% by chiral HPLC (see HPLC trace below). $[\alpha]_D$ = +48.0° (c 2.2, CH_2Cl_2); R_f = 0.33 (1:5 EtOAc/hexanes); ^{1}H NMR (400 MHz, $CDCl_3$) δ 7.60-7.55 (m, 1H), 7.45-7.39 (m, 2H), 7.33-7.24 (m, 4H), 7.12-7.06 (m, 1H), 5.69 (dddd, *J* = 17.1 Hz, 10.4 Hz, 7.5 Hz, 6.9 Hz, 1H), 5.11-5.02 (m, 2H), 4.46 (s, 1H), 3.69 (d, *J* = 17.1 Hz, 1H), 3.39 (d, *J* = 17.1 Hz, 1H), 2.65-2.52 (m, 2H); ^{13}C NMR (100 MHz, $CDCl_3$) δ 205.3, 144.6, 141.3, 133.7, 132.8, 132.1, 131.3, 128.7, 127.5, 127.0, 119.0, 118.6, 75.7, 51.5, 47.8; IR (cast film) 3495, 3074, 2978, 2908, 1687, 1587 cm^{-1}; APCI LRMS *m/z* 407.01 ([M–OH]$^+$, 100).

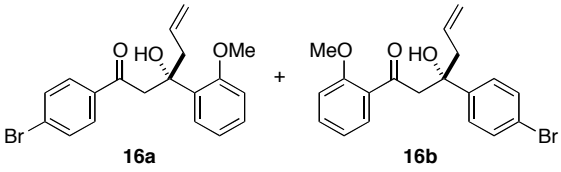

Compound 16a: This reaction was performed according to general procedure 1 (0.21 mmol of *p*-bromo *o*-methoxy dione in $CHCl_3$ at 23 °C for 15 h). Purification by flash chromatography (1:5 EtOAc/hexanes) afforded minor regioisomer **16b** (15 mg, 19%) as pale yellow oil and a mixture of major regioisomer **16a** and trace amounts of unreacted starting material, which co-elute. This mixture was further purified again by flash chromatography (4:1 CH_2Cl_2/hexanes) to afford **16a** (50 mg, 63%) as pale yellow oil. The regioselectivity was determined by ^{1}H NMR analysis of the crude product mixture to be 4:1 (**16a**:**16b**, see HMBC spectrum below). The enantiomeric excess of **16a** was determined to be 95% by chiral HPLC (see HPLC traces below). Data for the major regioisomer **16a**: $[\alpha]_D$ = +77.5° (c 2.55, CH_2Cl_2); R_f = 0.44 (1:5 EtOAc/hexanes); ^{1}H NMR (400 MHz, $CDCl_3$) 7.74-7.68 (m, 2H), 7.66 (dd, *J* = 7.8 Hz, 1.7 Hz, 1H), 7.57-7.52 (m, 2H), 7.18 (ddd, *J* = 8.1 Hz, 7.5 Hz, 1.8 Hz, 1H), 6.97 (ddd, *J* = 7.6 Hz, 7.6 Hz, 1.1 Hz, 1H), 6.77 (dd, *J* = 8.2 Hz, 0.9 Hz, 1H), δ 5.74 (dddd, *J* = 17.1 Hz, 10.1 Hz, 7.9 Hz, 6.3 Hz, 1H), 5.09-4.99 (m, 2H), 4.76 (s, 1H), 4.23 (d, *J* = 16.4 Hz, 1H), 3.76 (s, 3H), 3.19 (d, *J* = 16.4 Hz, 1H), 2.86 (dd, *J* = 13.8 Hz, 6.2 Hz, 1H), 2.70 (dd, 13.9 Hz, 8.0 Hz, 1H); ^{13}C NMR (75 MHz, $CDCl_3$) δ 201.2, 155.1, 136.1, 134.1, 132.8, 131.8, 129.7, 128.5, 128.4, 128.0, 120.9, 117.7, 110.8, 75.2, 55.1, 45.7, 44.8; IR (cast film) 3473, 3073, 2909, 2836, 1670, 1584, 1235 cm^{-1}; APCI LRMS *m/z* 356.46 ([M–OH]$^+$, 40), 176.9 ([M–C_8H_6BrO]$^+$, 100).

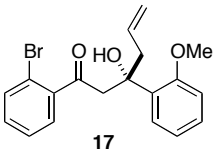

Compound 17: This reaction was performed according to general procedure 1 (0.24 mmol of 1-(1-bromophenyl)-3-(1-methoxyphenyl)-1,3-propanedione in $CHCl_3$ at 23 °C for 18 h). Purification by flash chromatography by first eluting with 2:1 CH_2Cl_2/hexanes to remove trace amounts of unreacted starting material followed by 5% EtOAc/CH_2Cl_2 to afford **17** (81 mg, 89% yield) as a yellow oil. The regioselectivity was determined by ^{1}H NMR analysis of the crude product mixture to be >20:1 (see HMBC spectrum below). The enantiomeric excess of **17** was determined to be 95% by chiral HPLC (see HPLC trace below). $[\alpha]_D$ = +12.8° (c 4.6, CH_2Cl_2); R_f = 0.38 (1:5 EtOAc/hexanes); ^{1}H NMR (400 MHz, $CDCl_3$) δ 7.62 (dd, *J* = 7.7 Hz, 1.8 Hz, 1H), 7.54-7.50 (m, 1H), 7.23-7.14 (m, 3H), 6.97 (ddd, *J* = 7.6 Hz, 7.6 Hz, 1.1 Hz, 1H), 6.83-6.78 (m, 1H), 6.66 (dd, *J* = 8.2 Hz, 0.8 Hz, 1H), 5.75 (dddd, *J* = 17.0 Hz, 10.2 Hz, 8.0 Hz, 6.3 Hz, 1H), 5.08-5.00 (m, 2H), 4.41 (s, 1H), 4.26 (d, *J* = 15.5 Hz, 1H), 3.56 (s, 3H), 3.24 (dd, *J* = 15.5 Hz, 1H), 2.82 (dd, *J* = 13.9 Hz, 6.1 Hz, 1H), 2.70 (dd, *J* = 13.9 Hz, 8.0 Hz, 1H); ^{13}C NMR (100 MHz, $CDCl_3$) δ 206.5, 155.2, 141.9, 134.0, 133.2, 132.3, 131.5, 128.6, 128.5, 128.0, 127.1,

120.7, 118.6, 117.8, 110.6, 75.5, 54.7, 50.3, 44.5; IR (cast film) 3495, 3073, 2939, 2836, 1682, 1586, 1237 cm^{-1}; APCI LRMS *m/z* 356.46 ($[M–OH]^+$, 35), 176.9 ($[M–C_8H_6BrO]^+$, 100).

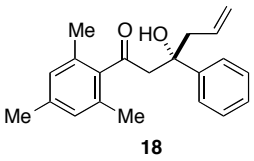

18

Compound 18: This reaction was performed according to general procedure 1 (0.23 mmol of mesitoylbenzoylmethane in $CHCl_3$ at 23 °C for 27 h). Purification by flash chromatography (5% EtOAc/hexanes) afforded **18** (68 mg, 94% yield) as a pale yellow oil. The regioselectivity was determined by ^1H NMR analysis of the crude product mixture to be >20:1 (see HMBC spectrum below). The enantiomeric excess of **18** was determined to be 83% by chiral HPLC (see HPLC trace below). $[\alpha]_D$ = +42.1° (c 3.8, CH_2Cl_2); R_f = 0.31 (10% EtOAc/hexanes); ^1H NMR (400 MHz, $CDCl_3$) δ 7.47-7.41 (m, 2H), 7.36-7.29 (m, 2H), 7.26-7.20 (m, 1H), 6.78 (s, 2H), 5.73 (dddd, *J* = 16.0 Hz, 10.9 Hz, 7.2 Hz, 7.2 Hz, 1H), 5.19-5.00 (m, 2H), 4.86 (s, 1H), 3.45 (d, *J* = 18.0 Hz, 1H), 3.22 (d, *J* = 18.1 Hz, 1H), 2.65-2.55 (m, 2H), 2.25 (s, 3H), 1.98 (s, 6H); ^{13}C NMR (100 MHz, $CDCl_3$) δ 212.1, 145.7, 139.0, 138.6, 133.4, 133.0, 128.7, 128.1, 126.8, 125.1, 118.4, 75.5, 53.6, 47.9, 21.0, 19.0; IR (cast film) 3474, 3073, 3026, 2977, 2920, 1686, 1610 cm^{-1}; APCI LRMS *m/z* 291.02 ($[M–OH]^+$, 5), 179.05 ($[M–C_{11}H_{13}O+MeOH]^+$, 50), 163.08 ($[M–C_{10}H_8O]^+$, 70), 147.05 ($[M–C_{11}H_{13}O]^+$, 100).

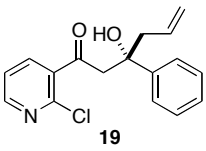

19

Compound 19: This reaction was performed according to general procedure 1 (0.39 mmol of 2-cloro-3-pyridoylbenzoylmethane in $CHCl_3$ at 23 °C for 19 h). Purification by flash chromatography (1:5:5 EtOAc/hexanes/CH_2Cl_2) afforded **19** (74 mg, 62% yield) as a pale yellow oil. The regioselectivity was determined by ^1H NMR analysis of the crude product mixture to be 5:1 (see HMBC spectra below). The enantiomeric excess of **19** was determined to be 84% by chiral HPLC (see HPLC trace below). $[\alpha]_D$ = 50.4° (c 3.7, CH_2Cl_2); R_f = 0.40 (1:5:5 EtOAc/hexanes/CH_2Cl_2); ^1H NMR (400 MHz, $CDCl_3$) δ 8.43 (dd, *J* = 4.8 Hz, 2.0 Hz, 1H), 7.38-7.33 (m, 3H), 7.31-7.26 (m, 2H), 7.23-7.17 (m, 2H), 5.78-5.65 (m, 1H), 5.13-5.07 (m, 2H), 4.09 (s, 1H), 3.83 (d, *J* = 16.4 Hz, 1H), 3.40 (d, *J* = 16.4 Hz, 1H), 2.70-2.55 (m, 2H); ^{13}C NMR (100 MHz, $CDCl_3$) δ 203.2, 151.3, 147.0, 145.1, 137.9, 135.9, 132.9, 128.2, 127.0, 125.0, 122.4, 119.1, 75.9, 52.1, 47.9; IR (cast film) 3488, 3076, 2980, 1688, 1575, 1397 cm^{-1}; APCI LRMS *m/z* 301.59 ($[M+H]^+$, 30), 283.62 ($[M–OH]^+$, 5), 155.80 ($[M–C_{10}H_9O]^+$, 100).

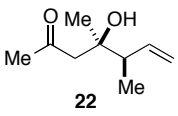

22

Compound 22: This reaction was performed according to general procedure 1 (0.48 mmol of acetylacetone in $CHCl_3$ at 23 °C for 40 h). Purification by flash chromatography (25% Et_2O/pentane) afforded **22** (52 mg, 69% yield) as a yellow oil. The diastereoselectivity was determined by GC analysis of the crude product mixture to be 99:1. The enantiomeric excess of **22** was determined to be 89% by chiral GC (see GC trace below). $[\alpha]_D$ = +16.3° (c 3.5, CH_2Cl_2); R_f = 0.43 (25% Et_2O/pentane); ^1H NMR (400 MHz, $CDCl_3$) δ 5.73 (ddd, *J* = 16.4 Hz, 10.9 Hz, 8.7 Hz, 1H), 5.05-4.97 (m, 2H), 3.88 (s, 1H), 2.69 (d, *J* = 17.3 Hz, 1H), 2.50 (d, *J* = 17.3 Hz, 1H), 2.37 (dq, *J* = 8.6 Hz, 6.9 Hz, 1H), 2.15 (s, 3H), 1.03 (d, *J* = 6.9 Hz, 3H); ^{13}C NMR (100 MHz, $CDCl_3$) δ 211.5, 140.6, 115.7, 73.2, 50.9, 47.6, 31.9, 22.9, 14.2; IR (cast film) 3492, 3077, 2977, 2938, 1701, 1639 cm^{-1}; APCI LRMS *m/z* 157.32 ($[M+H]^+$, 5), 139.29 ($[M–OH]^+$, 100).

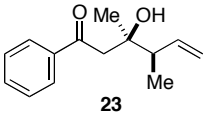

23

Compound 23: This reaction was performed according to general procedure 1 (0.17 mmol of benzoylacetone in $CHCl_3$ at 23 °C for 40 h). Purification by

flash chromatography (1:5 EtOAc/hexanes) afforded **23** (27 mg, 75% yield) as a yellowish-orange oil. The regioselectivity and diastereoselectivity were both determined by ^{1}H NMR analysis of the crude product mixture to be >20:1. The enantiomeric excess of **23** was determined to be 97% by chiral HPLC (see HPLC trace below). $[\alpha]_D = -18.1°$ (c 2.5, CH_2Cl_2); R_f = 0.38 (1:5 EtOAc/hexanes); ^{1}H NMR (300 MHz, $CDCl_3$) δ 7.97-7.88 (m, 2H), 7.62-7.54 (m, 1H), 7.51-7.42 (m, 2H), 5.80 (ddd, *J* = 17.0 Hz, 10.4 Hz, 8.7 Hz, 1H), 5.04-4.92 (m, 2H), 4.25 (s, 1H), 3.23 (d, *J* = 17.2 Hz, 1H), 3.03 (d, *J* = 17.2 Hz, 1H), 2.51 (dq, *J* = 8.3 Hz, 7.1 Hz, 1H), 1.23 (s, 3H), 1.11 (d, *J* = 6.9 Hz, 3H); ^{13}C NMR (75 MHz, $CDCl_3$) δ 202.4, 140.6, 137.5, 133.5, 128.7, 128.1, 115.9, 73.7, 47.7, 45.8, 23.2, 14.2; IR (cast film) 3494, 3069, 2976, 2937, 2885, 1670, 1597 cm^{-1}; APCI LRMS *m/z* 218.97 ($[M+H]^+$, 75), 201.01 ($[M-OH]^+$, 100).

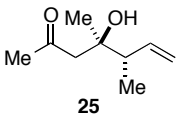

25

Compound 25: This reaction was performed according to general procedure 2 (0.088 mmol of acetylacetone in $CHCl_3$ at 23 °C for 67 h). Purification by flash chromatography (25% EtOAc/hexanes) afforded **25** (13 mg, 91% yield) as a pale orange oil (Note: color impurities could be removed with activated charcoal treatment resulting in a pale yellow oil). The diastereoselectivity was determined by GC analysis of the crude product mixture to be 49:1. The enantiomeric excess of **25** was determined to be 91% by chiral GC. **Note:** The reaction time was reduced to 6 h when carried out at 50 °C to obtain **25** in 71% yield, 58:1 diastereoselectivity, and 84% enantiomeric excess (see GC trace below). $[\alpha]_D = -19.4°$ (c 3.3, CH_2Cl_2; for 84% ee); R_f = 0.39 (25% EtOAc/hexanes); ^{1}H NMR (400 MHz, $CDCl_3$) δ 5.85 (ddd, *J* = 16.9 Hz, 10.7 Hz, 8.2 Hz, 1H), 5.09-5.00 (m, 2H), 3.74 (s, 1H), 2.66 (d, *J* = 16.8 Hz, 1H), 2.52 (d, *J* = 16.8 Hz, 1H), 2.25 (dq, *J* = 7.1 Hz, 7.7 Hz, 1H), 2.17 (s, 3H), 1.17 (s, 3H), 1.01 (d, *J* = 6.9 Hz, 3H); ^{13}C NMR (100 MHz, $CDCl_3$) δ 211.3, 140.0, 115.7, 73.2, 50.3, 47.7, 32.1, 24.6, 14.4; IR (cast film) 3486, 3077, 2976, 2937, 2885, 1701, 1639 cm^{-1}; APCI LRMS *m/z* 157.24 ($[M+H]^+$, 10), 139.23 ($[M-OH]^+$, 100).

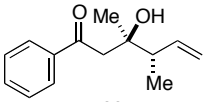

26

Compound 26: This reaction was performed according to general procedure 2 (0.065 mmol of benzoylacetone in $CHCl_3$ at 23 °C for 64 h). Purification by flash chromatography (1:4 EtOAc/hexanes) afforded **26** (10 mg, 71% yield) as a red oil that was a mixture of regioisomers. The regioselectivity was determined by ^{1}H NMR analysis of the crude product mixture to be 7:1 and the diastereoselectivity to be >20:1 for the major regioisomer. The enantiomeric excess of **26** was determined to be 96% by chiral HPLC. **Note:** The reaction time was reduced to 6 h when carried out at 50 °C to obtain **26** in 59% yield, 10:1 regioselectivity, >20:1 diastereoselectivity, and 94% enantiomeric excess (see HPLC trace below). $[\alpha]_D = -31.5°$ (c 2.8, CH_2Cl_2; for 94% ee); R_f = 0.42 (25% EtOAc/hexanes); ^{1}H NMR (400 MHz, $CDCl_3$) δ 7.97-7.92 (m, 2H), 7.62-7.55 (m, 1H), 7.52-7.44 (m, 2H), 5.86 (ddd, *J* = 17.8 Hz, 9.7 Hz, 8.0 Hz, 1H), 5.12-5.05 (m, 2H), 4.16 (s, 1H), 3.16 (d, *J* = 16.9 Hz, 1H), 3.10 (d, *J* = 16.8 Hz, 1H), 2.40 (dq, *J* = 7.8 Hz, 7.0 Hz, 1H), 1.27 (s, 3H), 1.08 (d, *J* = 6.9 Hz, 3H); ^{13}C NMR (100 MHz, $CDCl_3$) δ 202.3, 140.1, 137.5, 133.5, 128.7, 128.1, 115.7, 73.6, 47.8, 44.9, 24.9, 14.5; IR (cast film) 3487, 3069, 2975, 2936, 1670, 1597, 1216 cm^{-1}; LRMS (APCI) *m/z* 219.26 ($[M+H]^+$, 100), 201.25 ($[M-OH]^+$, 85).

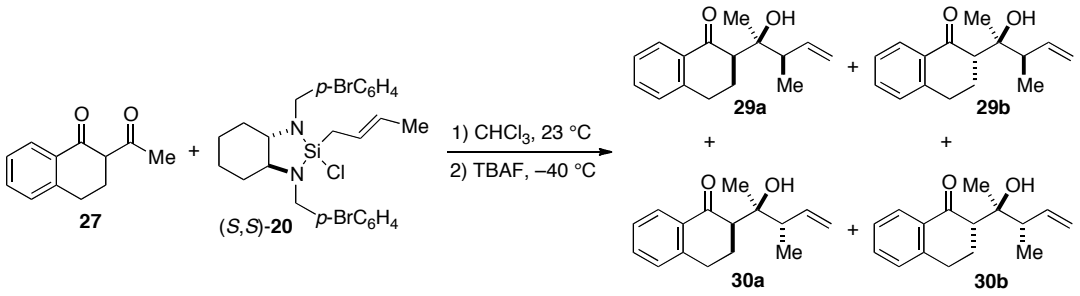

Compound 29a: This reaction was performed according to general procedure 1 (0.45 mmol of 2-acetyl-1-tetralone **27** in $CHCl_3$ at 23 °C for 43 h). Purification by flash chromatography (1:5 EtOAc/hexanes) afforded **29a** (76 mg, 69% yield) as an orange oil. The regioselectivity and the diastereoselectivity were determined by ^{1}H NMR analysis of the crude product mixture to be >20:1 and 94:4:2:0 (**29a**:**29b**:**30a**:**30b**), respectively. The enantiomeric excess of **29a** was determined to be 98% by chiral HPLC (see HPLC trace below). $[\alpha]_D = -48.1°$ (c 2.4, CH_2Cl_2); R_f = 0.28 (1:5 EtOAc/hexanes); ^{1}H NMR (300 MHz, $CDCl_3$) δ 7.99 (d, *J* = 7.8 Hz, 1H), 7.52-7.44 (m, 1H), 7.35-7.27 (m, 1H), 7.23 (d, *J* = 7.6 Hz, 1H), 5.86 (ddd, *J* = 17.8 Hz, 9.2 Hz, 9.0 Hz, 1H), 5.03-4.93 (m, 2H), 4.57 (s, 1H), 3.07-2.87 (m, 2H), 2.76-2.60 (m, 2H), 2.35-2.25 (m, 1H), 2.06 (dddd, *J* = 13.3 Hz, 13.3 Hz, 10.8 Hz, 6.1 Hz, 1H), 1.28 (s, 3H), 1.00 (d, *J* = 6.9 Hz, 3H); ^{13}C NMR (75 MHz, $CDCl_3$) δ 202.4, 144.0, 140.9, 133.6, 133.3, 128.5, 127.3, 126.7, 115.3, 76.1, 56.4, 45.2, 29.8, 25.3, 24.1, 16.1; IR (cast film) 3420, 3071, 2976, 2936, 2878, 1661, 1600 cm^{-1}; APCI LRMS *m/z* 245.29 ($[M+H]^+$, 70), 227.30 ($[M–OH]^+$, 40), 147.17 ($[M–C_6H_9O]^+$, 100).

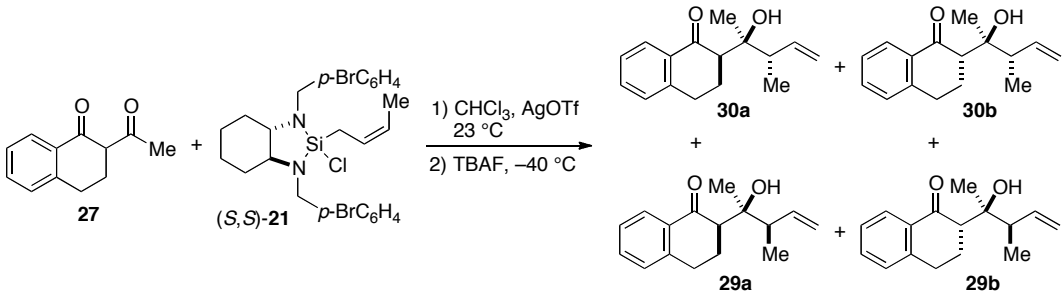

Compound 30a: This reaction was performed according to general procedure 2 (0.31 mmol of 2-acetyl-1-tetralone **27** in $CHCl_3$ at rt for 48 h). Purification by flash chromatography (1:4 EtOAc/hexanes) afforded **30a** (45 mg, 59% yield) as a red oil. The regioselectivity and the diastereoselectivity were determined by ^{1}H NMR analysis of the crude product mixture to be >20:1 and 88:10:2:0 (**30a**:**30b**:**29a**:**29b**), respectively. The enantiomeric excess of **30a** was determined to be 96% by chiral HPLC (see HPLC trace below). $[\alpha]_D = -43.0°$ (c 2.1, CH_2Cl_2); R_f = 0.31 (1:4 EtOAc/hexanes); ^{1}H NMR (300 MHz, $CDCl_3$) δ 7.95 (d, *J* = 7.7 Hz, 1H), 7.50-7.41 (m, 1H), 7.34-7.25 (m, 1H), 7.21 (d, *J* = 7.6 Hz, 1H), 5.84 (ddd, *J* = 17.3 Hz, 10.2 Hz, 9.1 Hz, 1H), 4.92-4.79 (m, 2H), 4.54 (s, 1H), 3.09-2.85 (m, 2H), 2.70-2.56 (m, 2H), 2.33-2.21 (m, 1H), 2.07 (dddd, *J* = 13.0 Hz, 13.0 Hz, 11.7 Hz, 5.0 Hz, 1H), 1.31 (s, 3H), 1.07 (d, *J* = 6.8 Hz, 3H); ^{13}C NMR (75 MHz, $CDCl_3$) δ 202.1, 143.7, 141.4, 133.7, 133.3, 128.3, 127.4, 126.6, 115.0, 76.7, 56.1, 45.2, 29.6, 24.8, 24.6, 14.8; IR (cast film) 3415, 3071, 2975, 2936, 2878, 1679, 1658, 1600, 1223 cm^{-1}; APCI LRMS *m/z* 245.33 ($[M+H]^+$, 50), 227.33 ($[M–OH]^+$, 30), 147.18 ($[M–C_6H_9O]^+$, 100).

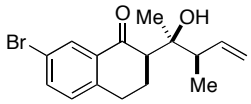

S1

Compound S1: This reaction was performed according to general procedure 1 (0.18 mmol of bromotetralone in $CHCl_3$ at rt for 38 h). Purification by flash chromatography (1:4 EtOAc/hexanes) afforded **S1** (29 mg, 49% yield) as an orange-red oil. The regioselectivity was determined by ^{1}H NMR analysis of the crude product mixture to be >20:1 and the diastereoselectivity to be 85:10:5:0. The enantiomeric excess of **S1** was determined to be 94% by chiral HPLC (see HPLC trace below). $[\alpha]_D$ = +20.7° (c 1.76, EtOH); R_f = 0.31 (25% EtOAc/hexanes); ^{1}H NMR (300 MHz, $CDCl_3$) δ 8.10 (d, *J* = 2.2 Hz, 1H), 7.58 (dd, *J* = 8.2 Hz, 2.2 Hz, 1H), 7.12 (d, 8.2 Hz, 1H), 5.86 (ddd, *J* = 17.7 Hz, 9.6 Hz, 9.0 Hz, 1H), 5.04-4.96 (m, 2H), 4.06 (s, 1H), 3.04-2.80 (m, 2H), 2.77-2.63 (m, 2H), 2.38-2.26 (m, 1H), 2.06 (dddd, *J* = 13.3 Hz, 13.3 Hz, 12.0 Hz, 4.8 Hz, 1H), 1.28 (s, 3H), 1.00 (d, *J* = 6.9 Hz, 3H); ^{13}C NMR (100 MHz, $CDCl_3$) δ 200.8, 142.6, 140.7, 136.3, 134.9, 130.3, 130.2, 120.7, 115.6, 75.9, 56.1, 45.1, 29.3, 25.0, 23.7, 15.9; IR (cast film) 3441, 3071, 2974, 2934, 2877, 1678, 1589, 1214 cm^{-1}; APCI LRMS *m/z* 322.93 ([M+H]$^+$, 25), 304.92 ([M–OH]$^+$, 100).

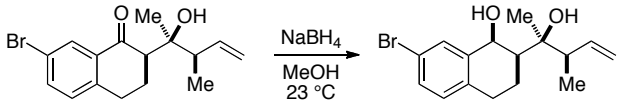

S1 **S2**

Compound S2: To a solution of **S1** (14 mg, 0.043 mmol) in MeOH (3 mL) was added $NaBH_4$ (4 mg, 0.11 mmol). The mixture was stirred at 23 °C until the reaction was complete by TLC (2:1 CH_2Cl_2/hexanes, $KMnO_4$); 3 h. The reaction was quenched with H_2O (3 mL), extracted with 2 × 10 mL Et_2O and the organic phased combined. The organic phase was washed with H_2O (5 mL), brine (5 mL) and dried over $MgSO_4$. The mixture was filtered and concentrated in vacuo to yield **S2** (14 mg, quantitative) as a pale yellow oil. The diastereoselectivity was determined by ^{1}H NMR to be 5:1. R_f = 0.31 (25% EtOAc/hexanes); ^{1}H NMR (400 MHz, $CDCl_3$) δ 7.44 (d, *J* = 2.1 Hz, 1H), 7.34 (dd, *J* = 8.1 Hz, 2.1 Hz, 1H), 7.01 (d, *J* = 8.2 Hz, 1H), 5.63 (ddd, *J* = 17.1 Hz, 10.3 Hz, 9.3 Hz, 1H), 5.10-4.95 (m, 3H), 3.02 (bs, 1H), 2.91 (ddd, *J* = 17.1 Hz, 5.1 Hz, 2.4 Hz, 1H), 2.78-2.57 (m, 3H), 2.05-1.88 (m, 2H), 1.76 (ddd, *J* = 11.8 Hz, 3.0 Hz, 3.0 Hz, 1H), 1.35 (s, 3H), 1.10 (d, *J* = 6.7 Hz, 3H); ^{13}C NMR (100 MHz, $CDCl_3$) δ 140.5, 140.3, 136.1, 132.5, 131.3, 130.7, 119.4, 115.6, 75.9, 69.6, 44.9, 43.9, 29.0, 20.1, 16.3, 14.2; IR (cast film) 3358, 3074, 2976, 2933 cm^{-1}; LRMS (APCI) 307.05 [M–OH]$^+$, 20), 251.1 ([M–OH–C_4H_7]$^+$, 100).

Mechanism Discussion

We conducted an experiment where only a *trans*-silyl enol ether could form (**S3**) to provide evidence that allylation does not occur via this isomer due to the silicon atom's inability to reach the β-carbonyl and provide the intramolecular Lewis acid activation needed for allylation to occur (Supplementary Figure 1). The reaction of β-diketone **5** with allylsilane (*S*,*S*)-**3** lead to the clean formation of **S3**, as determined by ^{1}H NMR spectroscopy, but did not undergo allylation to provide product **S4**.

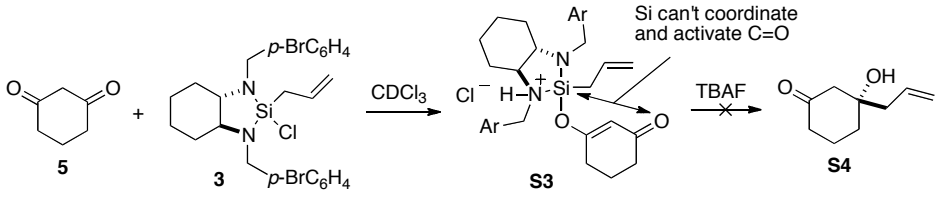

Supplementary Figure 1 | Attempted allylation of β-diketone **5**.

To provide evidence that the enol tautomer is required for the allylation of β-diketones compound **6** was mixed with allylsilane (*S*,*S*)-**3**, which resulted in no reaction even after heating to 60 °C for 3 days (Supplementary Figure 2).

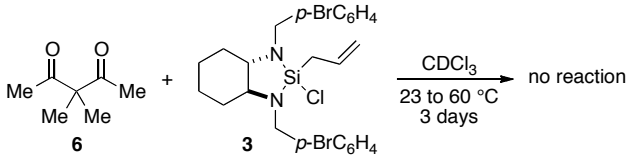

Supplementary Figure 2 | Control experiment to show that β-diketones that have a very low (or zero) concentration of enol tautomer do not undergo allylation with (*S*,*S*)-**3**.

The formation of *cis* and *trans* isomers of the silyl enol ethers was determined my ^{1}H NMR spectroscopy by mixing acetylacetone with *cis*-crotylsilane reagent (*S*,*S*)-**21** in the presence of silver triflate following the general procedure and observing the formation of two sets of intermediate silyl enol ether peaks that we have assigned to *cis*- and *trans*-silyl enol ethers **S5** and **S6**, respectively, in a ratio of *ca*. 1:1 (Supplementary Figure 3). It is interesting to note that the formation of **S5** and **S6** is rapid for the enol tautomer of acetylacetone with a much slower disappearance of the dione tautomer. The emergence of product **S7** can be seen by the formation of a new singlet upfield at 4.41 ppm representing the vinyl proton signal of **S7** (Supplementary Figure 3a) and new methyl signals at 1.77 and 1.22 ppm (Supplementary Figure 3b). The signals for intermediates **S5** and **S6** disappear at approximately the same rate suggesting that the two isomers are in rapid equilibrium where only intermediate **S5** can lead to product **S7**, as previously discussed in Supplementary Figure 1. Further evidence that supports this premise is that the isolated yield for this reaction was 69%, which is higher than would be expected from a 1:1 mixture of **S5** and **S6** if isomerization was not occuring.

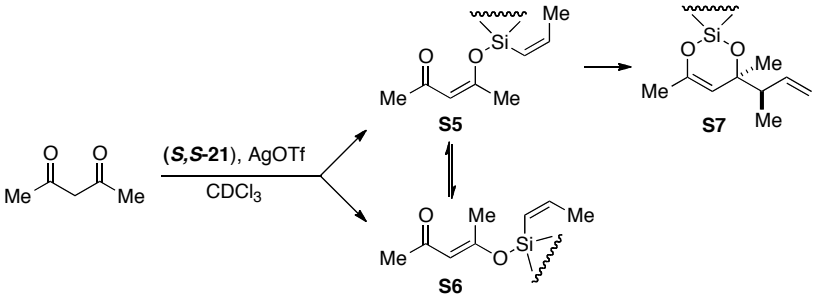
Me
O
O
Me
(S,S-21), AgOTf
CDCl3
Si
O
Me
S5
S6
S7

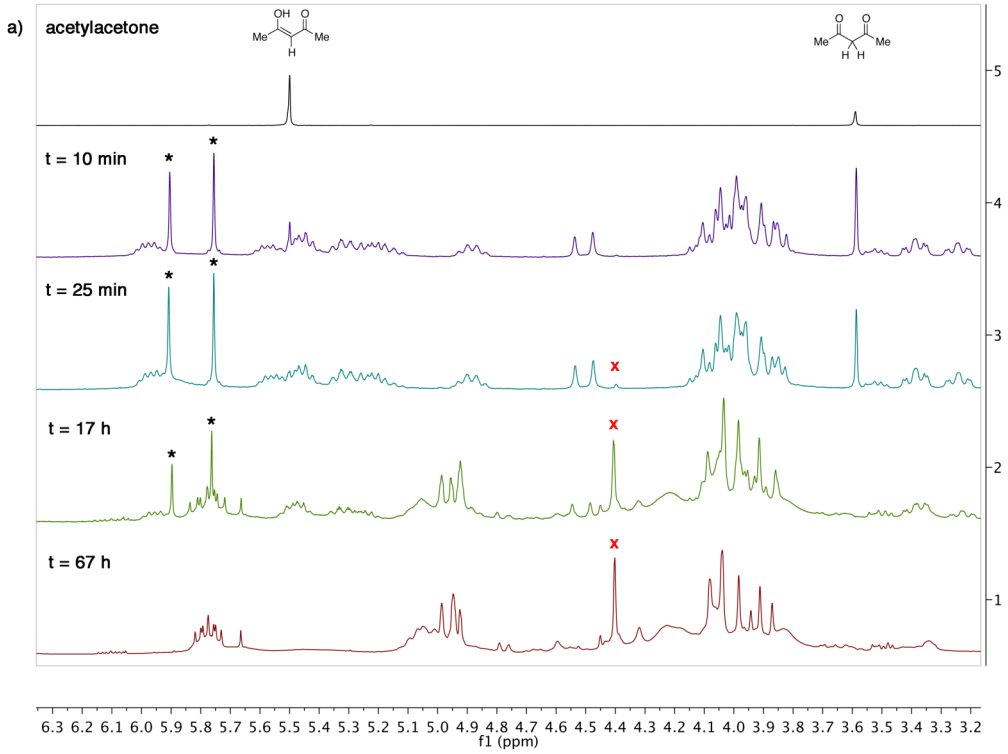
a)
acetylacetone
t = 10 min
t = 25 min
t = 17 h
t = 67 h
*
x
6.3 6.2 6.1 6.0 5.9 5.8 5.7 5.6 5.5 5.4 5.3 5.2 5.1 5.0 4.9 4.8 4.7 4.6 4.5 4.4 4.3 4.2 4.1 4.0 3.9 3.8 3.7 3.6 3.5 3.4 3.3 3.2
f1 (ppm)

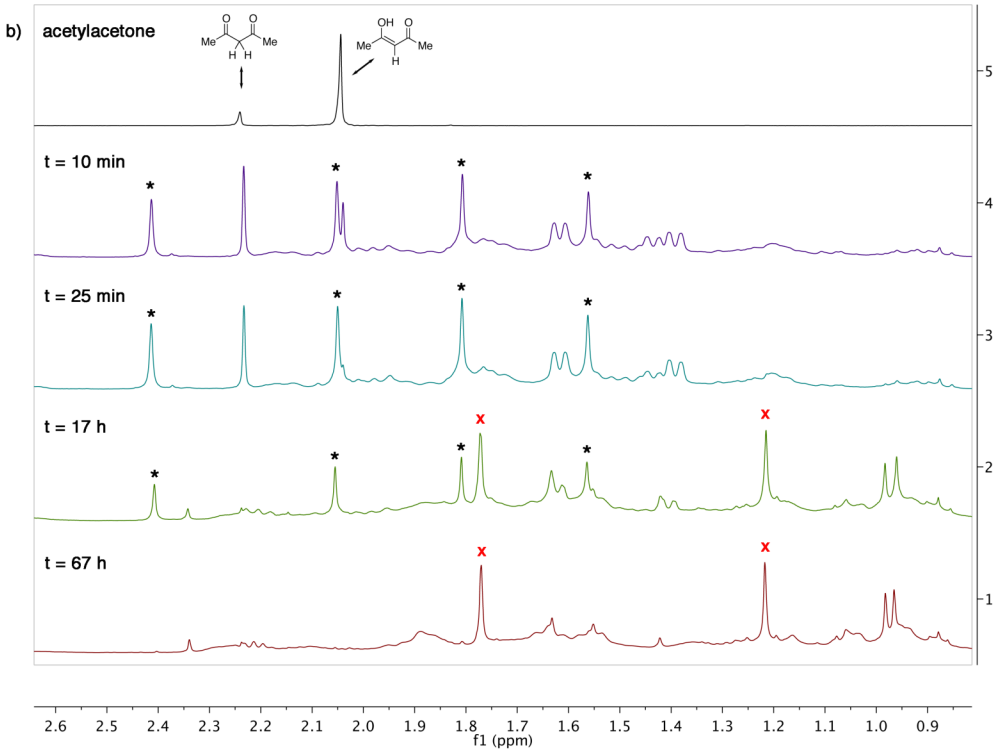

Supplementary Figure 3 | Time dependant ^{1}H NMR analysis of the **a)** vinyl region and the **b)** methyl region of the spectrum for the crotylation of acetylacetone. The spectra show the rapid formation of intermediates **S5** and **S6** (black asterisk, *cis*/*trans* ratio ca. 1:1) and the slow growth of product **S7** (red X), taking ca. 67 h for the crotylation reaction to complete.

The crotylation of 2-acetyl-1-tetralone **27** with (*S*,*S*)-**21** was carried out following the general procedure and the reaction progress was followed by ^{1}H NMR spectroscopy which provides evidence that silyl tautomerization is occurring in the reaction mechanism. Silyl enol ether isomers **S8-S10** are formed in an unassigned ratio of 2:3.4:1 once all starting material was consumed, as determined by ^{1}H NMR spectroscopy, based of the formation of 3 new singlets in at 2.53, 2.11 and 1.97 ppm (Supplementary Figure 4). It is clear that a substantial portion of silyl enol ether is present as either **S9** or **S10** (unassigned) based on the presence and proportions of these 3 peaks and since the regioselectivity of isolated product **30** is >20:1, the results suggest that tautomerization is occurring and is fast and reversible compared to the crotylation step leading preferentially to product **S11** via intermediate **S8**.

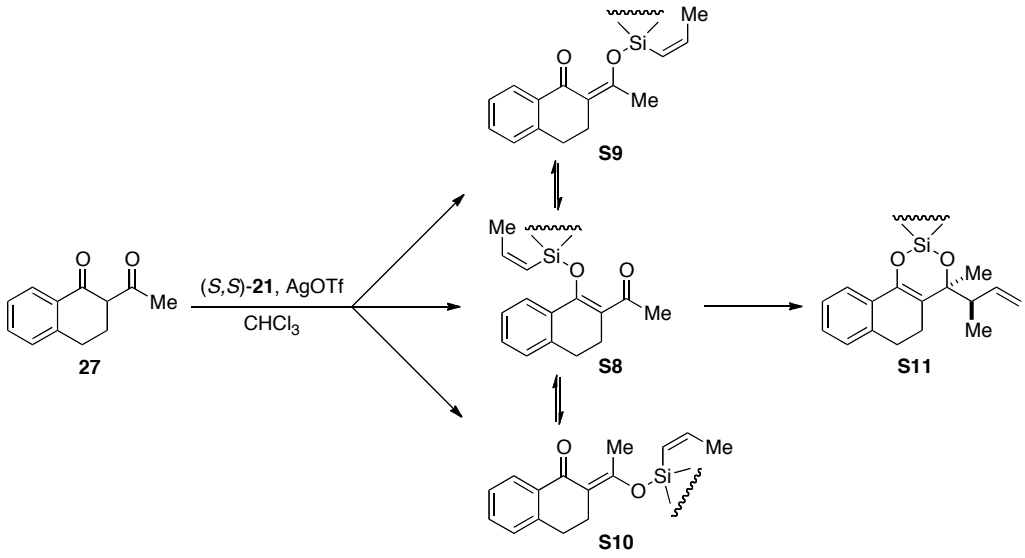

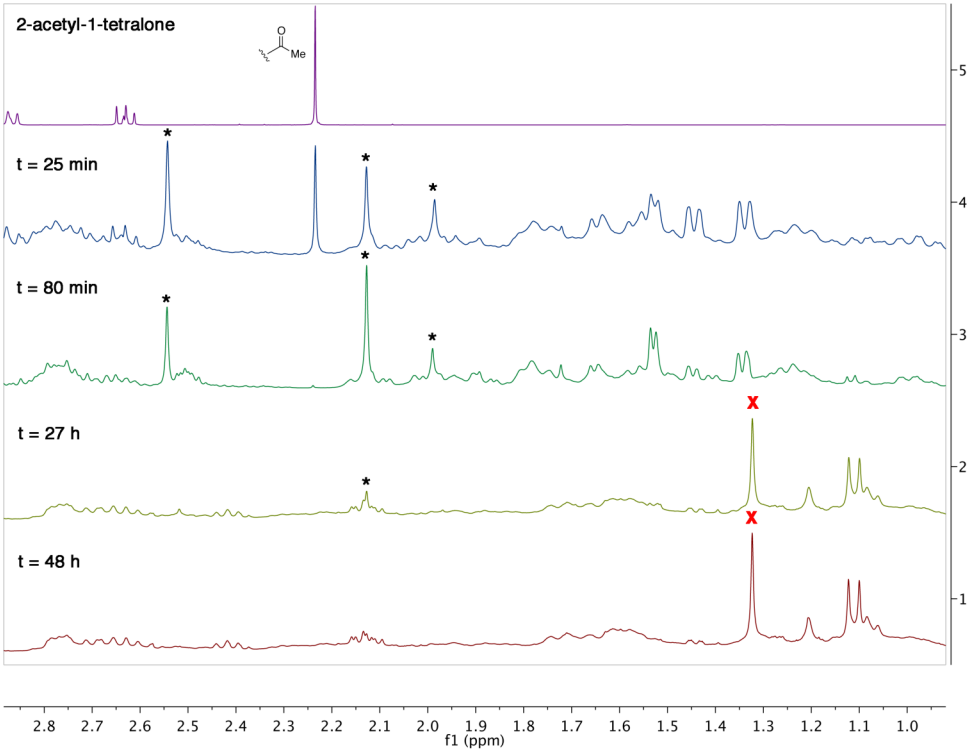

Supplementary Figure 4 | Time dependant ^{1}H NMR analysis of the methyl region of the spectrum for the crotylation of **27** showing the rapid formation of intermediates **S8**, **S9**, and **S10** (black asterisk, *ca*. 2:3.4:1 ratio at 80 min) and the slow growth of product **S11** (red X), taking ca. 48 h for the crotylation to complete.

Determination of relative and absolute stereochemistry

Single crystals suitable for X-ray crystallographic analysis were grown by slow evaporation of a solution of **S2** in hexanes (Supplementary Figure 5). This structure allowed the assignment of absolute configuration as shown. The absolute configuration of all other products was assigned by analogy. We thank Prof. Ged Parkin and Mr. Wesley Sattler for the x-ray structure analysis, and the National Science Foundation (CHE-0619638) is thanked for acquisition of an X-ray diffractometer. CCDC 874744 contains the supplementary crystallographic data for this paper. These data can be obtained free of charge from The Cambridge Crystallographic Data Centre via www.ccdc.cam.ac.uk/data_request/cif.

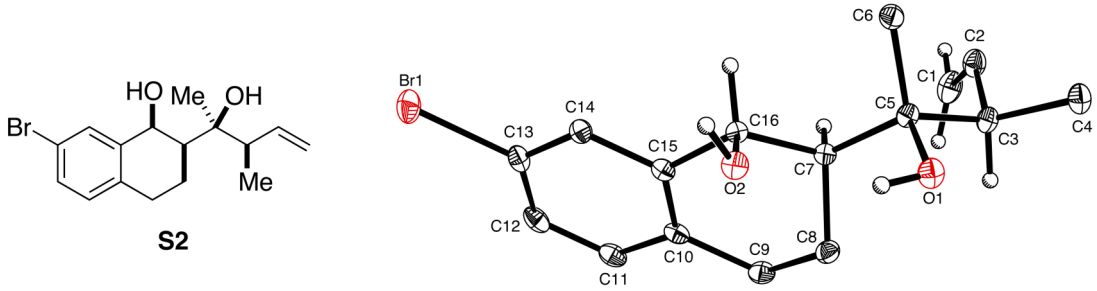

Supplementary Figure 5 | X-ray crystal structure of **S2**.

Supplementary Table 1 | Crystal data and structure refinement for **S2**.

_audit_creation_method	SHELXL-97
_chemical_formula_sum	'C16 H21 Br O2'
_chemical_formula_weight	325.24
_chemical_absolute_configuration	AD
_atom_type_scat_source	'C' 'C' 0.0033 0.0016
'International Tables Vol C Tables 4.2.6.8 and 6.1.1.4'	
'H' 'H' 0.0000 0.0000	
'International Tables Vol C Tables 4.2.6.8 and 6.1.1.4'	
'O' 'O' 0.0106 0.0060	
'International Tables Vol C Tables 4.2.6.8 and 6.1.1.4'	
'Br' 'Br' -0.2901 2.4595	
'International Tables Vol C Tables 4.2.6.8 and 6.1.1.4'	

_symmetry_cell_setting	Orthorhombic
_symmetry_space_group_name_H-M	P2(1)2(1)2(1)

_symmetry_equiv_pos_as_xyz
'x, y, z'
'-x+1/2, -y, z+1/2'
'-x, y+1/2, -z+1/2'
'x+1/2, -y+1/2, -z'

_cell_length_a	8.5529(6)
_cell_length_b	8.8479(7)
_cell_length_c	19.3771(14)
_cell_angle_alpha	90.00
_cell_angle_beta	90.00
_cell_angle_gamma	90.00
_cell_volume	1466.37(19)
_cell_formula_units_Z	4
_cell_measurement_temperature	150(2)
_cell_measurement_reflns_used	9914
_cell_measurement_theta_min	2.53
_cell_measurement_theta_max	31.55
_exptl_crystal_description	BLOCK
_exptl_crystal_colour	COLORLESS
_exptl_crystal_size_max	0.69
_exptl_crystal_size_mid	0.54
_exptl_crystal_size_min	0.15
_exptl_crystal_density_meas	?
_exptl_crystal_density_diffrn	1.473
_exptl_crystal_density_method	'not measured'
_exptl_crystal_F_000	672
_exptl_absorpt_coefficient_mu	2.799
_exptl_absorpt_correction_type	EMPIRICAL
_exptl_absorpt_correction_T_min	0.2483
_exptl_absorpt_correction_T_max	0.6788
_exptl_absorpt_process_details	SADABS
_diffrn_ambient_temperature	150(2)
_diffrn_radiation_wavelength	0.71073
_diffrn_radiation_type	MoK\a
_diffrn_radiation_source	'fine-focus sealed tube'
_diffrn_radiation_monochromator	graphite
_diffrn_measurement_device_type	'Bruker APEX-II CCD'
_diffrn_measurement_method	'\f and \w scans'
_diffrn_detector_area_resol_mean	?
_diffrn_reflns_number	25387
_diffrn_reflns_av_R_equivalents	0.0402
_diffrn_reflns_av_sigmaI/netI	0.0358
_diffrn_reflns_limit_h_min	-12
_diffrn_reflns_limit_h_max	12
_diffrn_reflns_limit_k_min	-13
_diffrn_reflns_limit_k_max	13

_diffrn_reflns_limit_l_min	-29
_diffrn_reflns_limit_l_max	29
_diffrn_reflns_theta_min	2.10
_diffrn_reflns_theta_max	32.68
_reflns_number_total	5169
_reflns_number_gt	4014
_reflns_threshold_expression	>2sigma(I)

_computing_data_collection	'Bruker APEX2'
_computing_cell_refinement	'Bruker SAINT'
_computing_data_reduction	'Bruker SAINT'
_computing_structure_solution	'SHELXS-97 (Sheldrick, 2008)'
_computing_structure_refinement	'SHELXL-97 (Sheldrick, 2008)'
_computing_molecular_graphics	'Bruker SHELXTL'
_computing_publication_material	'Bruker SHELXTL'

_refine_special_details

Refinement of F^2^ against ALL reflections. The weighted R-factor wR and goodness of fit S are based on F^2^, conventional R-factors R are based on F, with F set to zero for negative F^2^. The threshold expression of F^2^ > 2sigma(F^2^) is used only for calculating R-factors(gt) etc. and is not relevant to the choice of reflections for refinement. R-factors based on F^2^ are statistically about twice as large as those based on F, and R- factors based on ALL data will be even larger.

_refine_ls_structure_factor_coef	Fsqd
_refine_ls_matrix_type	full
_refine_ls_weighting_scheme	calc

_refine_ls_weighting_details

'calc w=1/[\s^2^(Fo^2^)+(0.0525P)^2^+0.2811P] where P=(Fo^2^+2Fc^2^)/3'

_atom_sites_solution_primary	direct
_atom_sites_solution_secondary	difmap
_atom_sites_solution_hydrogens	geom
_refine_ls_hydrogen_treatment	CONSTR
_refine_ls_extinction_method	none
_refine_ls_extinction_coef	?

_refine_ls_abs_structure_details

'Flack H D (1983), Acta Cryst. A39, 876-881'

_refine_ls_abs_structure_Flack	-0.025(10)
_refine_ls_number_reflns	5169
_refine_ls_number_parameters	177
_refine_ls_number_restraints	0
_refine_ls_R_factor_all	0.0624
_refine_ls_R_factor_gt	0.0401

_refine_ls_wR_factor_ref 0.1012
_refine_ls_wR_factor_gt 0.0919
_refine_ls_goodness_of_fit_ref 1.053
_refine_ls_restrained_S_all 1.053
_refine_ls_shift/su_max 0.001
_refine_ls_shift/su_mean 0.000

_atom_site_label
_atom_site_type_symbol
_atom_site_fract_x
_atom_site_fract_y
_atom_site_fract_z
_atom_site_U_iso_or_equiv
_atom_site_adp_type
_atom_site_occupancy
_atom_site_symmetry_multiplicity
_atom_site_calc_flag
_atom_site_refinement_flags
_atom_site_disorder_assembly
_atom_site_disorder_group
Br1 Br -0.08420(3) -0.74198(3) 0.000713(13) 0.03718(8) Uani 1 1 d . . .
O1 O -0.11593(18) 0.00015(18) 0.26803(9) 0.0256(3) Uani 1 1 d . . .
H1A H -0.0430 -0.0377 0.2447 0.031 Uiso 1 1 calc R . .
O2 O -0.00327(17) -0.22570(18) 0.18106(8) 0.0228(3) Uani 1 1 d . . .
H2A H 0.0571 -0.2926 0.1964 0.027 Uiso 1 1 calc R . .
C1 C -0.6489(3) -0.1255(3) 0.26613(16) 0.0361(6) Uani 1 1 d . . .
H1B H -0.6514 -0.0700 0.2242 0.043 Uiso 1 1 calc R . .
H1C H -0.7331 -0.1908 0.2777 0.043 Uiso 1 1 calc R . .
C2 C -0.5293(3) -0.1119(3) 0.30807(13) 0.0286(5) Uani 1 1 d . . .
H2B H -0.5321 -0.1696 0.3494 0.034 Uiso 1 1 calc R . .
C3 C -0.3881(3) -0.0135(2) 0.29688(12) 0.0230(4) Uani 1 1 d . . .
H3A H -0.4155 0.0618 0.2604 0.028 Uiso 1 1 calc R . .
C4 C -0.3537(3) 0.0745(3) 0.36312(13) 0.0281(5) Uani 1 1 d . . .
H4A H -0.4463 0.1328 0.3764 0.042 Uiso 1 1 calc R . .
H4B H -0.2658 0.1434 0.3552 0.042 Uiso 1 1 calc R . .
H4C H -0.3269 0.0036 0.4001 0.042 Uiso 1 1 calc R . .
C5 C -0.2458(2) -0.1047(2) 0.27069(11) 0.0192(4) Uani 1 1 d . . .
C6 C -0.2048(3) -0.2322(3) 0.32101(11) 0.0250(4) Uani 1 1 d . . .
H6A H -0.1024 -0.2743 0.3090 0.038 Uiso 1 1 calc R . .
H6B H -0.2843 -0.3118 0.3180 0.038 Uiso 1 1 calc R . .
H6C H -0.2017 -0.1922 0.3681 0.038 Uiso 1 1 calc R . .
C7 C -0.2754(2) -0.1655(2) 0.19689(10) 0.0184(4) Uani 1 1 d . . .
H7A H -0.3808 -0.2144 0.1975 0.022 Uiso 1 1 calc R . .

C8 C -0.2800(3) -0.0450(2) 0.14016(12) 0.0240(4) Uani 1 1 d . . .
H8A H -0.3449 0.0414 0.1556 0.029 Uiso 1 1 calc R . .
H8B H -0.1729 -0.0073 0.1313 0.029 Uiso 1 1 calc R . .
C9 C -0.3477(3) -0.1106(3) 0.07426(12) 0.0262(5) Uani 1 1 d . . .
H9A H -0.4625 -0.1193 0.0794 0.031 Uiso 1 1 calc R . .
H9B H -0.3268 -0.0399 0.0357 0.031 Uiso 1 1 calc R . .
C10 C -0.2815(2) -0.2644(3) 0.05597(10) 0.0222(4) Uani 1 1 d . . .
C11 C -0.3161(3) -0.3309(3) -0.00746(12) 0.0276(5) Uani 1 1 d . . .
H11A H -0.3789 -0.2774 -0.0396 0.033 Uiso 1 1 calc R . .
C12 C -0.2612(3) -0.4724(3) -0.02460(12) 0.0292(5) Uani 1 1 d . . .
H12A H -0.2869 -0.5169 -0.0678 0.035 Uiso 1 1 calc R . .
C13 C -0.1676(3) -0.5487(3) 0.02251(12) 0.0252(4) Uani 1 1 d . . .
C14 C -0.1331(3) -0.4869(3) 0.08570(11) 0.0217(4) Uani 1 1 d . . .
H14A H -0.0699 -0.5410 0.1176 0.026 Uiso 1 1 calc R . .
C15 C -0.1911(2) -0.3438(3) 0.10313(11) 0.0194(4) Uani 1 1 d . . .
C16 C -0.1596(2) -0.2866(2) 0.17521(10) 0.0179(4) Uani 1 1 d . . .
H16A H -0.1693 -0.3735 0.2079 0.021 Uiso 1 1 calc R . .

_atom_site_aniso_label
_atom_site_aniso_U_11
_atom_site_aniso_U_22
_atom_site_aniso_U_33
_atom_site_aniso_U_23
_atom_site_aniso_U_13
_atom_site_aniso_U_12
Br1 0.04343(15) 0.03449(13) 0.03363(13) -0.01411(12) -0.00080(11) 0.00400(11)
O1 0.0200(8) 0.0270(8) 0.0298(8) -0.0056(6) -0.0002(6) -0.0058(6)
O2 0.0142(6) 0.0270(8) 0.0271(7) -0.0007(6) -0.0026(6) 0.0003(6)
C1 0.0240(12) 0.0335(13) 0.0508(16) -0.0099(12) -0.0003(12) 0.0032(10)
C2 0.0244(11) 0.0280(11) 0.0333(13) -0.0052(9) 0.0049(9) 0.0011(9)
C3 0.0208(11) 0.0211(10) 0.0270(11) -0.0036(8) 0.0003(8) 0.0024(8)
C4 0.0268(12) 0.0288(11) 0.0287(12) -0.0076(9) 0.0033(10) 0.0003(10)
C5 0.0162(10) 0.0184(9) 0.0230(10) -0.0016(7) -0.0009(8) -0.0019(7)
C6 0.0299(11) 0.0249(11) 0.0202(9) -0.0005(8) -0.0035(8) 0.0044(9)
C7 0.0162(9) 0.0199(9) 0.0192(9) 0.0008(7) -0.0010(8) -0.0001(8)
C8 0.0264(11) 0.0210(10) 0.0246(10) 0.0017(8) -0.0017(9) 0.0023(9)
C9 0.0269(12) 0.0284(11) 0.0233(10) 0.0060(9) -0.0050(9) 0.0029(9)
C10 0.0180(9) 0.0297(11) 0.0190(9) 0.0049(8) 0.0005(7) -0.0017(9)
C11 0.0243(11) 0.0389(12) 0.0195(11) 0.0048(9) -0.0032(9) -0.0024(8)
C12 0.0293(12) 0.0408(13) 0.0176(9) -0.0040(9) 0.0008(9) -0.0079(11)
C13 0.0230(10) 0.0289(11) 0.0236(10) -0.0063(8) 0.0048(8) -0.0038(9)
C14 0.0198(10) 0.0240(10) 0.0213(10) -0.0010(8) 0.0002(8) 0.0000(8)
C15 0.0145(9) 0.0247(10) 0.0189(9) 0.0010(8) -0.0005(7) -0.0025(7)

C16 0.0169(9) 0.0185(9) 0.0183(9) 0.0001(7) -0.0015(8) -0.0007(7)

_geom_special_details
All esds (except the esd in the dihedral angle between two l.s. planes) are estimated using the full covariance matrix. The cell esds are taken into account individually in the estimation of esds in distances, angles and torsion angles; correlations between esds in cell parameters are only used when they are defined by crystal symmetry. An approximate (isotropic) treatment of cell esds is used for estimating esds involving l.s. planes.

_geom_bond_atom_site_label_1
_geom_bond_atom_site_label_2
_geom_bond_distance
_geom_bond_site_symmetry_2
_geom_bond_publ_flag
Br1 C13 1.900(2) . ?
O1 C5 1.448(2) . ?
O2 C16 1.446(2) . ?
C1 C2 1.312(4) . ?
C2 C3 1.504(3) . ?
C3 C4 1.530(3) . ?
C3 C5 1.546(3) . ?
C5 C6 1.532(3) . ?
C5 C7 1.549(3) . ?
C7 C16 1.518(3) . ?
C7 C8 1.532(3) . ?
C8 C9 1.517(3) . ?
C9 C10 1.516(3) . ?
C10 C15 1.388(3) . ?
C10 C11 1.395(3) . ?
C11 C12 1.377(3) . ?
C12 C13 1.390(4) . ?
C13 C14 1.373(3) . ?
C14 C15 1.401(3) . ?
C15 C16 1.510(3) . ?

_geom_angle_atom_site_label_1
_geom_angle_atom_site_label_2
_geom_angle_atom_site_label_3
_geom_angle
_geom_angle_site_symmetry_1
_geom_angle_site_symmetry_3
_geom_angle_publ_flag
C1 C2 C3 126.1(3) . . ?

C2 C3 C4 109.1(2) . . ?
C2 C3 C5 112.21(17) . . ?
C4 C3 C5 112.92(19) . . ?
O1 C5 C6 108.63(17) . . ?
O1 C5 C3 106.36(16) . . ?
C6 C5 C3 110.80(18) . . ?
O1 C5 C7 108.37(17) . . ?
C6 C5 C7 111.64(17) . . ?
C3 C5 C7 110.84(18) . . ?
C16 C7 C8 108.05(17) . . ?
C16 C7 C5 113.22(17) . . ?
C8 C7 C5 115.12(17) . . ?
C9 C8 C7 110.33(18) . . ?
C10 C9 C8 113.43(18) . . ?
C15 C10 C11 119.0(2) . . ?
C15 C10 C9 120.57(19) . . ?
C11 C10 C9 120.4(2) . . ?
C12 C11 C10 121.6(2) . . ?
C11 C12 C13 118.6(2) . . ?
C14 C13 C12 121.1(2) . . ?
C14 C13 Br1 118.44(18) . . ?
C12 C13 Br1 120.50(18) . . ?
C13 C14 C15 119.9(2) . . ?
C10 C15 C14 119.7(2) . . ?
C10 C15 C16 122.6(2) . . ?
C14 C15 C16 117.58(19) . . ?
O2 C16 C15 111.25(16) . . ?
O2 C16 C7 108.59(16) . . ?
C15 C16 C7 112.10(17) . . ?

_geom_hbond_atom_site_label_D
_geom_hbond_atom_site_label_H
_geom_hbond_atom_site_label_A
_geom_hbond_distance_DH
_geom_hbond_distance_HA
_geom_hbond_distance_DA
_geom_hbond_angle_DHA
_geom_hbond_site_symmetry_A
O1 H1A O2 0.84 2.10 2.786(2) 138.8 .
O2 H2A O1 0.84 2.02 2.810(2) 155.9 3_545

_diffrn_measured_fraction_theta_max 0.975
_diffrn_reflns_theta_full 32.68

_diffrn_measured_fraction_theta_full	0.975
_refine_diff_density_max	0.743
_refine_diff_density_min	-0.432
_refine_diff_density_rms	0.082

Determination of regiochemistry in compounds 14-19:

The regioselectivity was assigned by observing relevant correlations in the HMBC spectra for compounds **14-19** (see below).

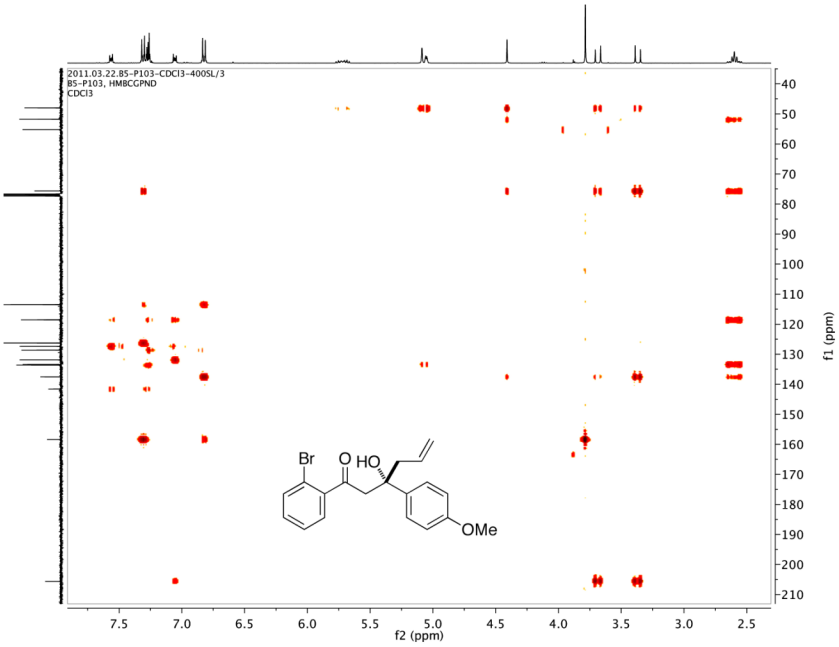

Supplementary Figure 6 | HMBC spectrum of compound **14**.

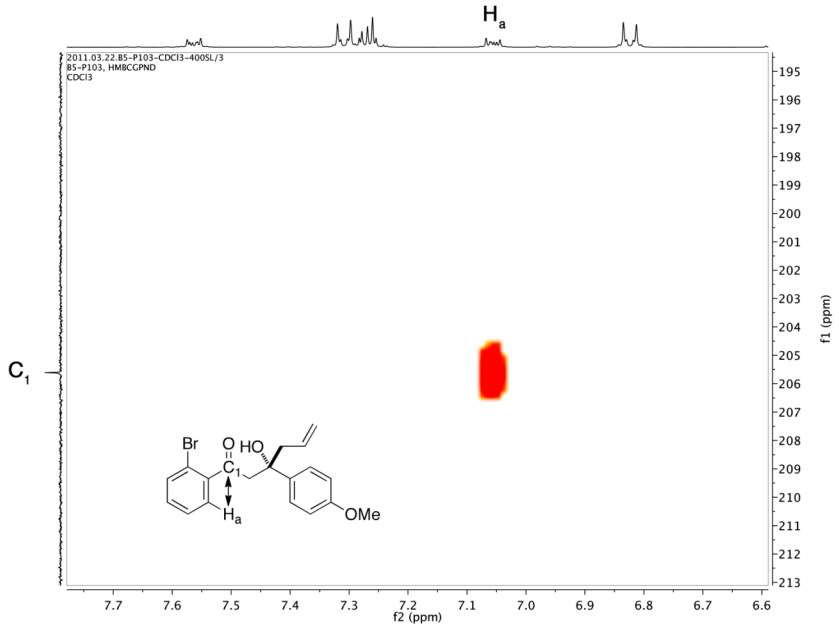

Supplementary Figure 7 | Expanded HMBC spectrum for compound **14** showing the $H_a \leftrightarrow C_1$ correlation. (H_a is believed to be shifted upfield due to the same reason we observe regioselectivity; steric inhibition of resonance (SIR) causing the aryl ring to twist out of planarity).

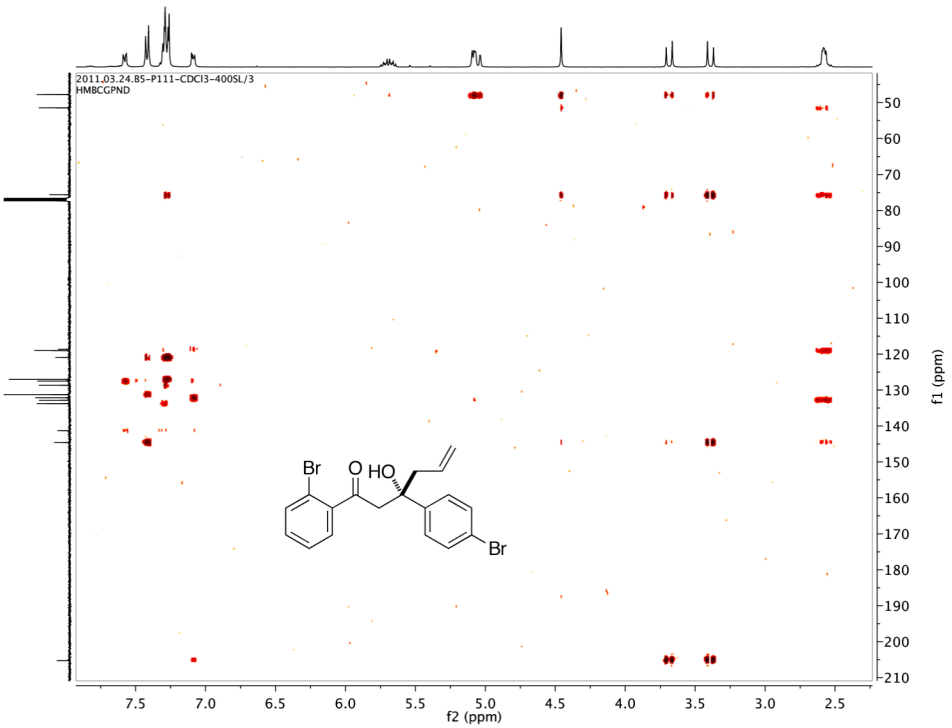

Supplementary Figure 8 | HMBC spectrum of compound **15**.

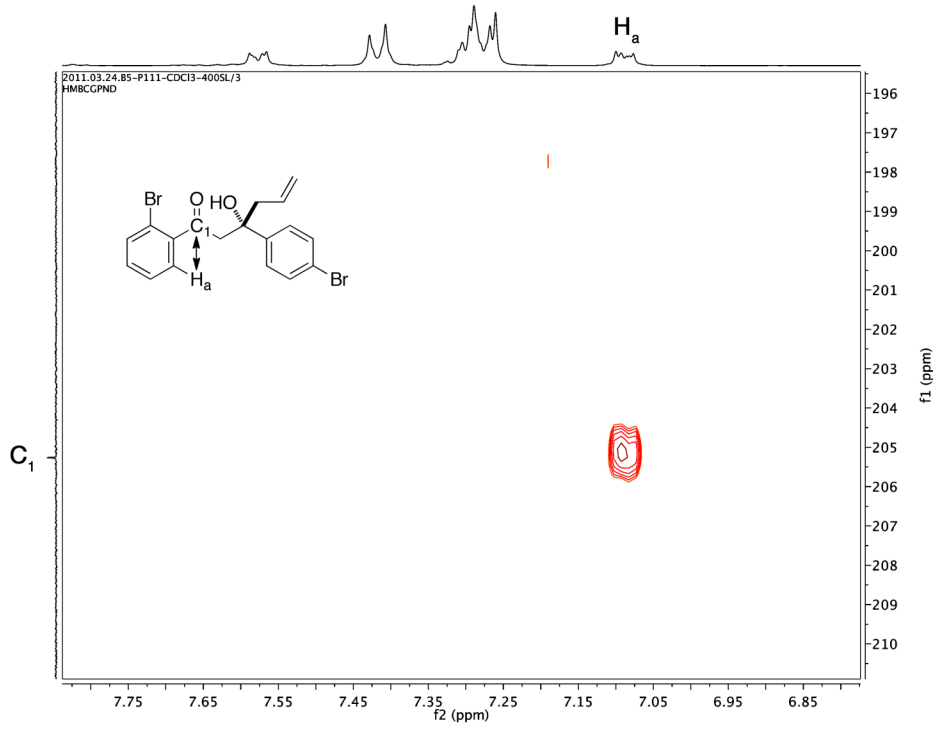

Supplementary Figure 9 | Expanded HMBC spectrum for compound **15** showing the $H_a \leftrightarrow C_1$ correlation.

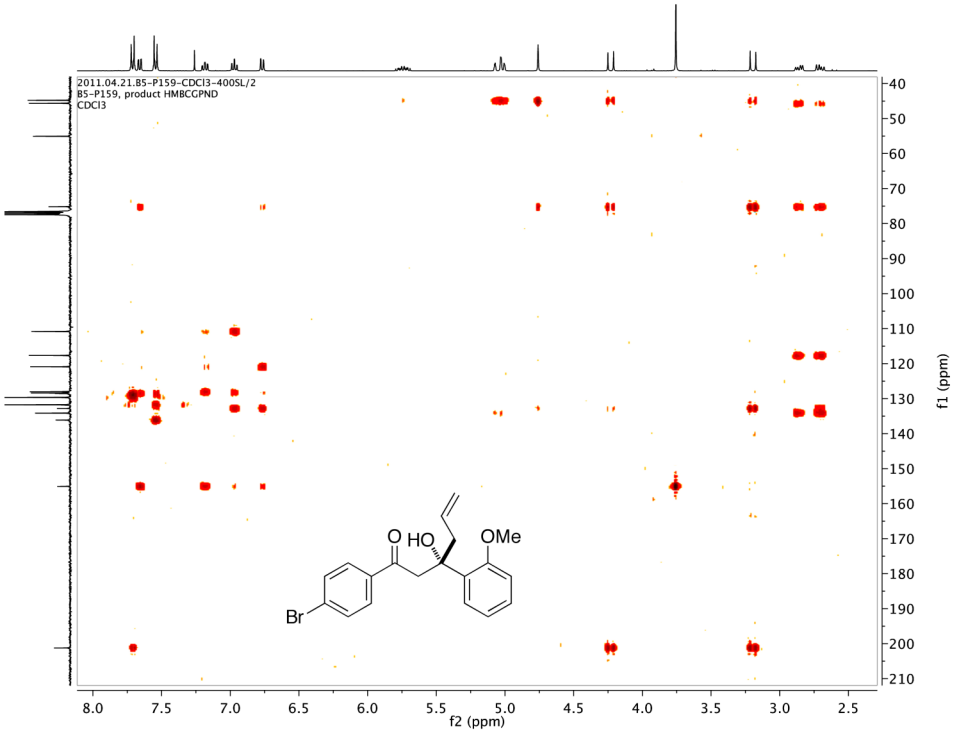

Supplementary Figure 10 | HMBC spectrum of compound **16a**.

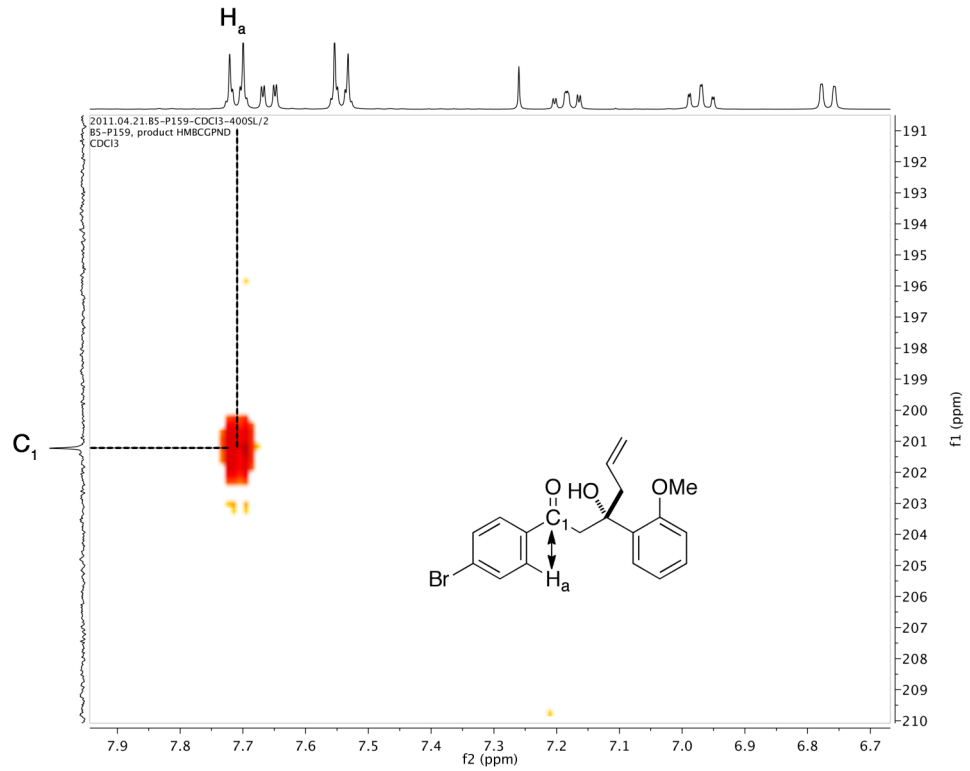

Supplementary Figure 11 | Expanded HMBC spectrum for compound **16a** showing the $H_a \leftrightarrow C_1$ correlation.

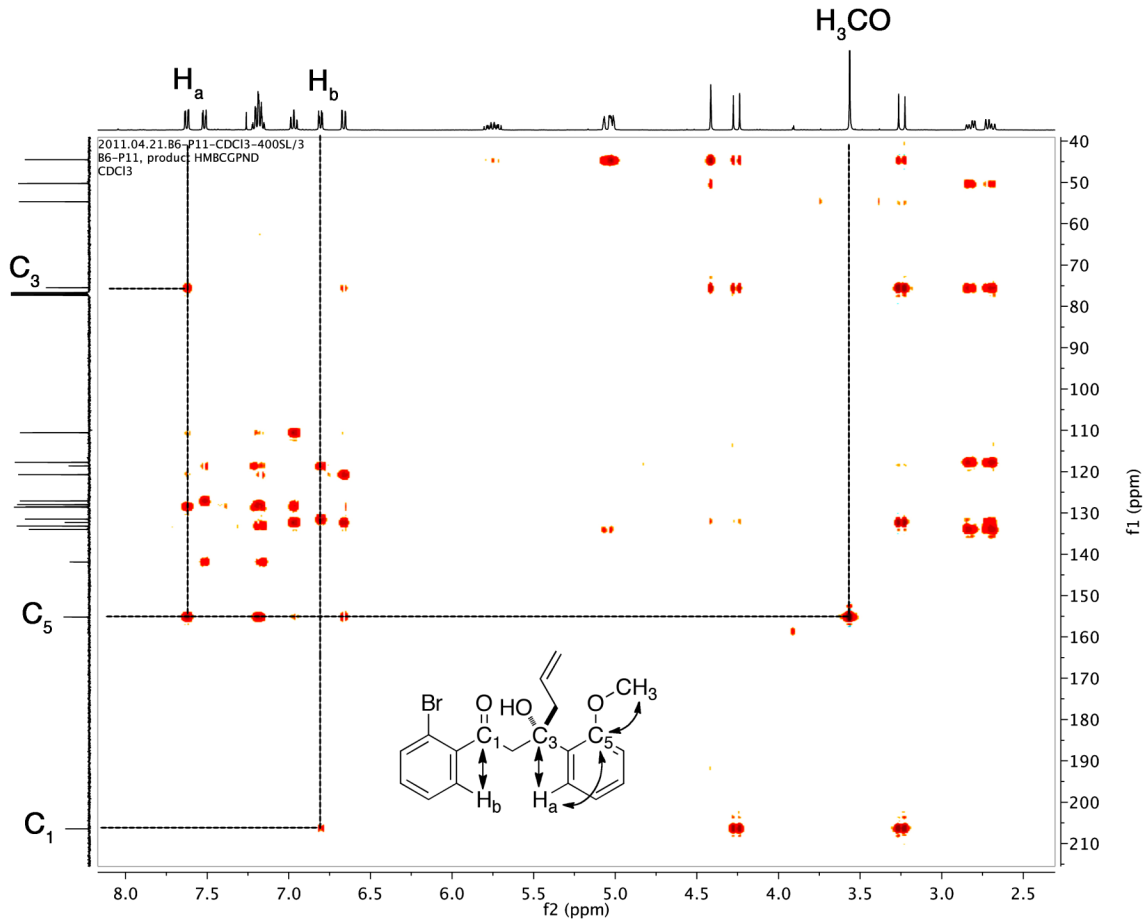

Supplementary Figure 12 | HMBC spectrum of compound **17**. Using the methyl group as an entry point for solving the regiochemistry of allylation we see that there is a $CH_3 \leftrightarrow C_5$ correlation, which in turn leads us to the $C_5 \leftrightarrow H_a$ correlation. Now that we have assigned H_a we can see that there is a $H_a \leftrightarrow C_3$ correlation, confirming the regiochemistry shown (dotted lines added as a guide to the eye to point out relevant correlations in assigning the structure).

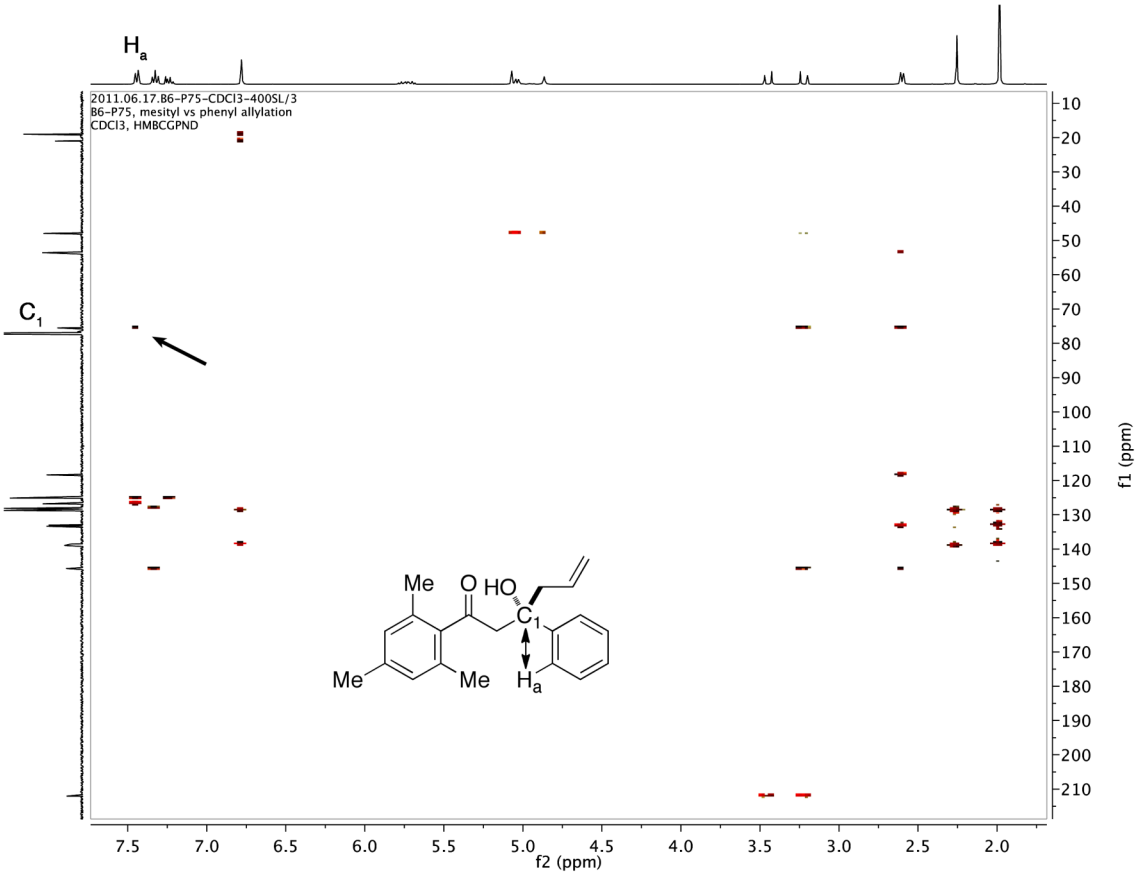

Supplementary Figure 13 | HMBC spectrum of compound **18** showing the $H_a \leftrightarrow C_1$ correlation (arrow).

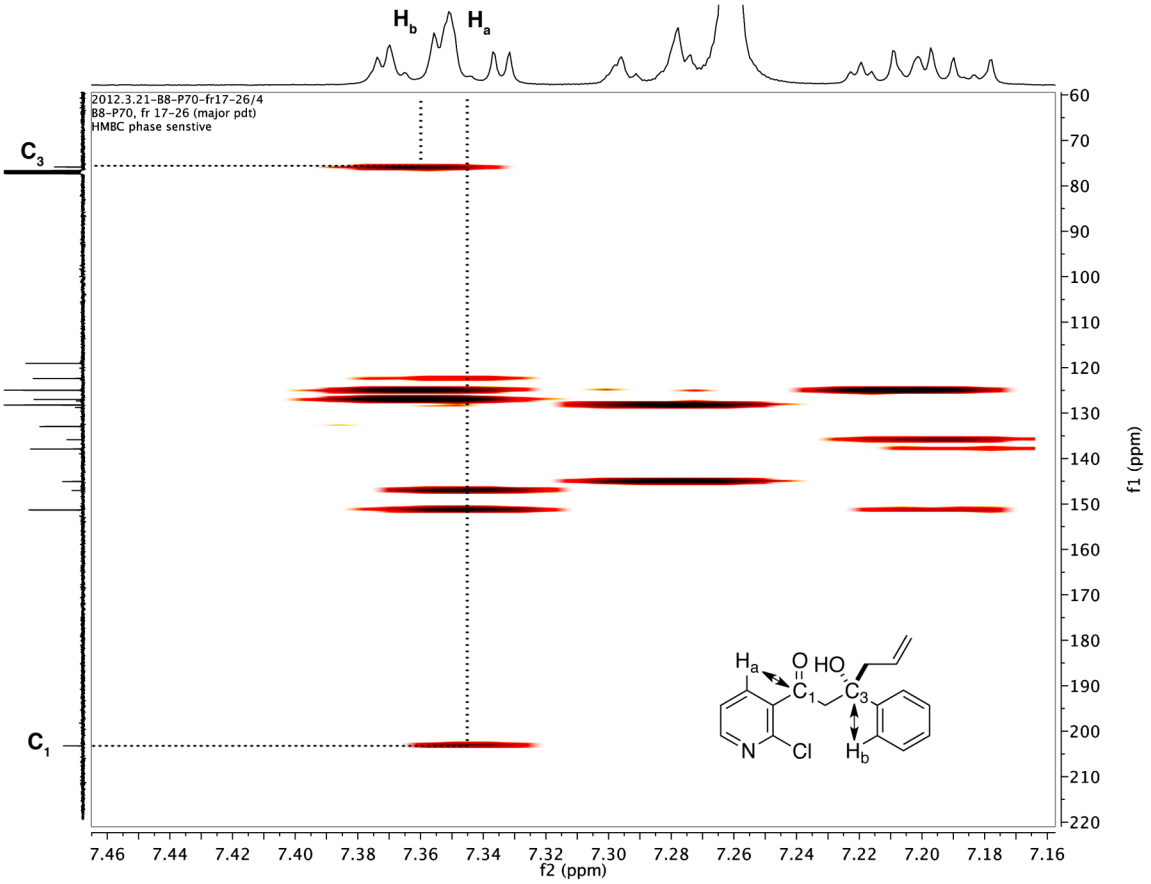

Supplementary Figure 14 | HMBC spectrum of compound **19**. One can see that there is ambiguity in the assignment of regiochemistry due to the similar chemical shifts of H_a and H_b. Although we can make a regiochemical assignment with confidence based on peak shape and the slight chemical shift difference, we can make a more convincing argument by looking at chemical shifts of H_b as well as HMBC correlations for the minor regioisomer of **19** (see Supplementary Figure 13).

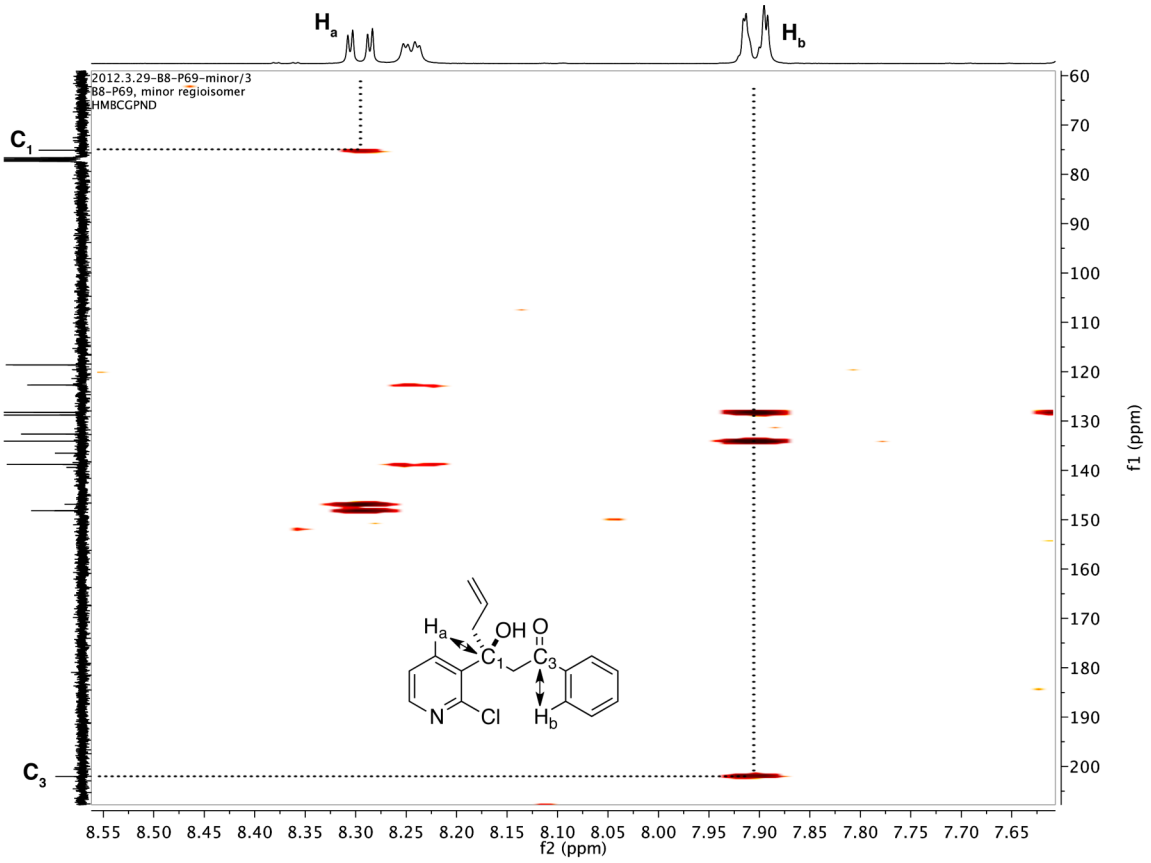

Supplementary Figure 15 | HMBC spectrum of the minor regioisomer from the allylation reaction to form compound **19**. One can clearly see the $H_a \leftrightarrow C_1$ correlation (H_a integration = 1) and the $H_b \leftrightarrow C_3$ correlation (H_b integration = 2). Since the regiochemical assignment of compound **19** is ambiguous, the clear assignment of the minor regioisomer shown above removes any doubt of the regioselectivity and major isomer formed in this reaction.

Determination of enantioselectivities:

NOTE: Racemic samples of the allylated products were either prepared following the procedure developed by Bartoli et al.[34] or using racemic allylsilane **3**, prepared by mixing equimolar amounts of allylsilane reagent (*S*,*S*)-**3** and (*R*,*R*)-**3**. Racemic samples of crotylated products were prepared by carrying out the crotylation reactions with racemic *cis*-**20** or *trans*-**21**, prepared by mixing equimolar amounts of the (*S*,*S*)- and (*R*,*R*)-crotylsilanes **20** or **21**. Slight deviations from 50:50 in the racemic GC or HPLC traces may therefore be attributed to the error inherent in this procedure.

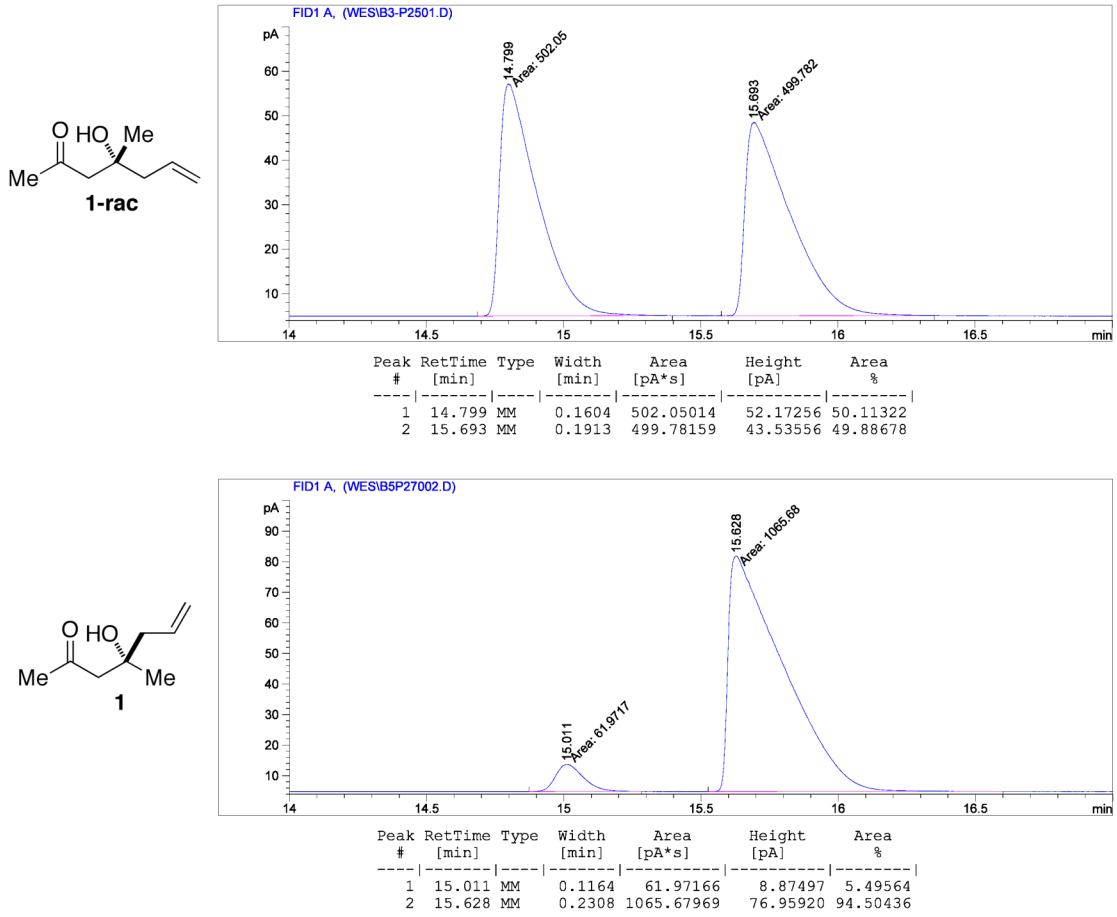

Supplementary Figure 16 | GC trace of **1** (β-dex 325, 1 mL/min, 90 °C isothermal).

[34] Bartoli, G.; Marcantoni, E.; Petrini, M. *Angew. Chem. Int. Ed. Engl.* **1993**, *32*, 1061.

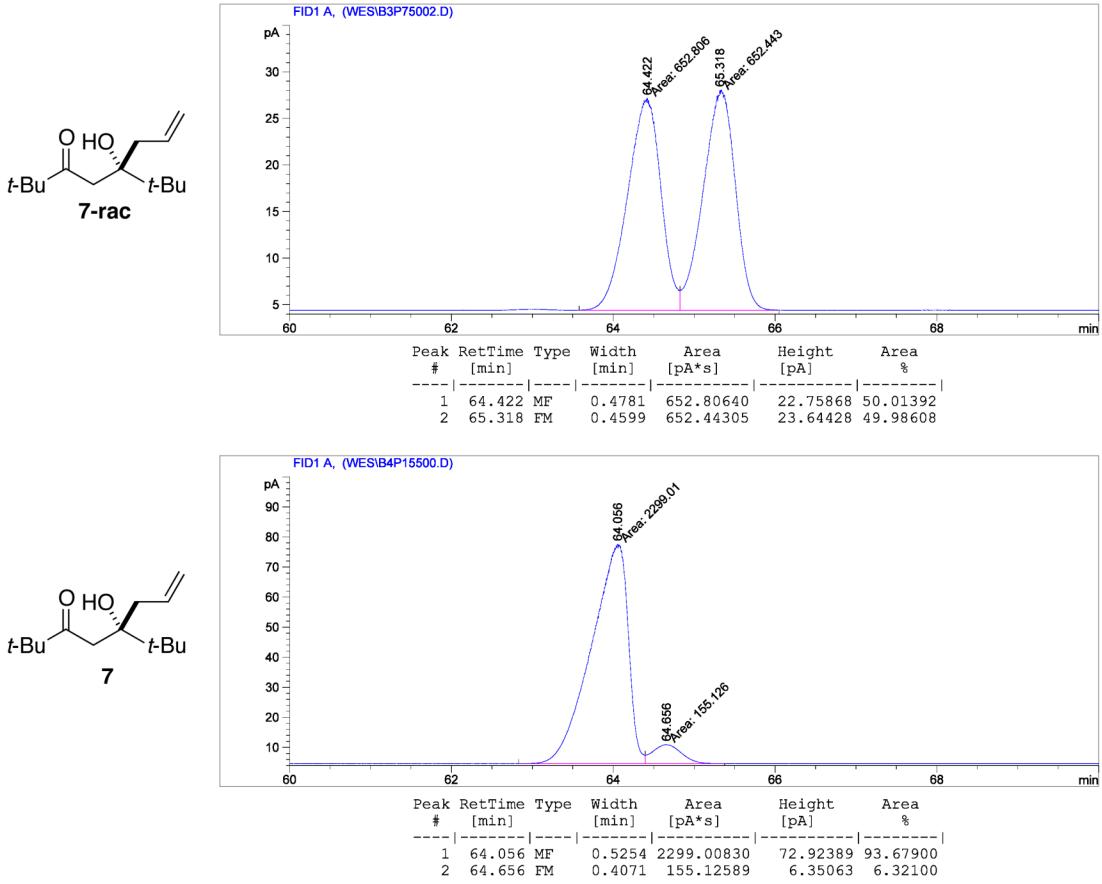

Peak #	RetTime [min]	Type	Width [min]	Area [pA*s]	Height [pA]	Area %
1	64.422	MF	0.4781	652.80640	22.75868	50.01392
2	65.318	FM	0.4599	652.44305	23.64428	49.98608

Peak #	RetTime [min]	Type	Width [min]	Area [pA*s]	Height [pA]	Area %
1	64.056	MF	0.5254	2299.00830	72.92389	93.67900
2	64.656	FM	0.4071	155.12589	6.35063	6.32100

Supplementary Figure 17 | GC trace of **7** (β-dex 325, 1 mL/min, 100 °C isothermal).

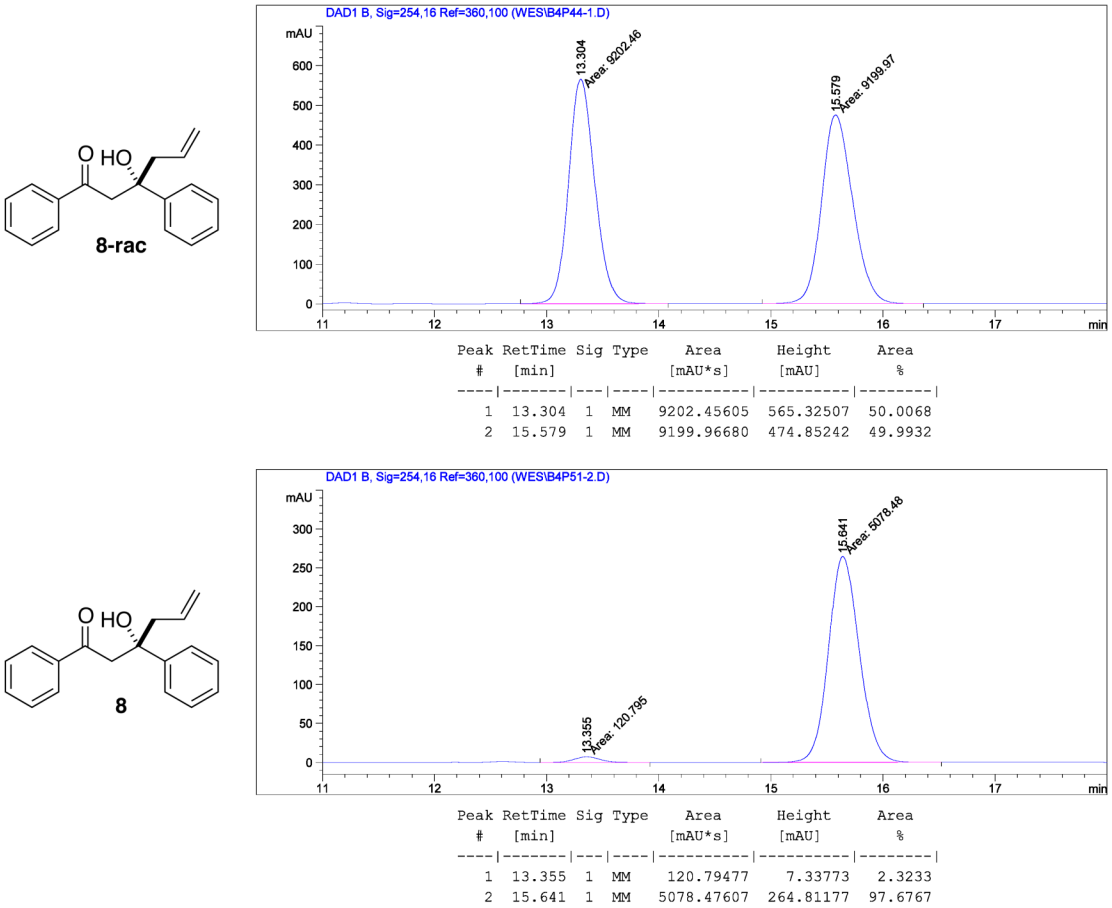

Supplementary Figure 18 | HPLC trace of **8** (Chiralpak AD-H, Hexanes:*i*-PrOH = 97:3, 1 mL/min, 254 nm).

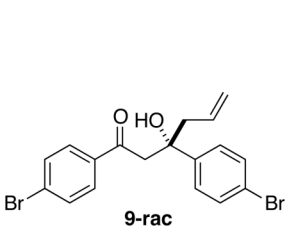

9-rac

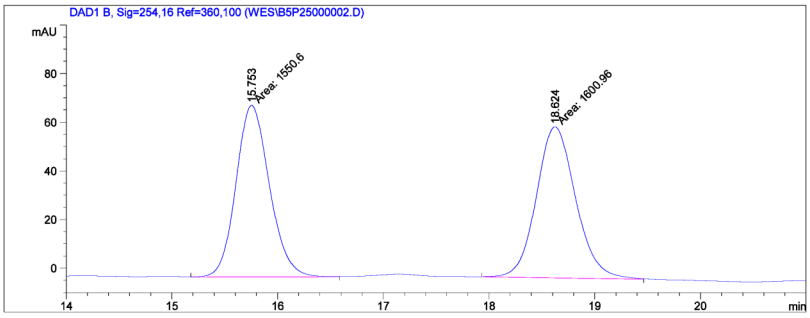

Peak #	RetTime [min]	Sig	Type	Area [mAU*s]	Height [mAU]	Area %
1	15.753	1	MM	1550.60010	70.54240	49.2011
2	18.624	1	MM	1600.95508	62.12122	50.7989

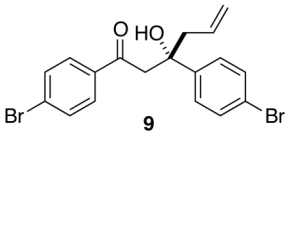

9

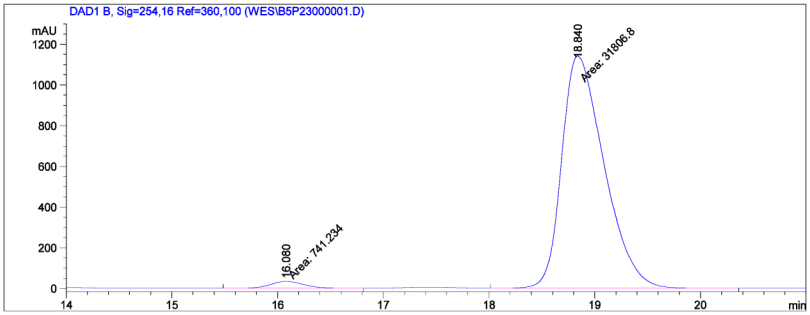

Peak #	RetTime [min]	Sig	Type	Area [mAU*s]	Height [mAU]	Area %
1	16.080	1	MM	741.23419	33.81213	2.2774
2	18.840	1	MM	3.18068e4	1141.39819	97.7226

Supplementary Figure 19 | HPLC trace of **9** (Chiralpak AD-H, Hexanes:*i*-PrOH = 96:4, 1 mL/min, 254 nm).

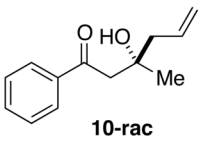

10-rac

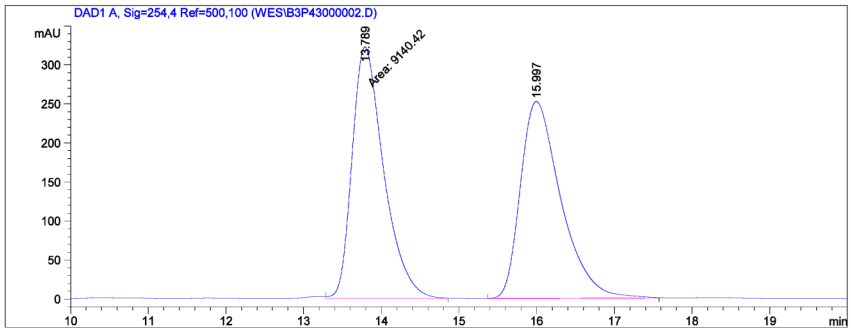

Peak #	RetTime [min]	Sig	Type	Area [mAU*s]	Height [mAU]	Area %
1	13.789	1	FM	9140.42285	322.36642	50.0088
2	15.997	1	BB	9137.22363	252.45828	49.9912

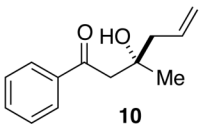

10

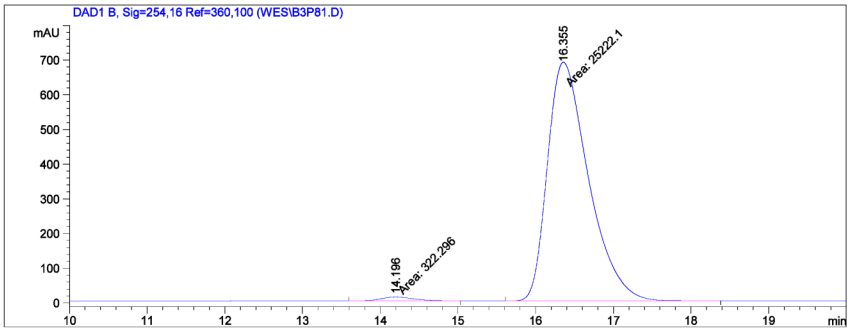

Peak #	RetTime [min]	Sig	Type	Area [mAU*s]	Height [mAU]	Area %
1	14.196	1	MM	322.29633	11.18189	1.2617
2	16.355	1	MM	2.52221e4	688.07141	98.7383

Supplementary Figure 20 | HPLC trace of **10** (Chiralcel OD, Hexanes:*i*-PrOH = 98:2, 1 mL/min, 254 nm).

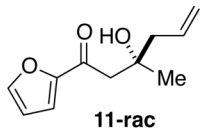

11-rac

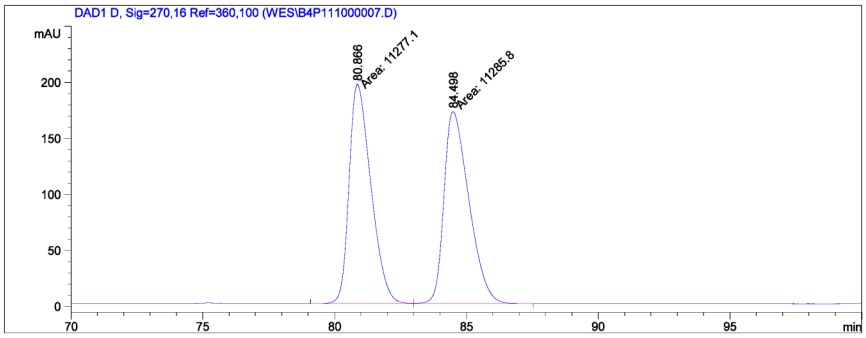

Peak #	RetTime [min]	Sig	Type	Area [mAU*s]	Height [mAU]	Area %
1	80.866	1	MF	1.12771e4	195.47859	49.9806
2	84.498	1	FM	1.12858e4	171.31721	50.0194

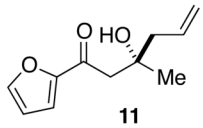

11

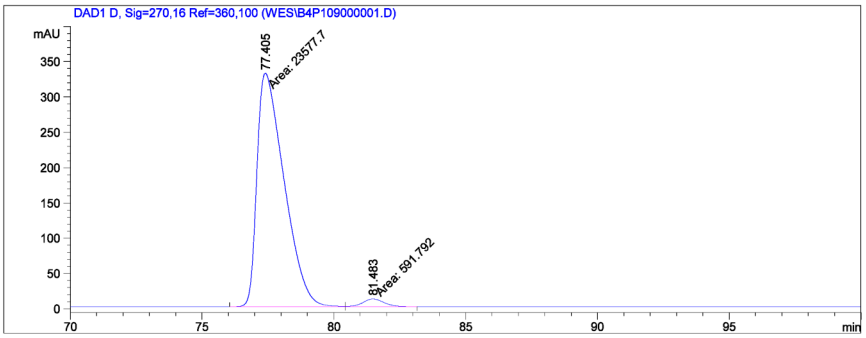

Peak #	RetTime [min]	Sig	Type	Area [mAU*s]	Height [mAU]	Area %
1	77.405	1	MF	2.35777e4	330.40732	97.5515
2	81.483	1	FM	591.79242	10.76878	2.4485

Supplementary Figure 21 | HPLC trace of **11** (Chiralpak AD-H, Hexanes:*i*-PrOH = 99:1 for 30 min then ramp to 98:2 over 30 min and hold, 1 mL/min, 270 nm).

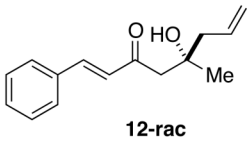

12-rac

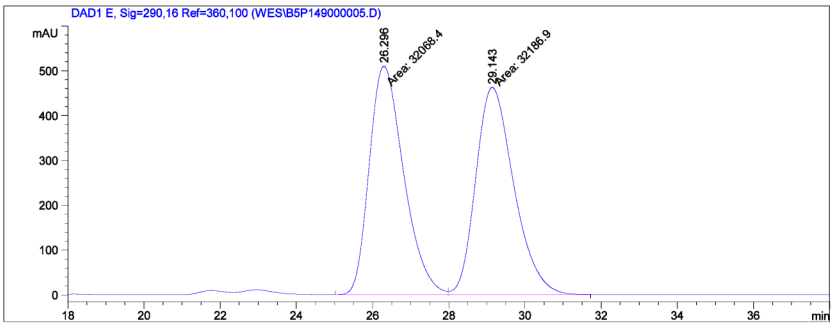

Peak #	RetTime [min]	Sig	Type	Area [mAU*s]	Height [mAU]	Area %
1	26.296	1	MF	3.20684e4	509.92322	49.9078
2	29.143	1	FM	3.21869e4	462.48792	50.0922

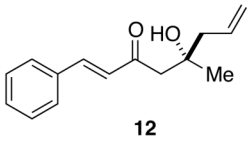

12

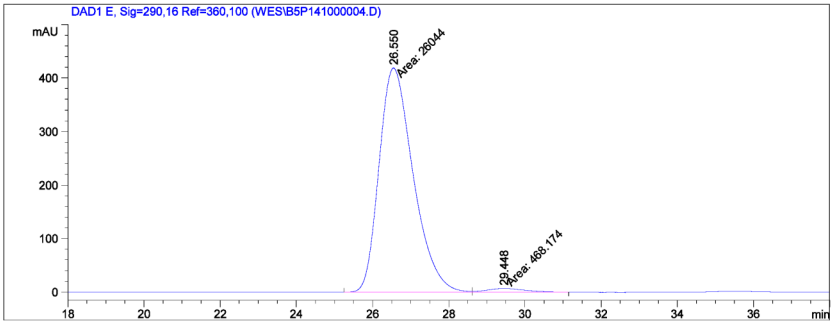

Peak #	RetTime [min]	Sig	Type	Area [mAU*s]	Height [mAU]	Area %
1	26.550	1	MF	2.60440e4	418.60898	98.2341
2	29.448	1	FM	468.17416	6.78201	1.7659

Supplementary Figure 22 | HPLC trace of **12** (Chiralcel OD, Hexanes:*i*-PrOH = 97:3, 1 mL/min, 290 nm).

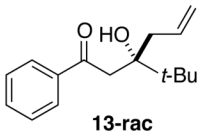

13-rac

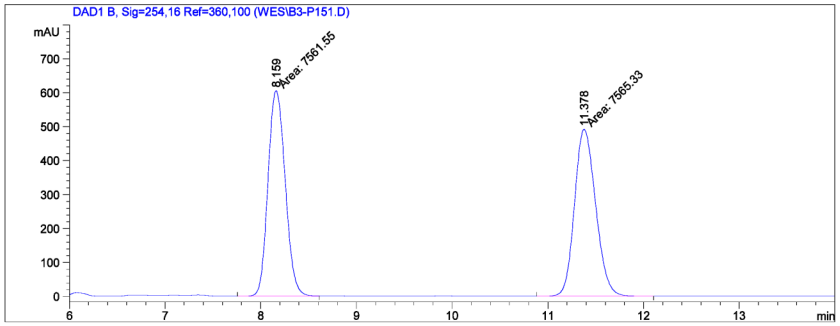

Peak #	RetTime [min]	Sig	Type	Area [mAU*s]	Height [mAU]	Area %
1	8.159	1	MM	7561.55078	604.46008	49.9875
2	11.378	1	MM	7565.33350	491.39420	50.0125

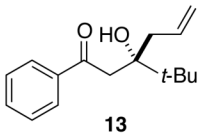

13

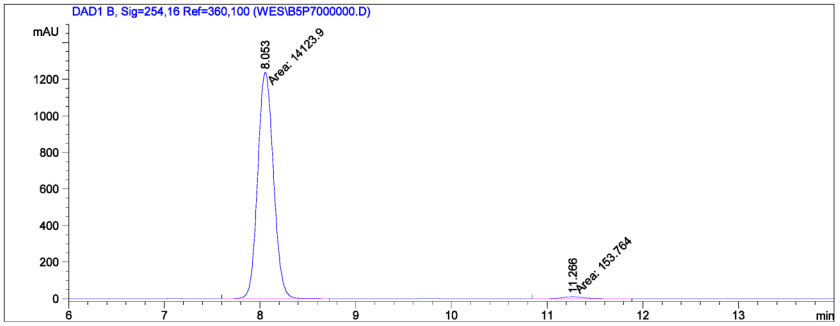

Peak #	RetTime [min]	Sig	Type	Area [mAU*s]	Height [mAU]	Area %
1	8.053	1	MF	1.41239e4	1236.87988	98.9230
2	11.266	1	MM	153.76422	10.31383	1.0770

Supplementary Figure 23 | HPLC trace of **13** (Chiralpak AD-H, Hexanes:*i*-PrOH = 98:2, 1 mL/min, 254 nm).

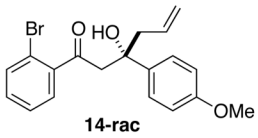

14-rac

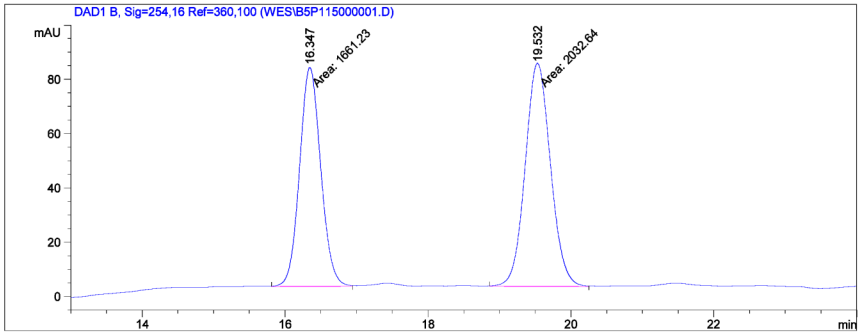

Peak #	RetTime [min]	Sig	Type	Area [mAU*s]	Height [mAU]	Area %
1	16.347	1	MM	1661.22888	80.70562	44.9726
2	19.532	1	MM	2032.63806	82.36096	55.0274

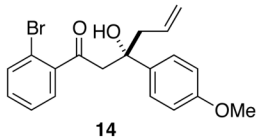

14

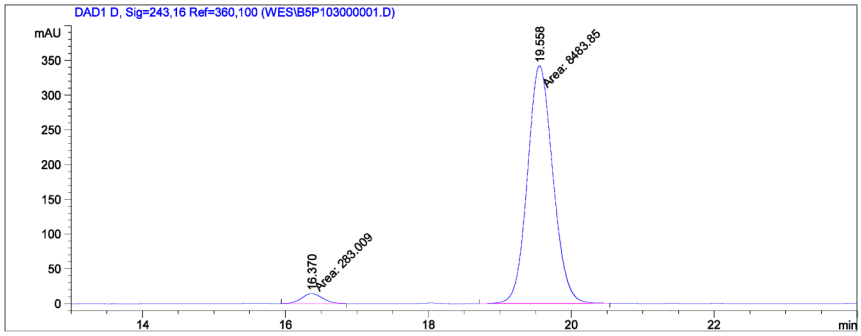

Peak #	RetTime [min]	Sig	Type	Area [mAU*s]	Height [mAU]	Area %
1	16.370	1	MM	283.00891	14.13829	3.2282
2	19.558	1	MM	8483.85449	342.52344	96.7718

Supplementary Figure 24 | HPLC trace of **14** (Chiralpak AD-H, Hexanes:*i*-PrOH = 96:4, 1 mL/min, 243 nm).

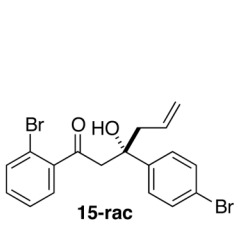

15-rac

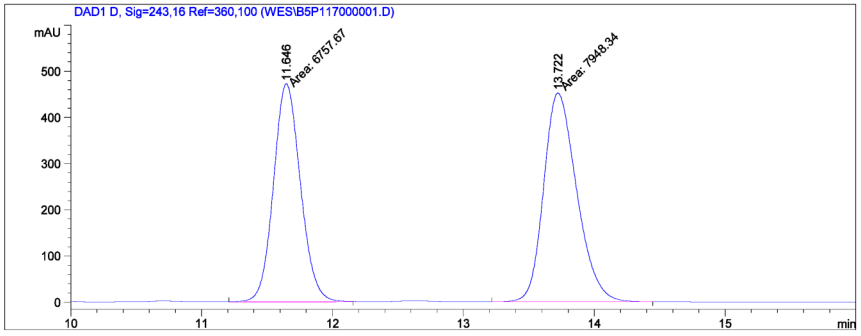

Peak #	RetTime [min]	Sig	Type	Area [mAU*s]	Height [mAU]	Area %
1	11.646	1	MM	6757.67041	471.98892	45.9518
2	13.722	1	MM	7948.33887	451.87305	54.0482

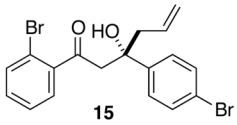

15

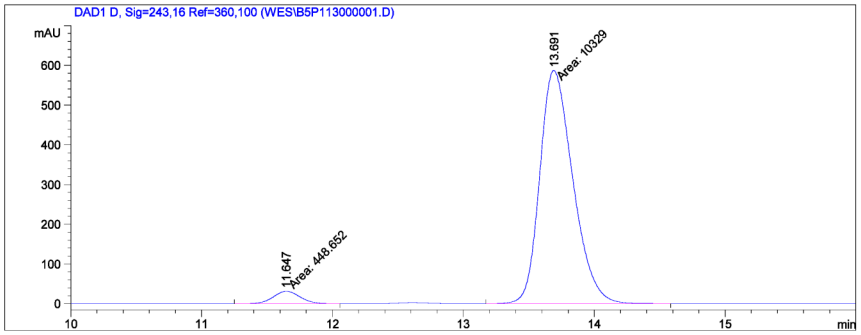

Peak #	RetTime [min]	Sig	Type	Area [mAU*s]	Height [mAU]	Area %
1	11.647	1	MM	448.65201	31.37775	4.1628
2	13.691	1	MM	1.03290e4	587.09650	95.8372

Supplementary Figure 25 | HPLC trace of **15** (Chiralpak AD-H, Hexanes:*i*-PrOH = 96:4, 1 mL/min, 243 nm).

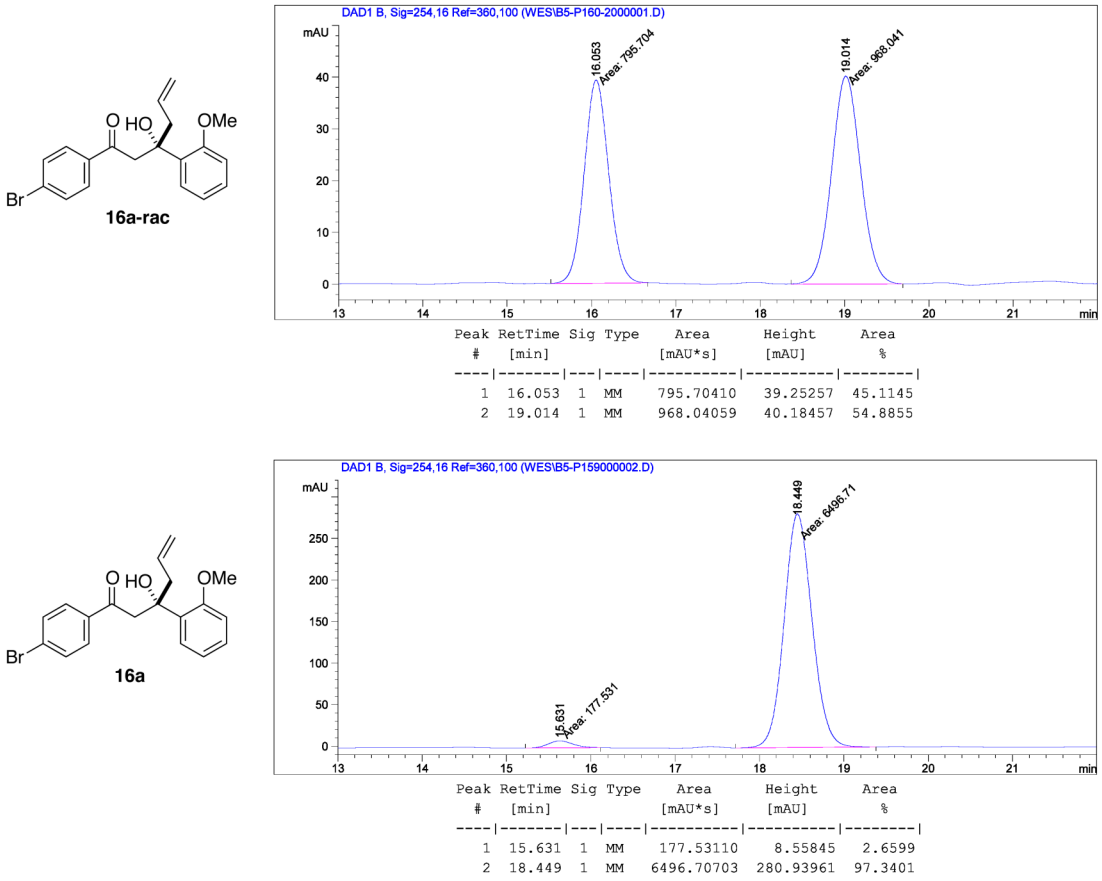

Supplementary Figure 26 | HPLC trace of **16a** (Chiralpak AD-H, Hexanes:*i*-PrOH = 96:4, 1 mL/min, 254 nm).

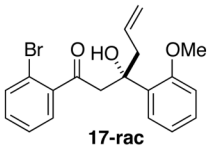

17-rac

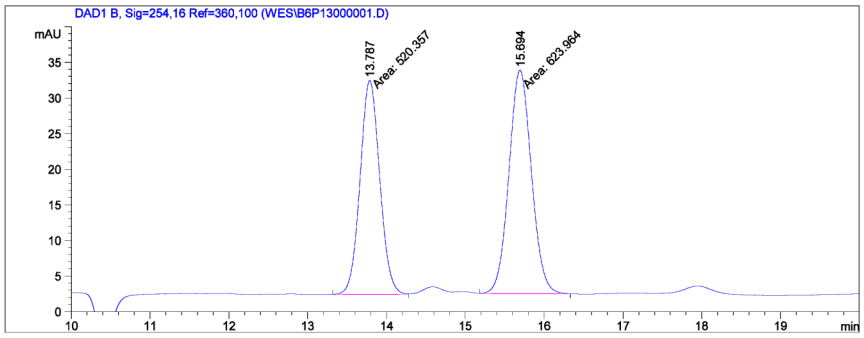

Peak #	RetTime [min]	Sig	Type	Area [mAU*s]	Height [mAU]	Area %
1	13.787	1	MM	520.35748	30.02085	45.4730
2	15.694	1	MM	623.96368	31.37293	54.5270

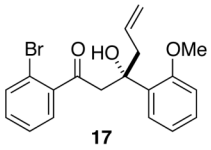

17

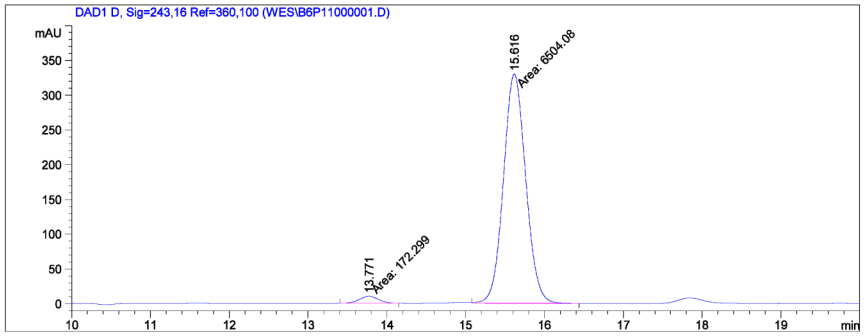

Peak #	RetTime [min]	Sig	Type	Area [mAU*s]	Height [mAU]	Area %
1	13.771	1	MM	172.29938	10.11165	2.5807
2	15.616	1	FM	6504.07861	329.91415	97.4193

Supplementary Figure 27 | HPLC trace of **17** (Chiralpak AD-H, Hexanes:*i*-PrOH = 96:4, 1 mL/min, 243 nm).

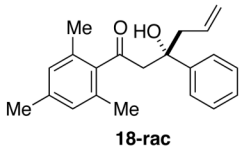

18-rac

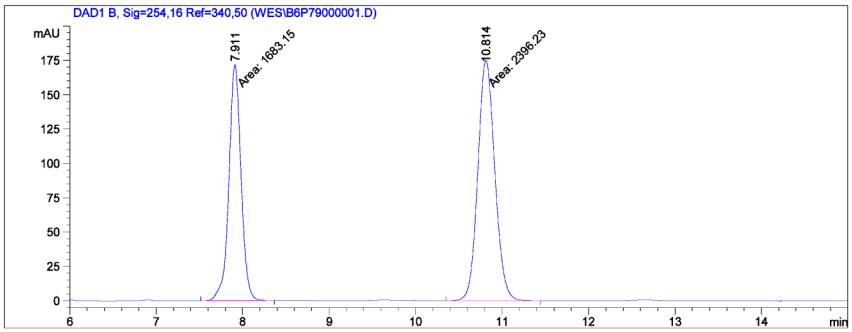

Peak #	RetTime [min]	Sig	Type	Area [mAU*s]	Height [mAU]	Area %
1	7.911	1	MM	1683.14990	171.94693	41.2600
2	10.814	1	MM	2396.22607	174.98244	58.7400

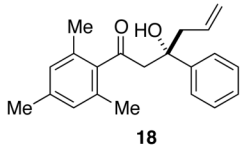

18

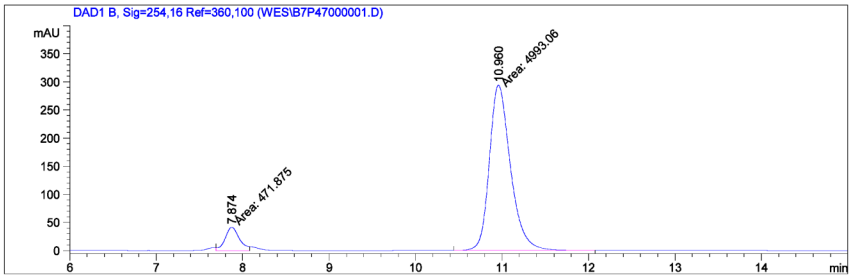

Peak #	RetTime [min]	Sig	Type	Area [mAU*s]	Height [mAU]	Area %
1	7.874	1	MF	471.87524	41.25963	8.6346
2	10.960	1	MM	4993.05908	293.93866	91.3654

Supplementary Figure 28 | HPLC trace of **18** (Chiralpak AD-H, Hexanes:*i*-PrOH = 98:2, 1 mL/min, 254 nm).

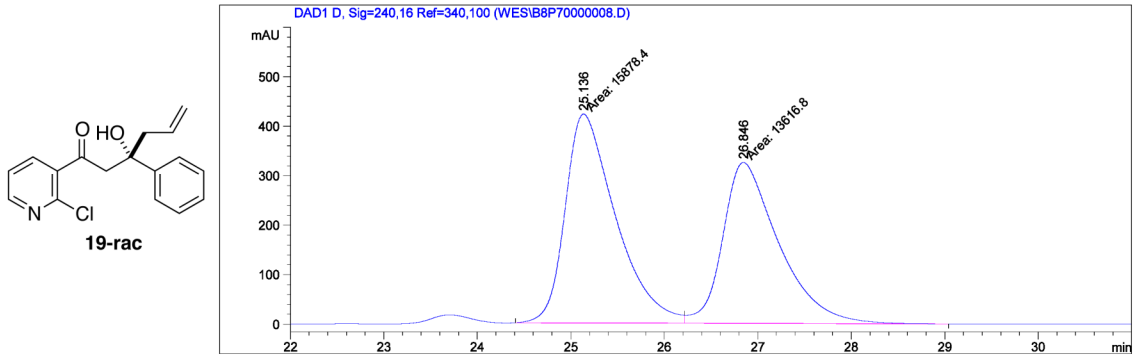

19-rac

Peak #	RetTime [min]	Sig	Type	Area [mAU*s]	Height [mAU]	Area %
1	25.136	1	MF	1.58784e4	422.21741	53.8338
2	26.846	1	FM	1.36168e4	325.34372	46.1662

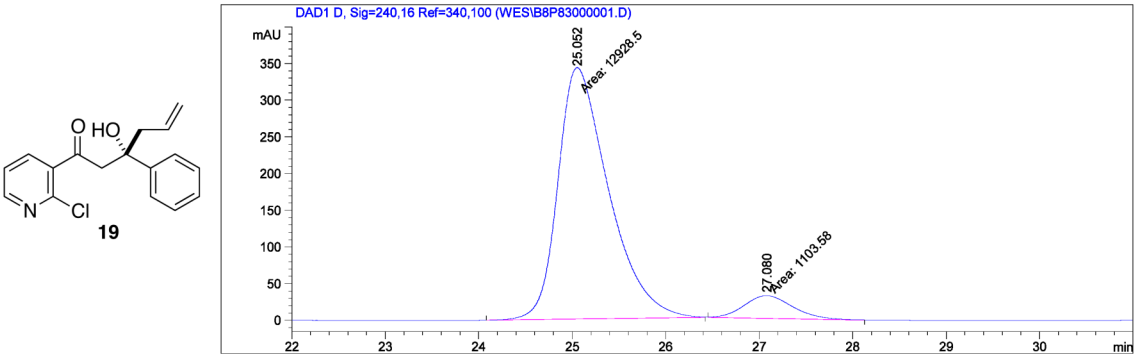

19

Peak #	RetTime [min]	Sig	Type	Area [mAU*s]	Height [mAU]	Area %
1	25.052	1	MM	1.29285e4	342.74216	92.1353
2	27.080	1	MM	1103.58301	30.82989	7.8647

Supplementary Figure 29 | HPLC trace of **19** (Chiralpak AD-H, Hexanes:EtOH = 96:4, 1 mL/min, 240 nm).

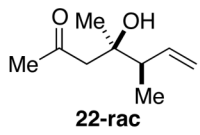

22-rac

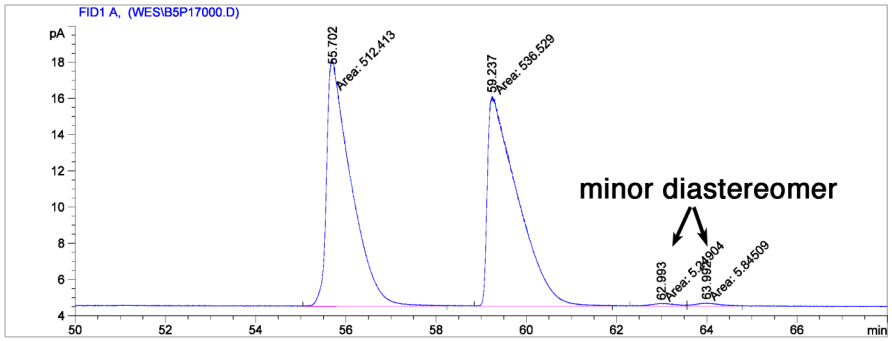

Peak #	RetTime [min]	Type	Width [min]	Area [pA*s]	Height [pA]	Area %
1	55.702	MM	0.6248	512.41321	13.66976	48.33923
2	59.237	MM	0.7717	536.52863	11.58691	50.61419
3	62.993	MF	0.5913	5.24904	1.47956e-1	0.49518
4	63.992	FM	0.5561	5.84509	1.75197e-1	0.55140

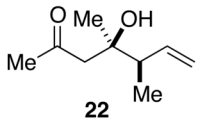

22

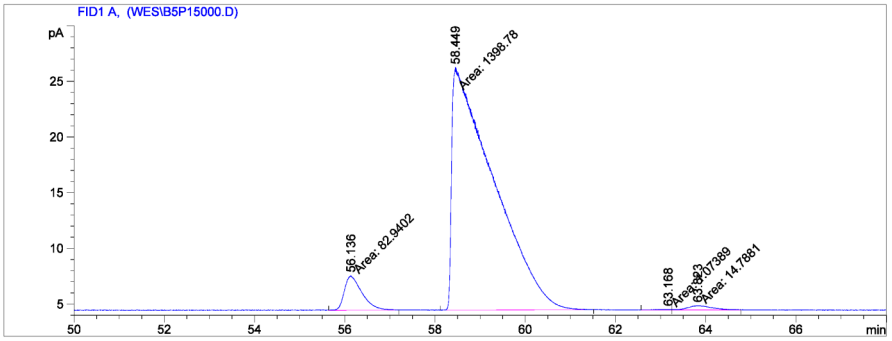

Peak #	RetTime [min]	Type	Width [min]	Area [pA*s]	Height [pA]	Area %
1	56.136	MM	0.4474	82.94016	3.08973	5.53827
2	58.449	MM	1.0711	1398.78101	21.76493	93.40256
3	63.168	MF	0.3607	1.07389	4.96209e-2	0.07171
4	63.823	FM	0.6202	14.78814	3.97405e-1	0.98747

Supplementary Figure 30 | GC trace of **22** (β-dex 325, 1 mL/min, 70 °C isothermal).

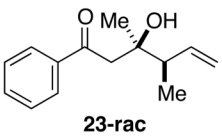

23-rac

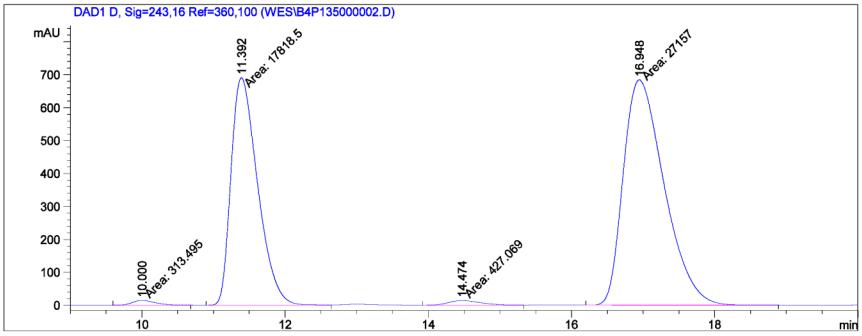

Peak #	RetTime [min]	Sig	Type	Area [mAU*s]	Height [mAU]	Area %
1	10.000	1	MM	313.49506	14.48387	0.6857
2	11.392	1	MF	1.78185e4	690.44305	38.9765
3	14.474	1	MM	427.06943	13.74351	0.9342
4	16.948	1	MM	2.71570e4	683.76666	59.4036

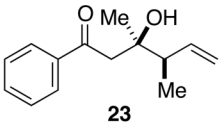

23

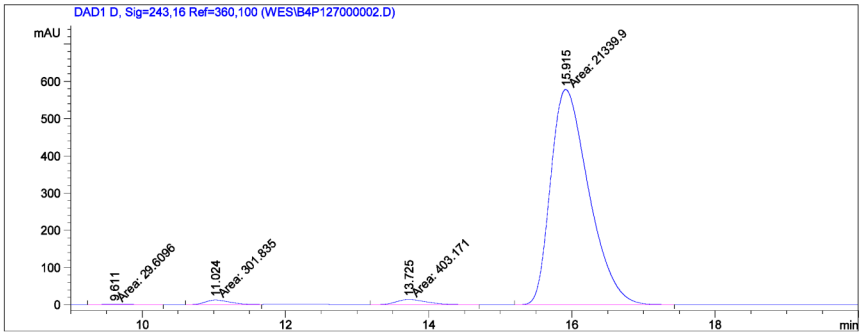

Peak #	RetTime [min]	Sig	Type	Area [mAU*s]	Height [mAU]	Area %
1	9.611	1	MM	29.60961	1.22936	0.1341
2	11.024	1	MF	301.83545	12.39983	1.3674
3	13.725	1	MM	403.17142	13.72319	1.8264
4	15.915	1	MF	2.13399e4	577.83069	96.6721

Supplementary Figure 31 | HPLC trace of **23** (Chiralcel OD, Hexanes:*i*-PrOH = 98:2, 1 mL/min, 243 nm).

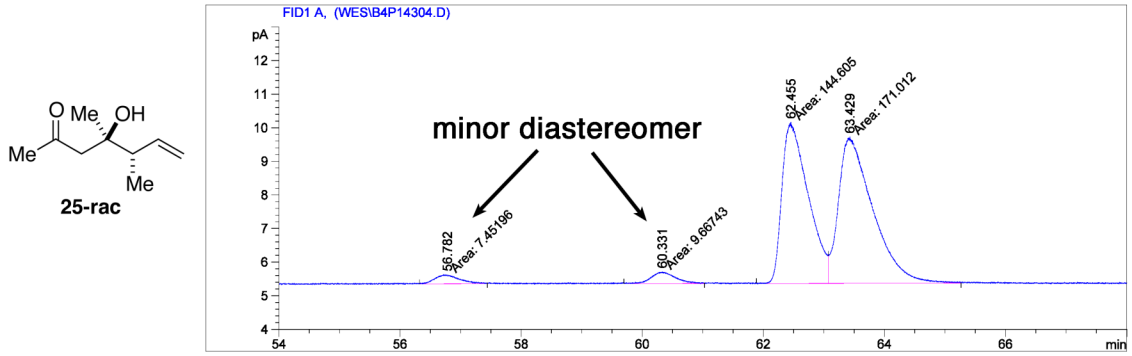

Peak #	RetTime [min]	Type	Width [min]	Area [pA*s]	Height [pA]	Area %
1	56.782	MM	0.4694	7.45196	2.64584e-1	2.23960
2	60.331	MM	0.4538	9.66743	3.55082e-1	2.90543
3	62.455	MF	0.5018	144.60495	4.80271	43.45933
4	63.429	FM	0.6537	171.01189	4.36033	51.39563

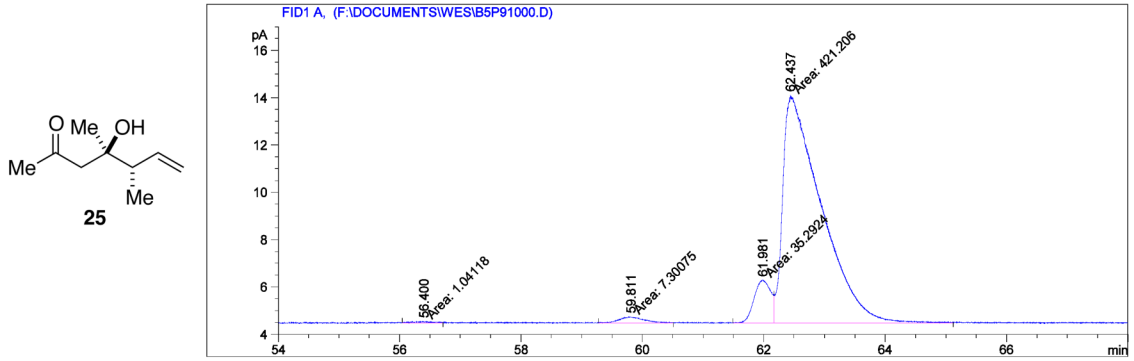

Peak #	RetTime [min]	Sig	Type	Area [pA*s]	Height [pA]	Area %
1	56.400	1	MM	1.04118	5.06219e-2	0.2240
2	59.811	1	MM	7.30075	2.61029e-1	1.5706
3	61.981	1	MF	35.29241	1.81944	7.5924
4	62.437	1	FM	421.20566	9.64233	90.6130

Supplementary Figure 32 | GC trace of **25** (β-dex 325, 1 mL/min, 70 °C isothermal).

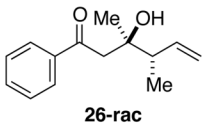

26-rac

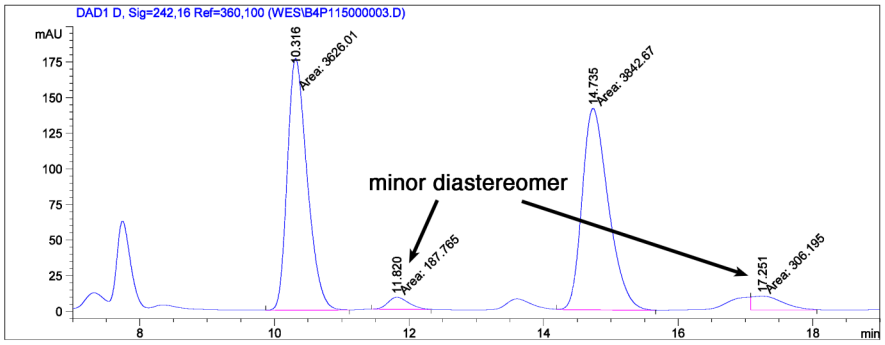

Peak #	RetTime [min]	Sig	Type	Area [mAU*s]	Height [mAU]	Area %
1	10.316	1	MM	3626.00903	176.72484	45.5378
2	11.820	1	MM	187.76537	8.61539	2.3581
3	14.735	1	MM	3842.66577	141.35040	48.2587
4	17.251	1	FM	306.19479	9.67964	3.8454

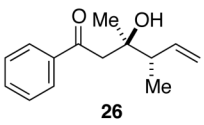

26

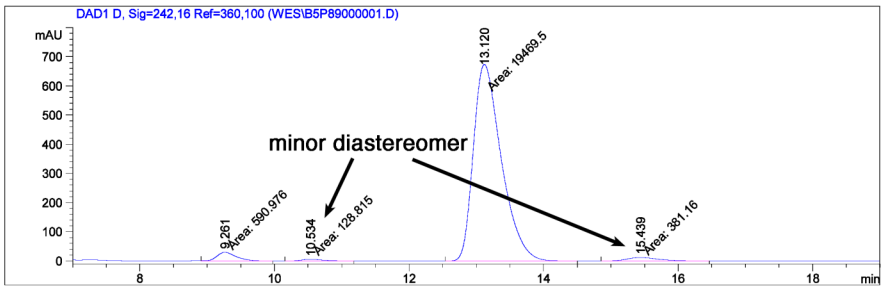

Peak #	RetTime [min]	Sig	Type	Area [mAU*s]	Height [mAU]	Area %
1	9.261	1	FM	590.97583	29.76722	2.8729
2	10.534	1	MM	128.81493	5.76914	0.6262
3	13.120	1	MM	1.94695e4	673.87292	94.6479
4	15.439	1	MM	381.15958	11.75626	1.8529

Supplementary Figure 33 | HPLC trace of **26** (Chiralcel OD, Hexanes:*i*-PrOH = 98:2, 1 mL/min, 242 nm).

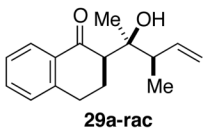

29a-rac

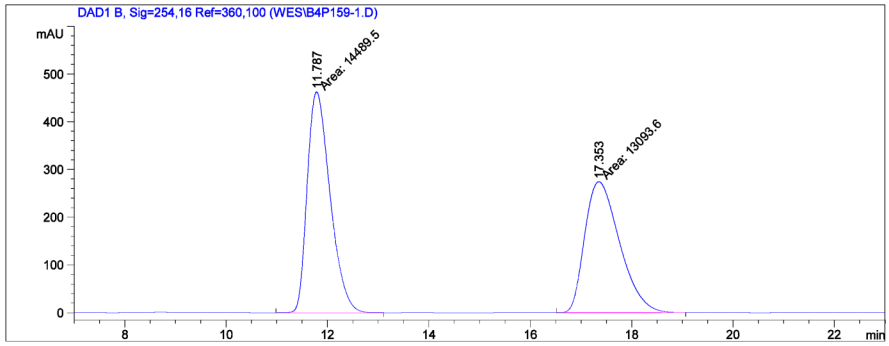

Peak #	RetTime [min]	Sig	Type	Area [mAU*s]	Height [mAU]	Area %
1	11.787	1	MM	1.44895e4	462.16232	52.5304
2	17.353	1	MM	1.30936e4	274.06464	47.4696

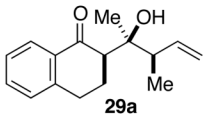

29a

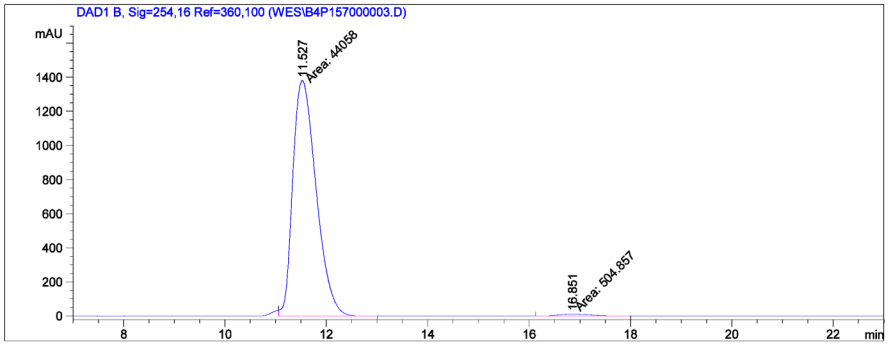

Peak #	RetTime [min]	Sig	Type	Area [mAU*s]	Height [mAU]	Area %
1	11.527	1	FM	4.40580e4	1379.53589	98.8671
2	16.851	1	MM	504.85675	11.81540	1.1329

Supplementary Figure 34 | HPLC trace of **29a** (Chiralcel OD, Hexanes:*i*-PrOH = 98:2, 1 mL/min, 254 nm).

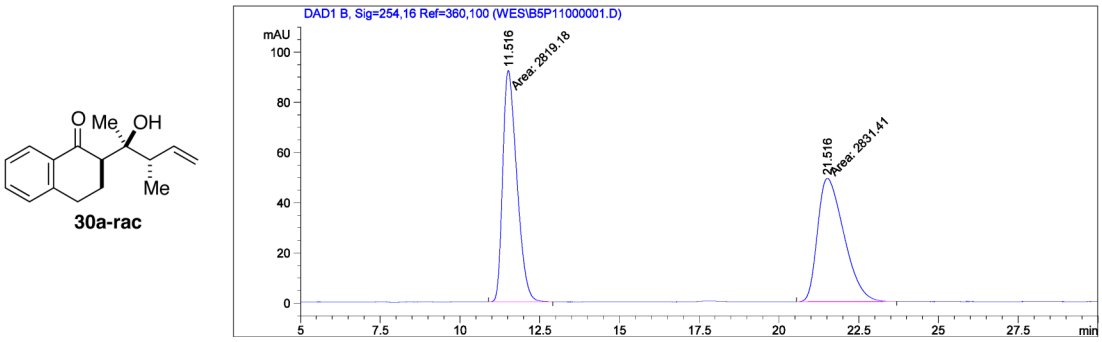

Peak #	RetTime [min]	Sig	Type	Area [mAU*s]	Height [mAU]	Area %
1	11.516	1	MM	2819.18384	92.13503	49.8918
2	21.516	1	MM	2831.41455	49.17508	50.1082

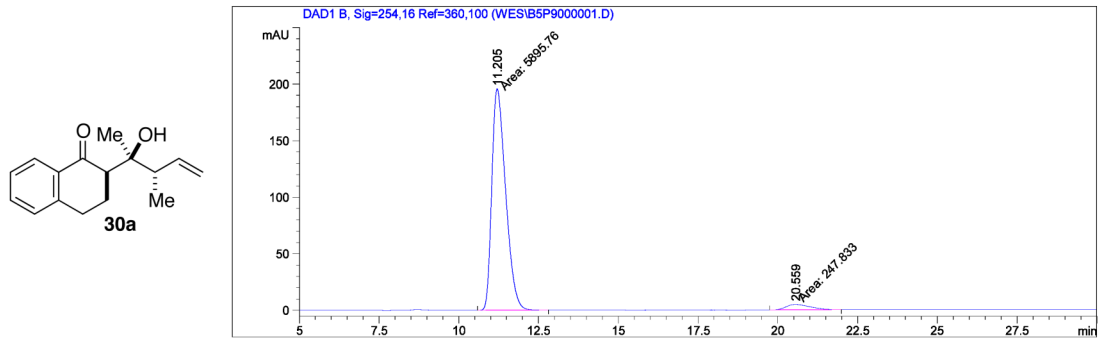

Peak #	RetTime [min]	Sig	Type	Area [mAU*s]	Height [mAU]	Area %
1	11.205	1	MM	5895.76270	195.59328	95.9660
2	20.559	1	MM	247.83327	4.78587	4.0340

Supplementary Figure 35 | HPLC trace of **30a** (Chiralcel OD, Hexanes:*i*-PrOH = 98:2, 1 mL/min, 254 nm).

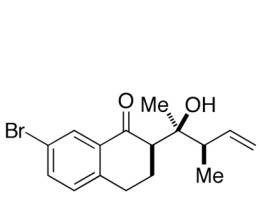

S1-rac

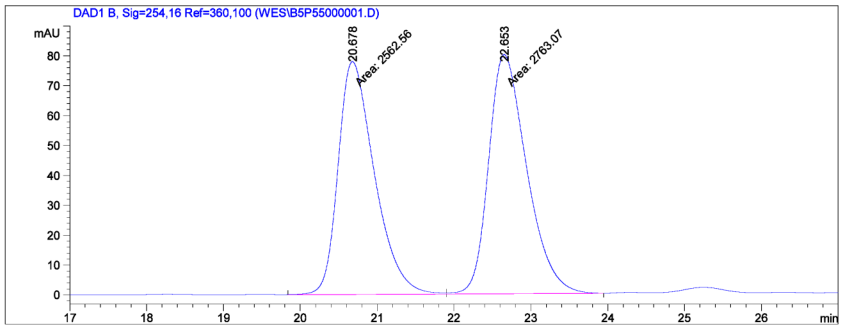

Peak #	RetTime [min]	Sig	Type	Area [mAU*s]	Height [mAU]	Area %
1	20.678	1	MF	2562.56079	77.92183	48.1175
2	22.653	1	FM	2763.07227	80.05615	51.8825

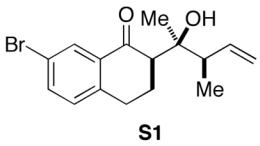

S1

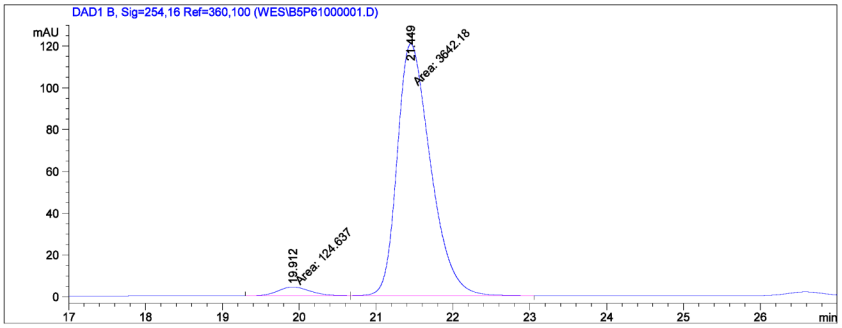

Peak #	RetTime [min]	Sig	Type	Area [mAU*s]	Height [mAU]	Area %
1	19.912	1	MF	124.63725	4.23498	3.3088
2	21.449	1	FM	3642.18311	120.62037	96.6912

Supplementary Figure 36 | HPLC trace of **S1** (Chiralpak AD-H, Hexanes:*i*-PrOH = 98:2, 1 mL/min, 254 nm).

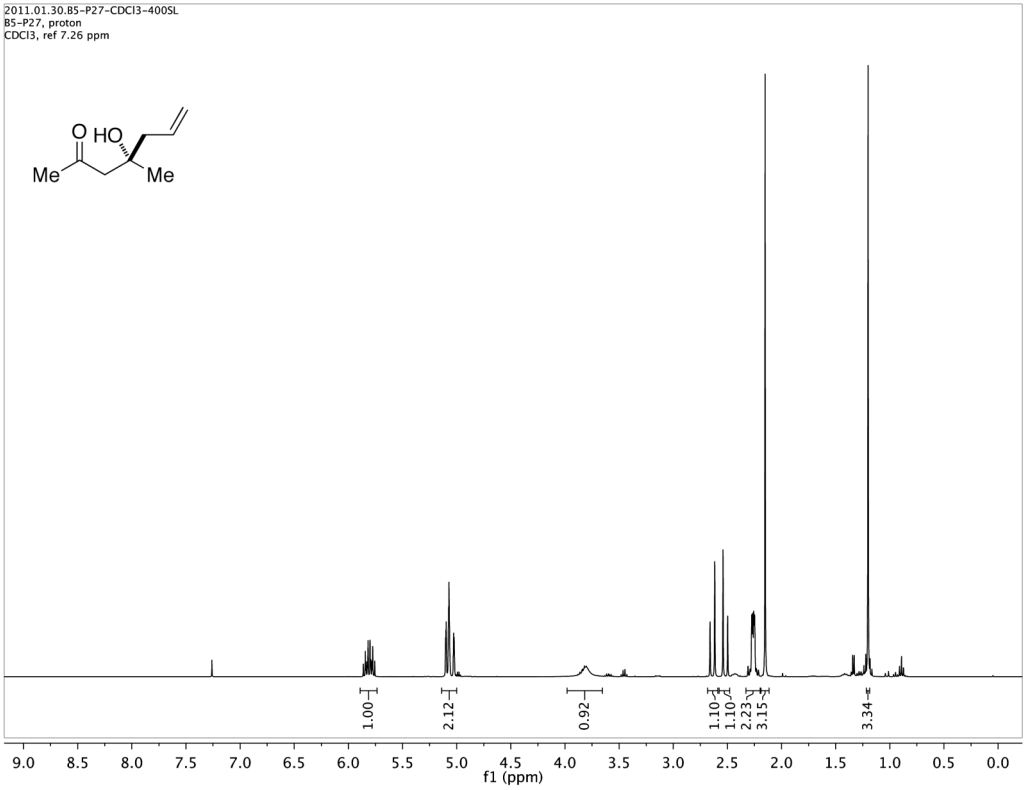

Supplementary Figure 37 | ^{1}H NMR spectrum of compound **1**.

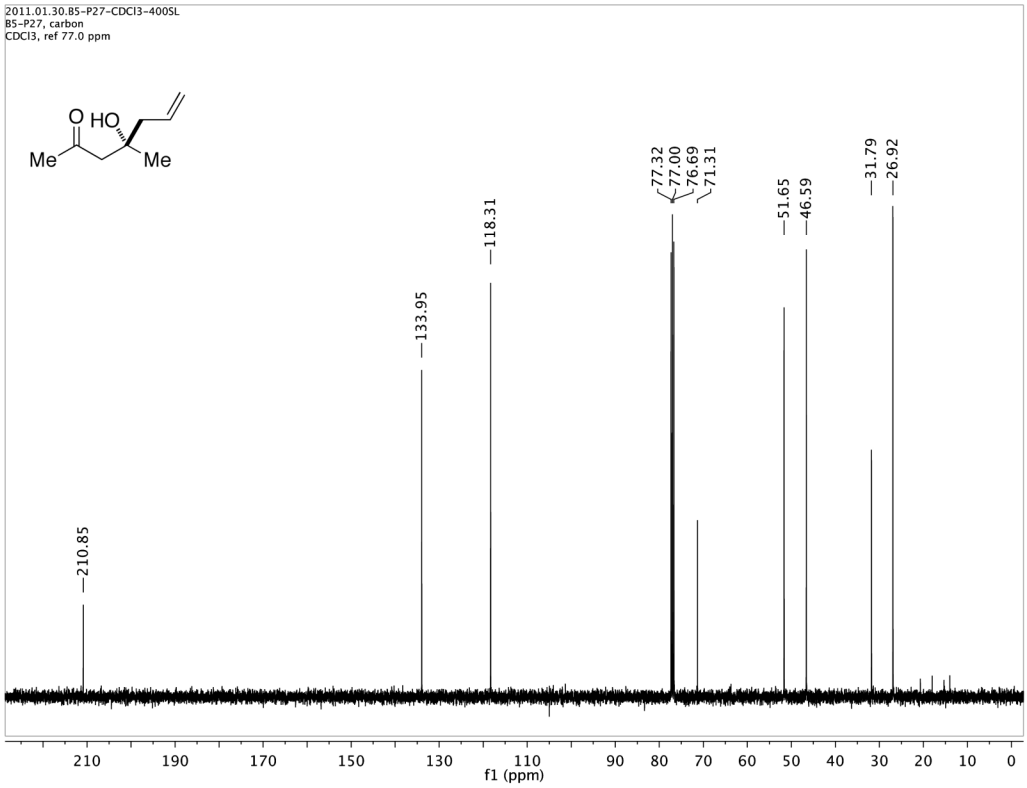

Supplementary Figure 38 | ^{13}C NMR spectrum of compound **1**.

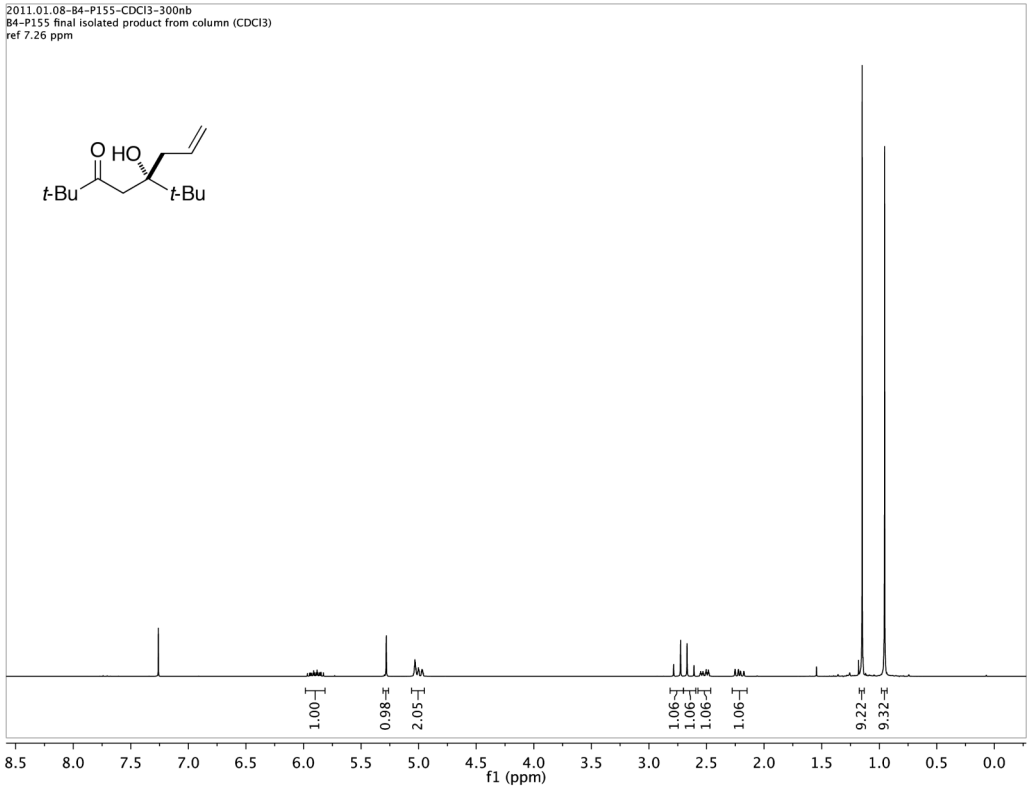

Supplementary Figure 39 | ^{1}H NMR spectrum of compound **7**.

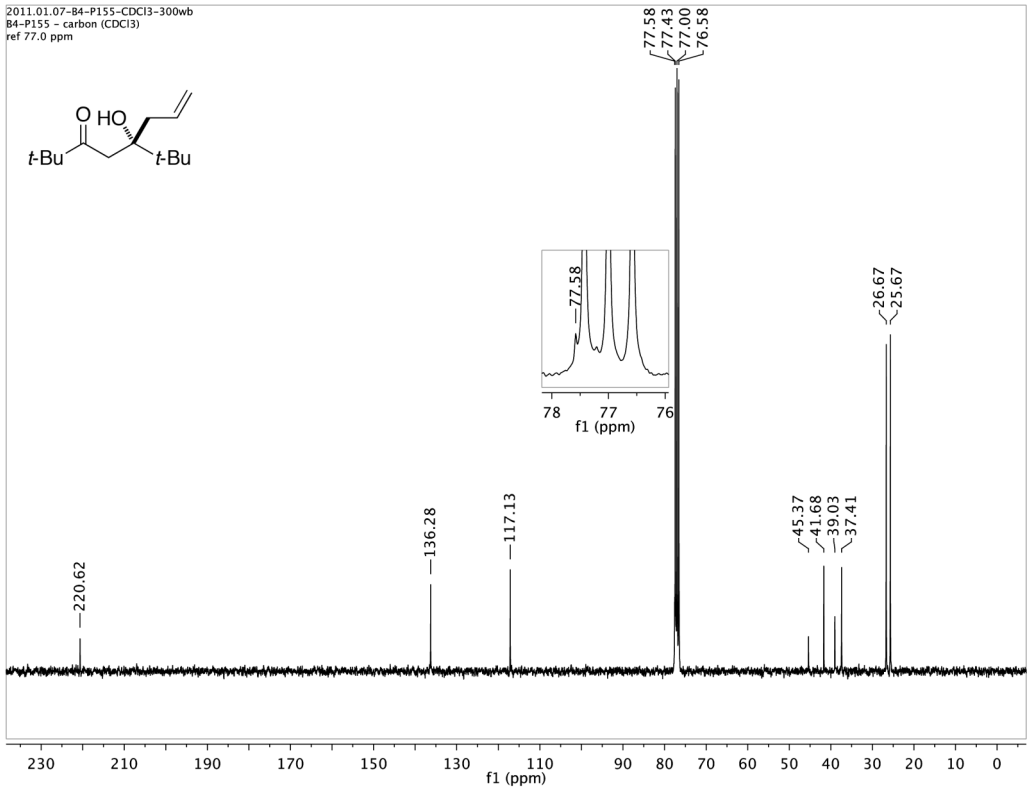

Supplementary Figure 40 | ^{13}C NMR spectrum of compound **7**.

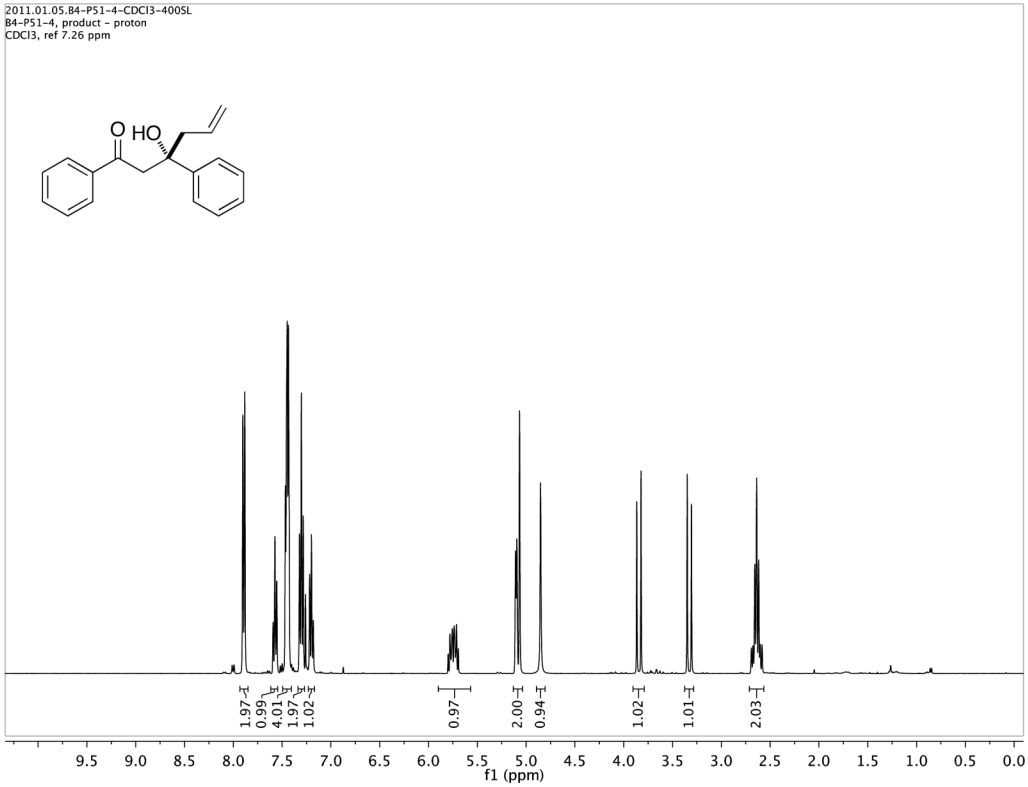

Supplementary Figure 41 | ^{1}H NMR spectrum of compound **8**.

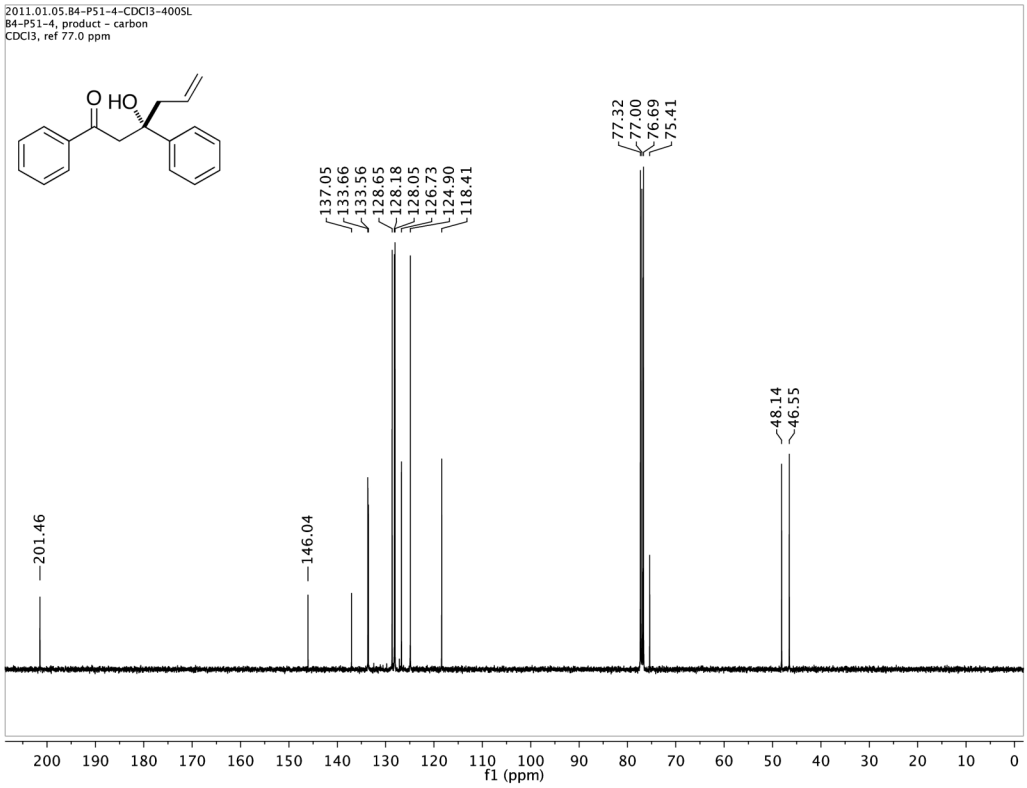

Supplementary Figure 42 | ^{13}C NMR spectrum of compound **8**.

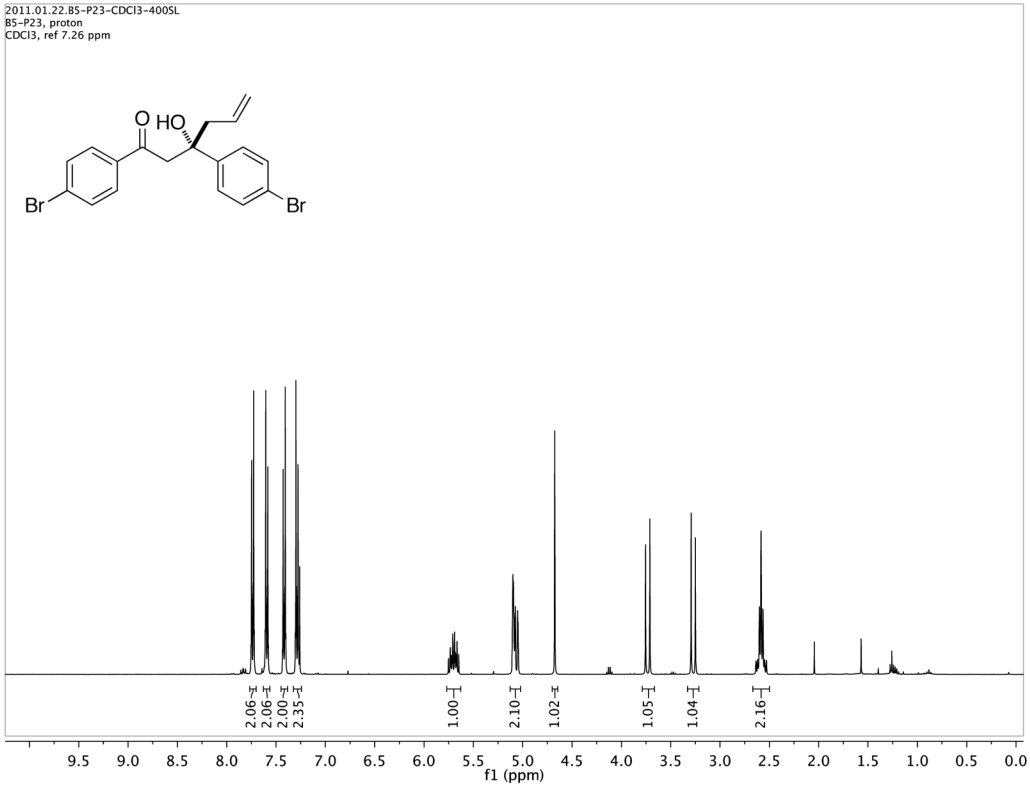

Supplementary Figure 43 | ^{1}H NMR spectrum of compound **9**.

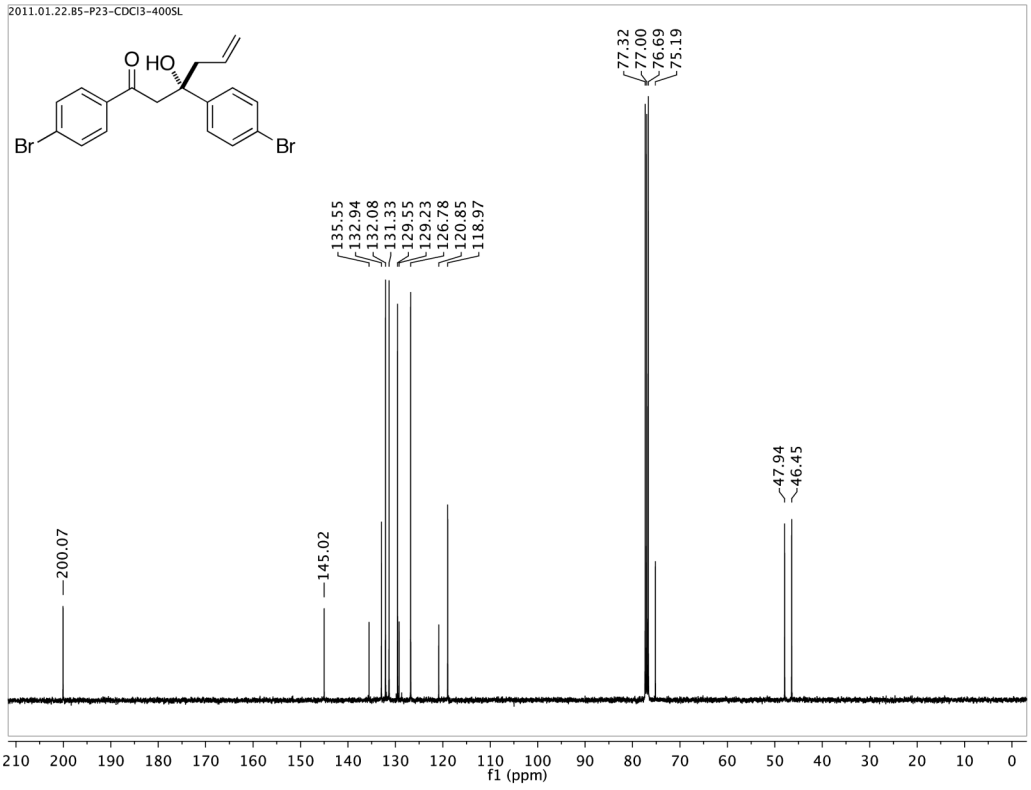

Supplementary Figure 44 | ^{13}C NMR spectrum of compound **9**.

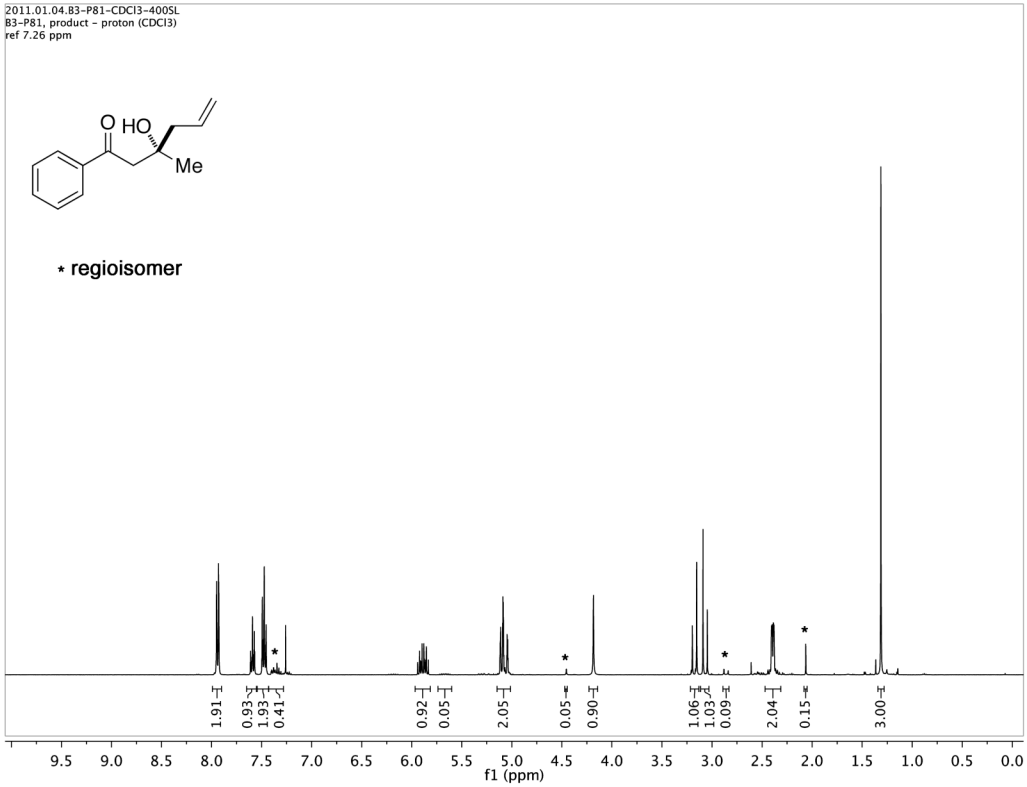

Supplementary Figure 45 | ^{1}H NMR spectrum of compound **10**.

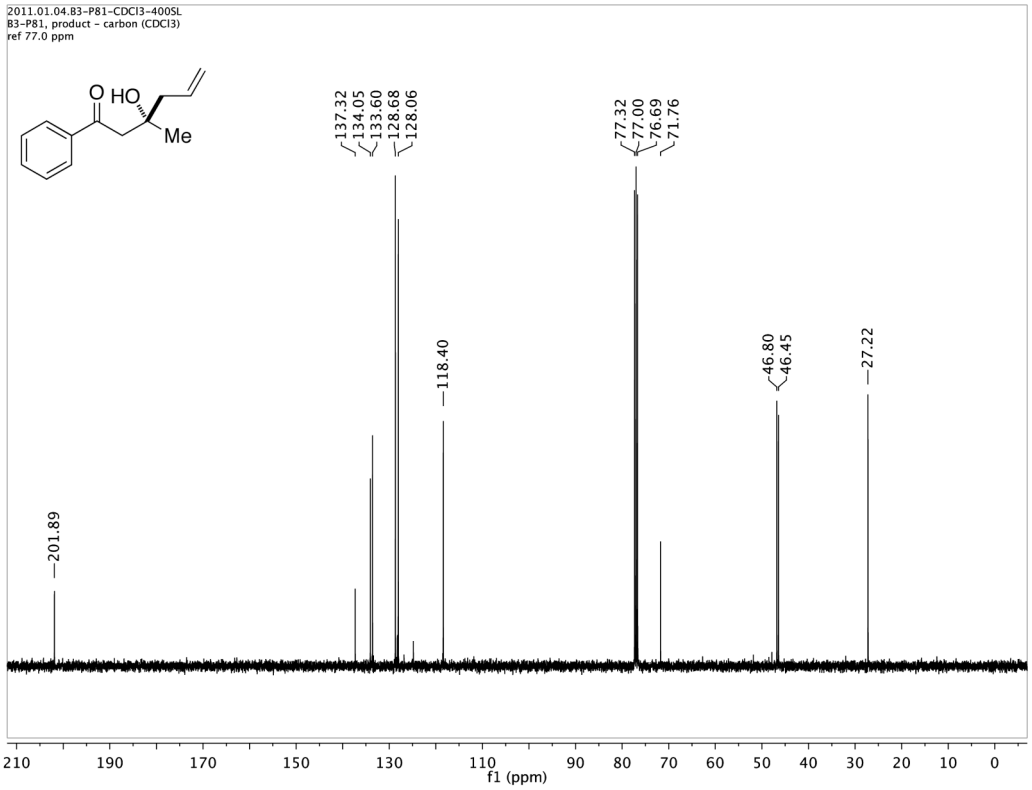

Supplementary Figure 46 | ^{13}C NMR spectrum of compound **10**.

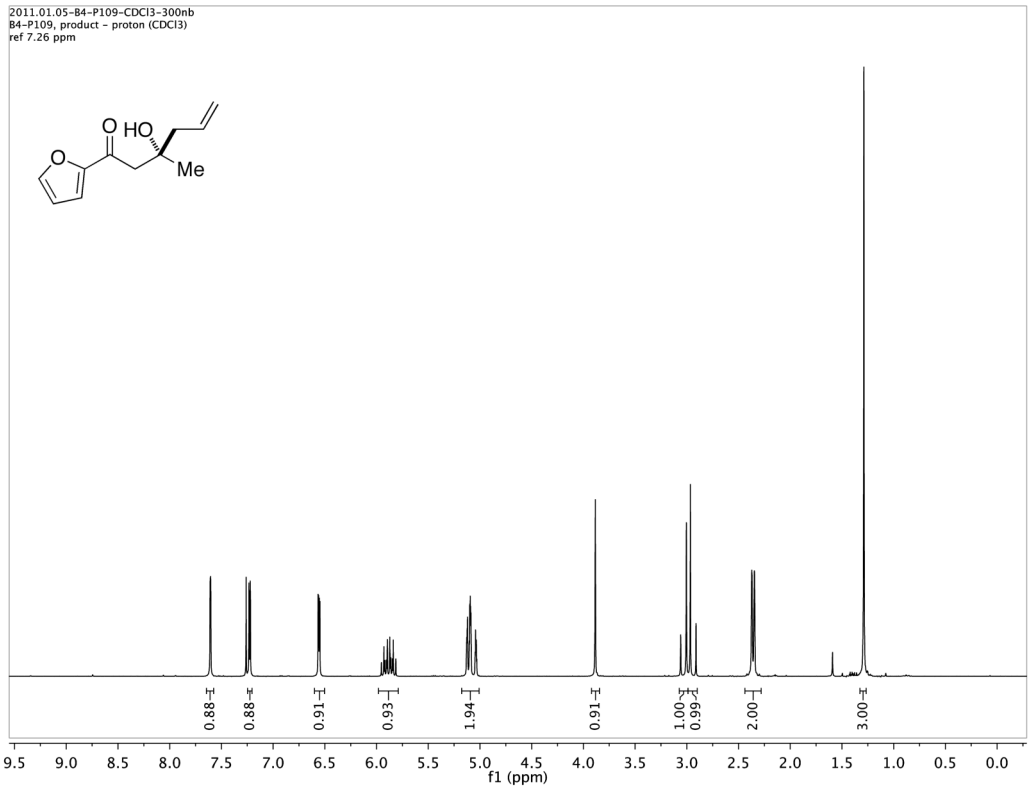

Supplementary Figure 47 | ^{1}H NMR spectrum of compound **11**.

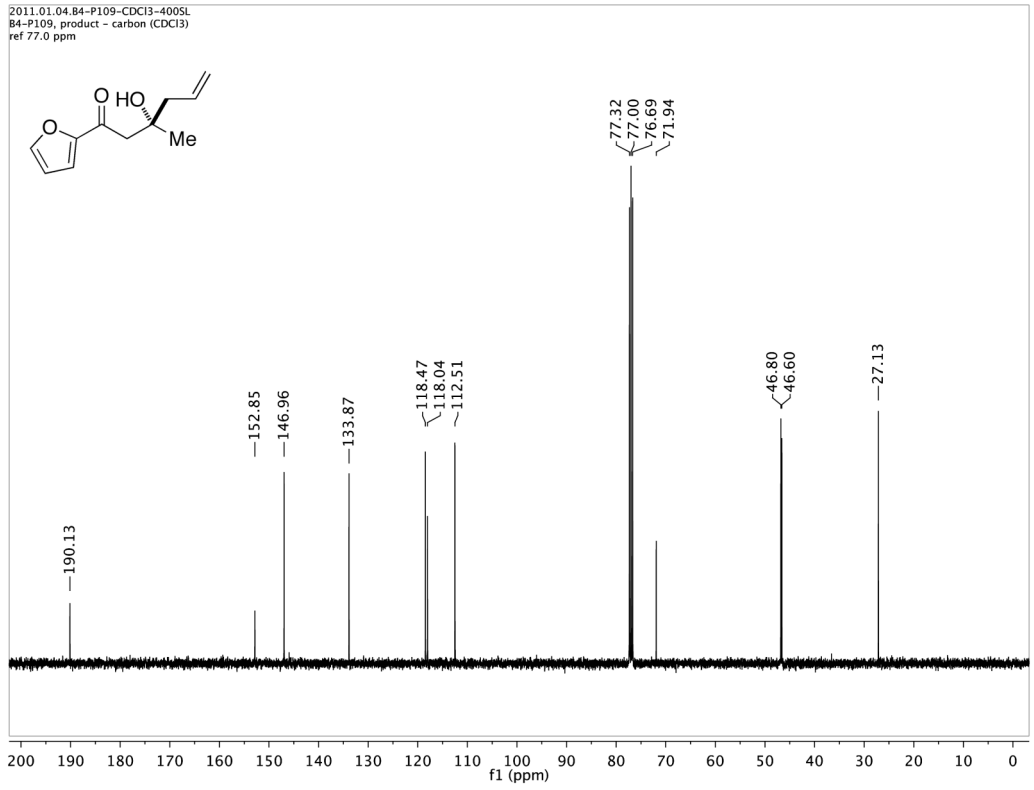

Supplementary Figure 48 | ^{13}C NMR spectrum of compound **11**.

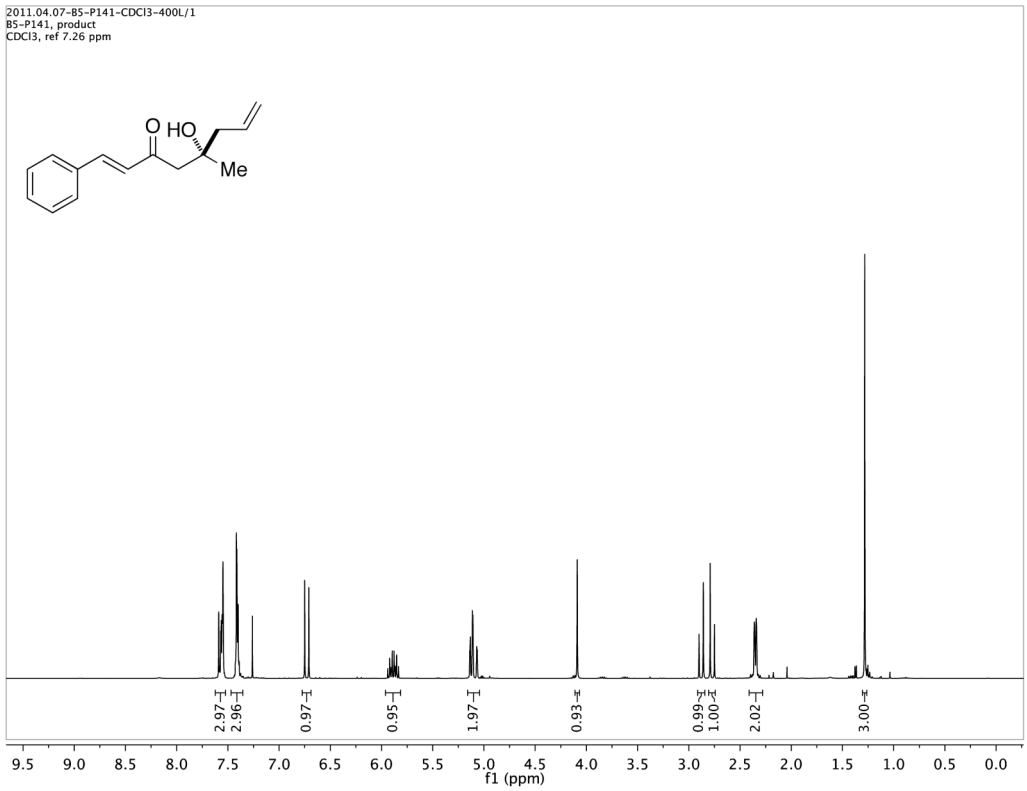

Supplementary Figure 49 | ^{1}H NMR spectrum of compound **12**.

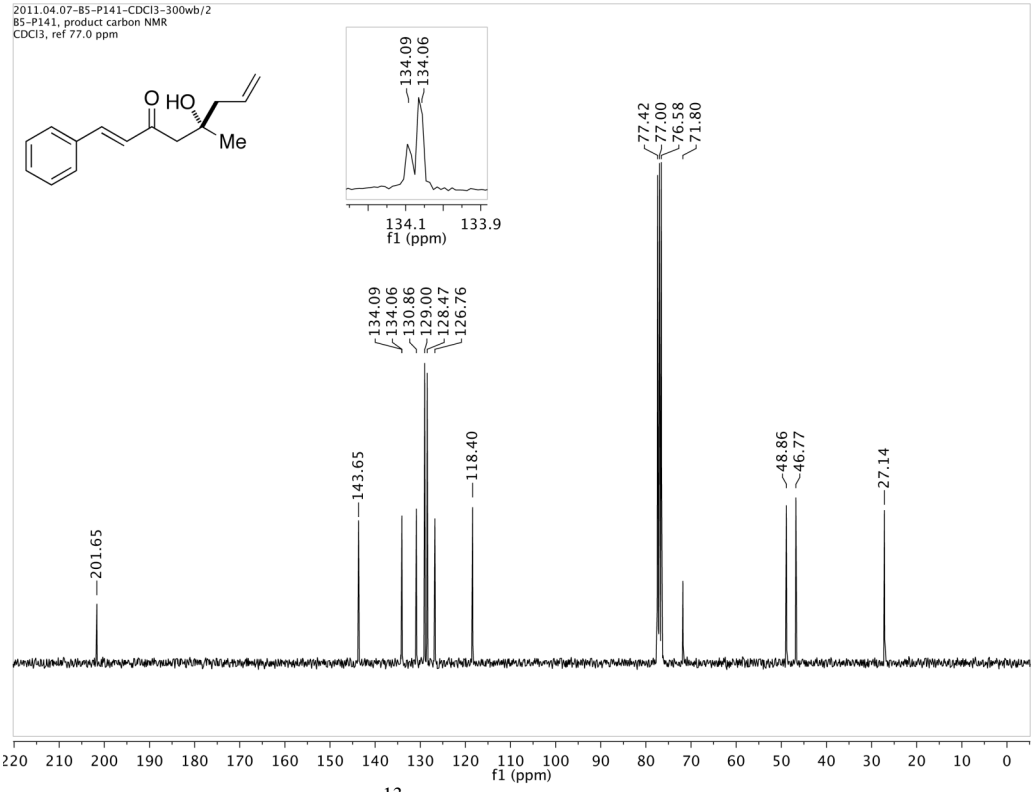

Supplementary Figure 50 | ^{13}C NMR spectrum of compound **12**.

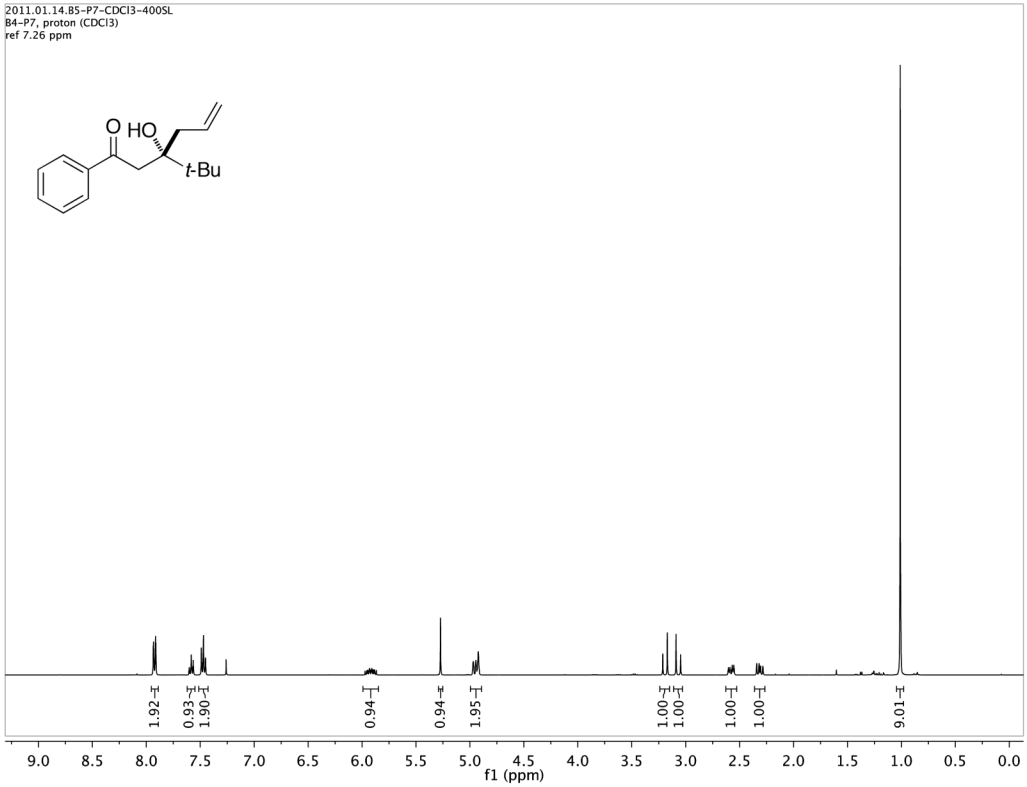

Supplementary Figure 51 | ^{1}H NMR spectrum of compound **13**.

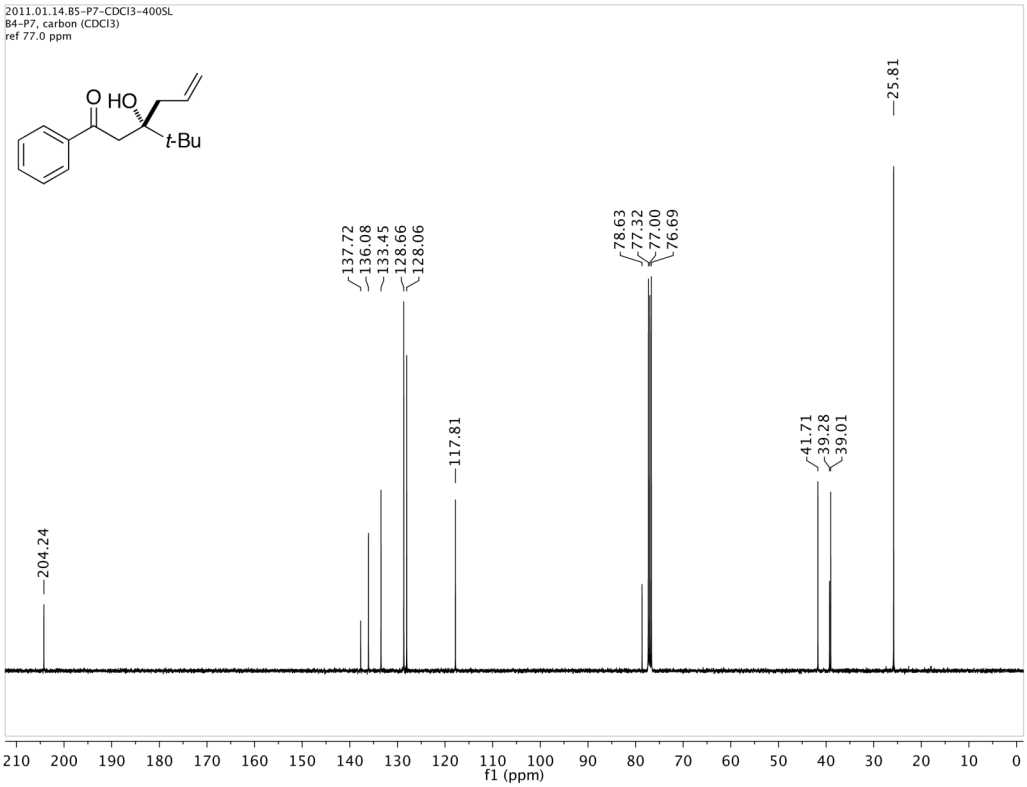

Supplementary Figure 52 | ^{13}C NMR spectrum of compound **13**.

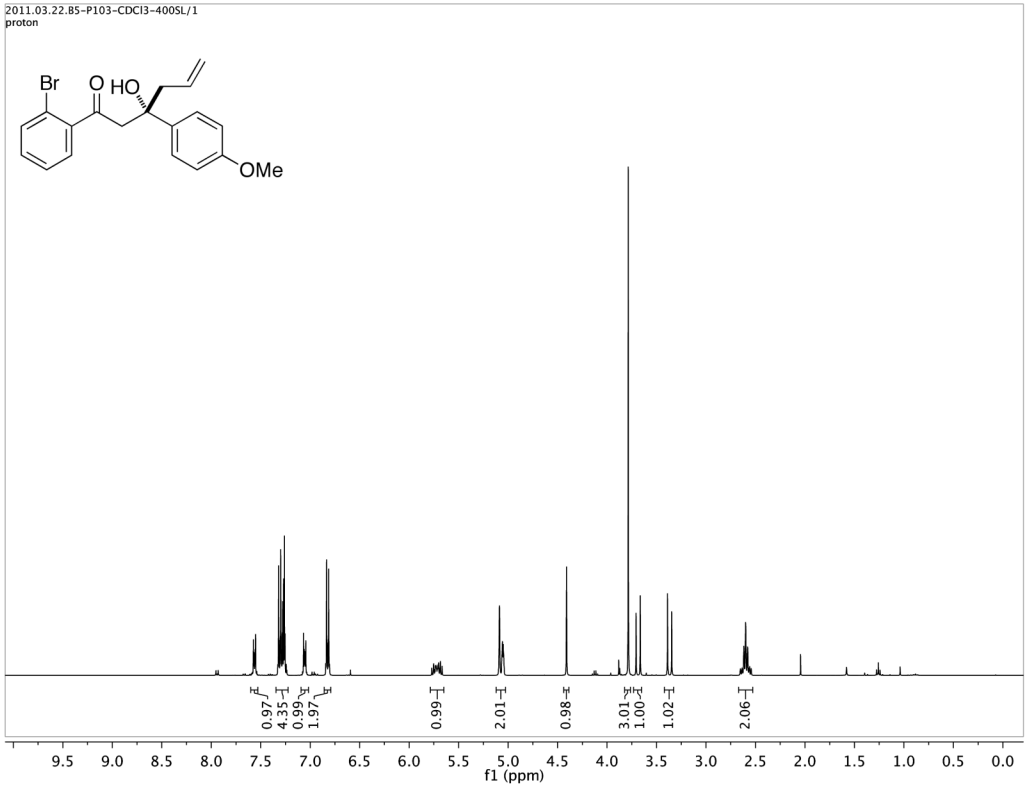

Supplementary Figure 53 | ^{1}H NMR spectrum of compound **14**.

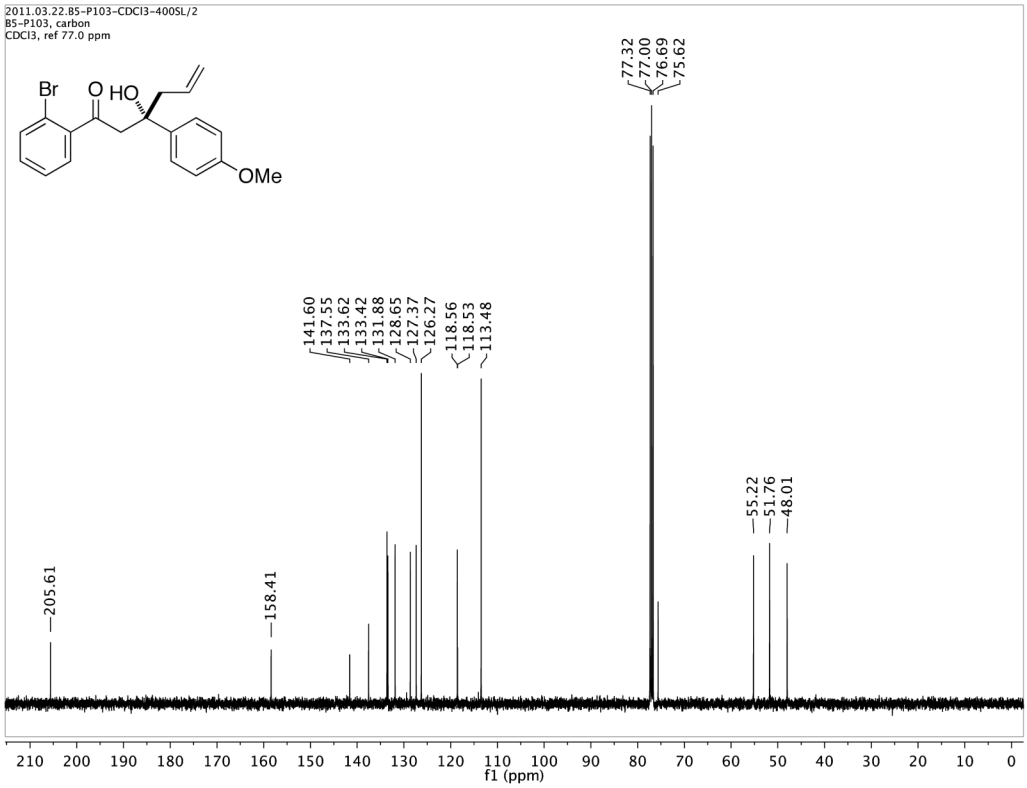

Supplementary Figure 54 | ^{13}C NMR spectrum of compound **14**.

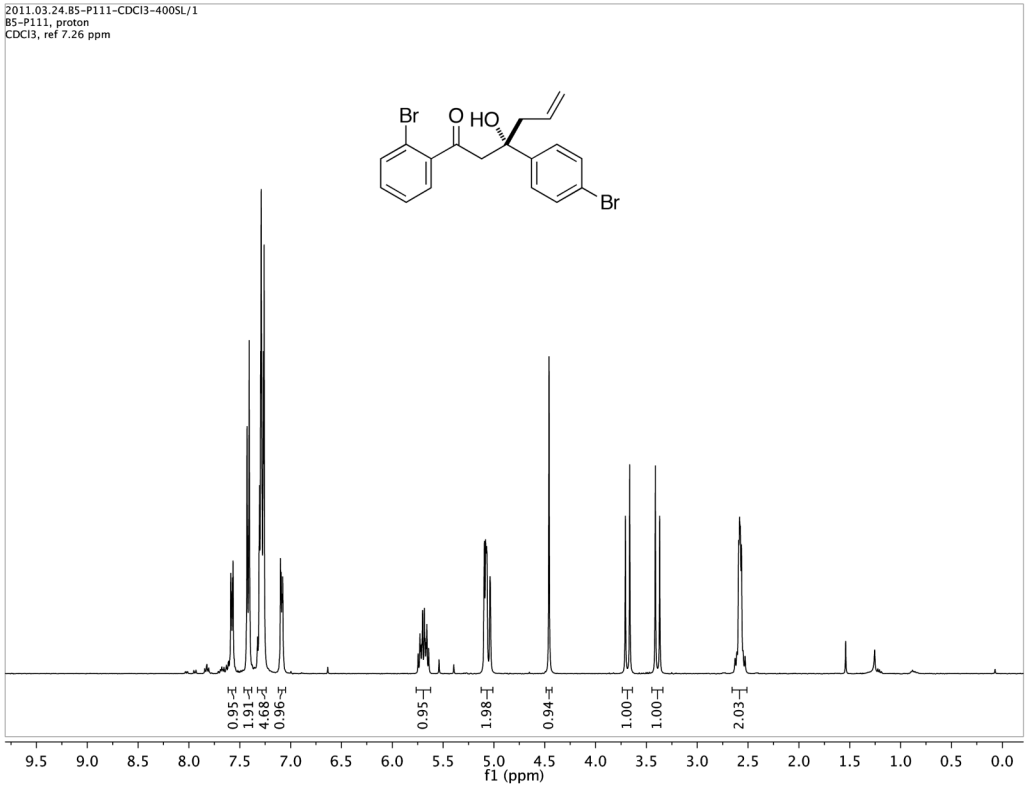

Supplementary Figure 55 | ^{1}H NMR spectrum of compound **15**.

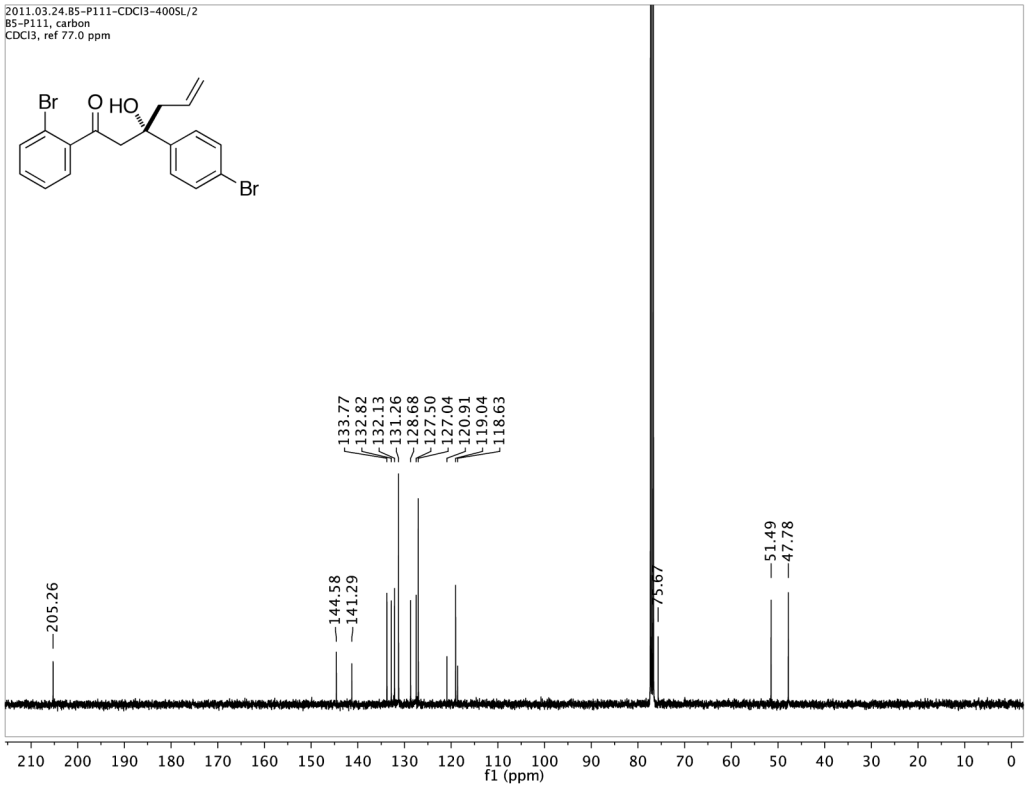

Supplementary Figure 56 | ^{13}C NMR spectrum of compound **15**.

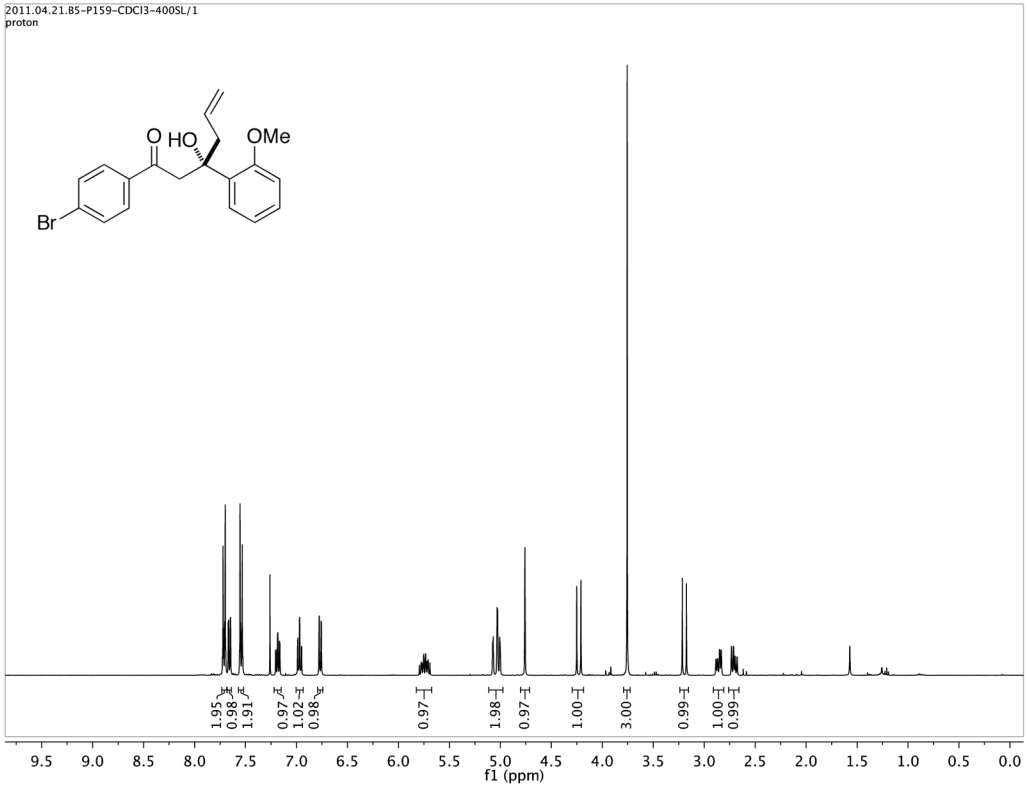

Supplementary Figure 57 | ^{1}H NMR spectrum of compound **16a**.

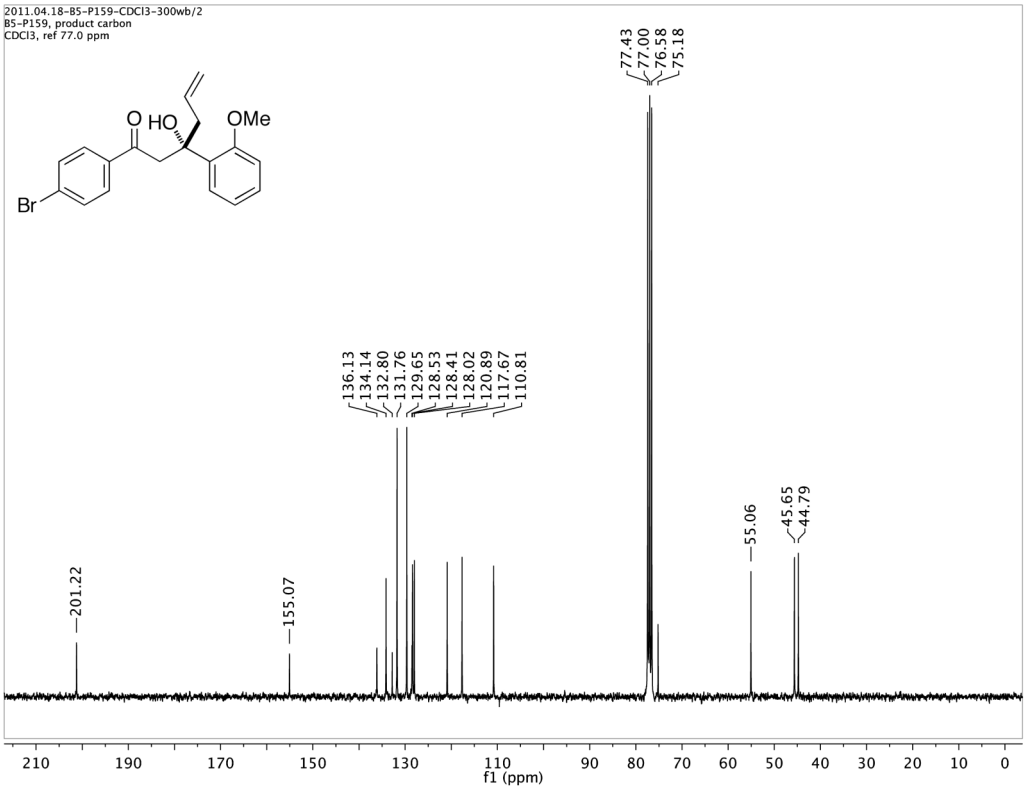

Supplementary Figure 58 | ^{13}C NMR spectrum of compound **16a**.

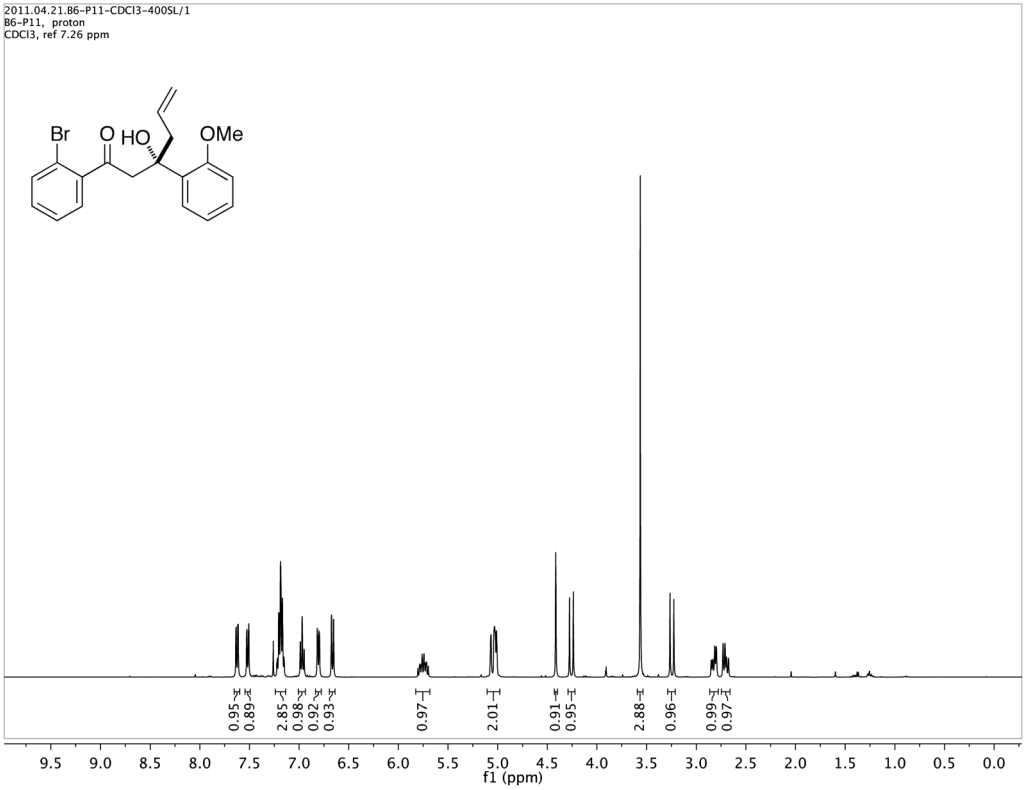

Supplementary Figure 59 | ^{1}H NMR spectrum of compound **17**.

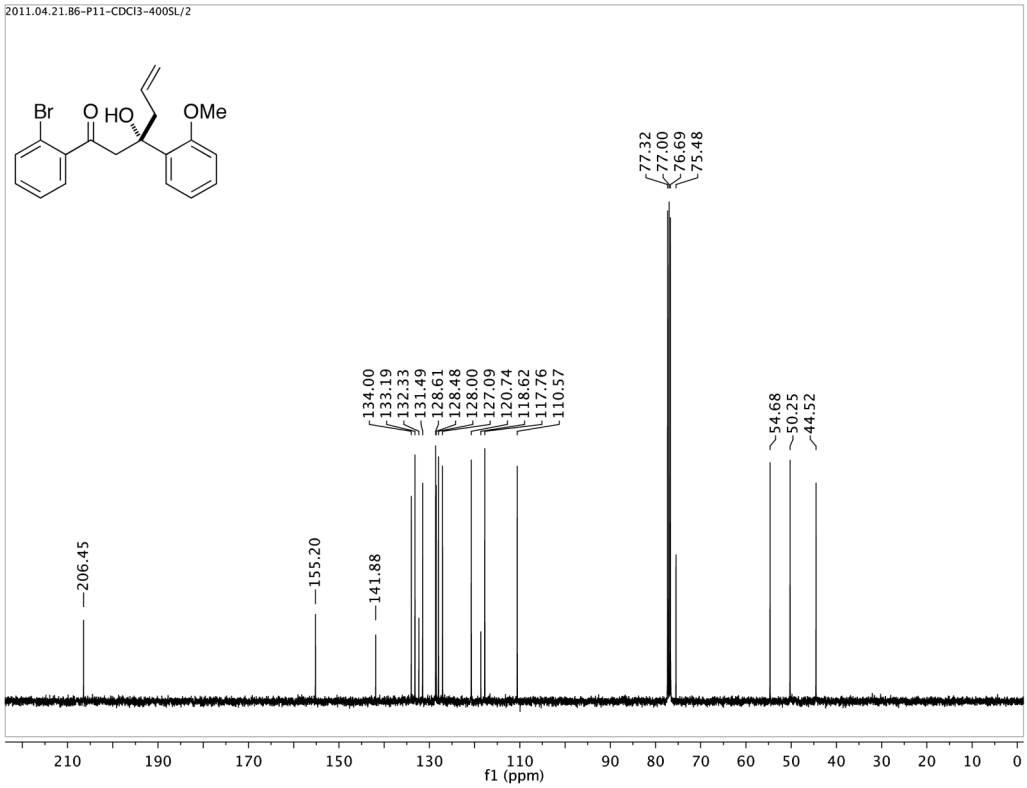

Supplementary Figure 60 | ^{13}C NMR spectrum of compound **17**.

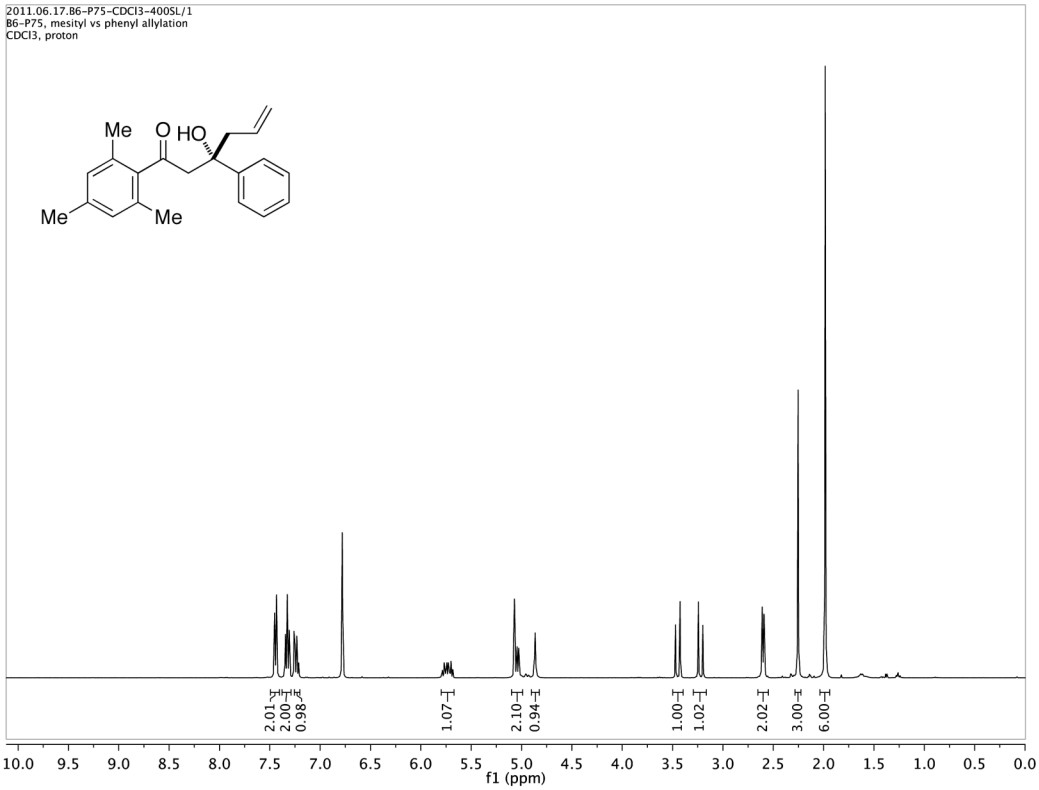

Supplementary Figure 61 | ^{1}H NMR spectrum of compound **18**.

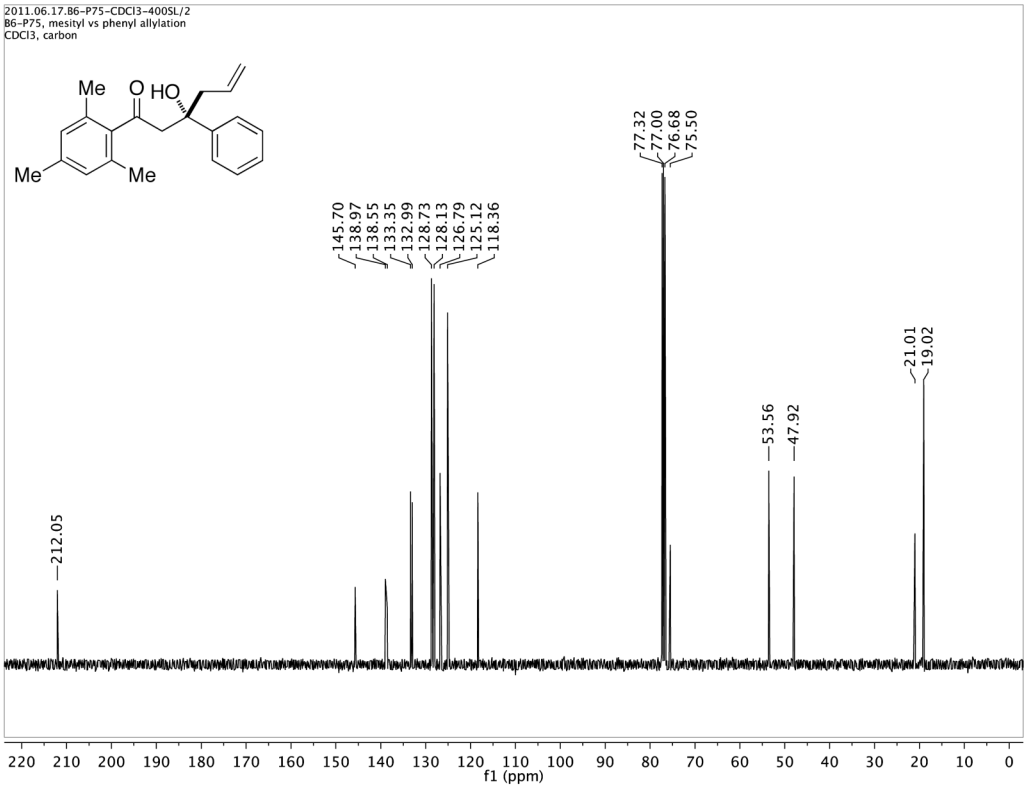

Supplementary Figure 62 | ^{13}C NMR spectrum of compound **18**.

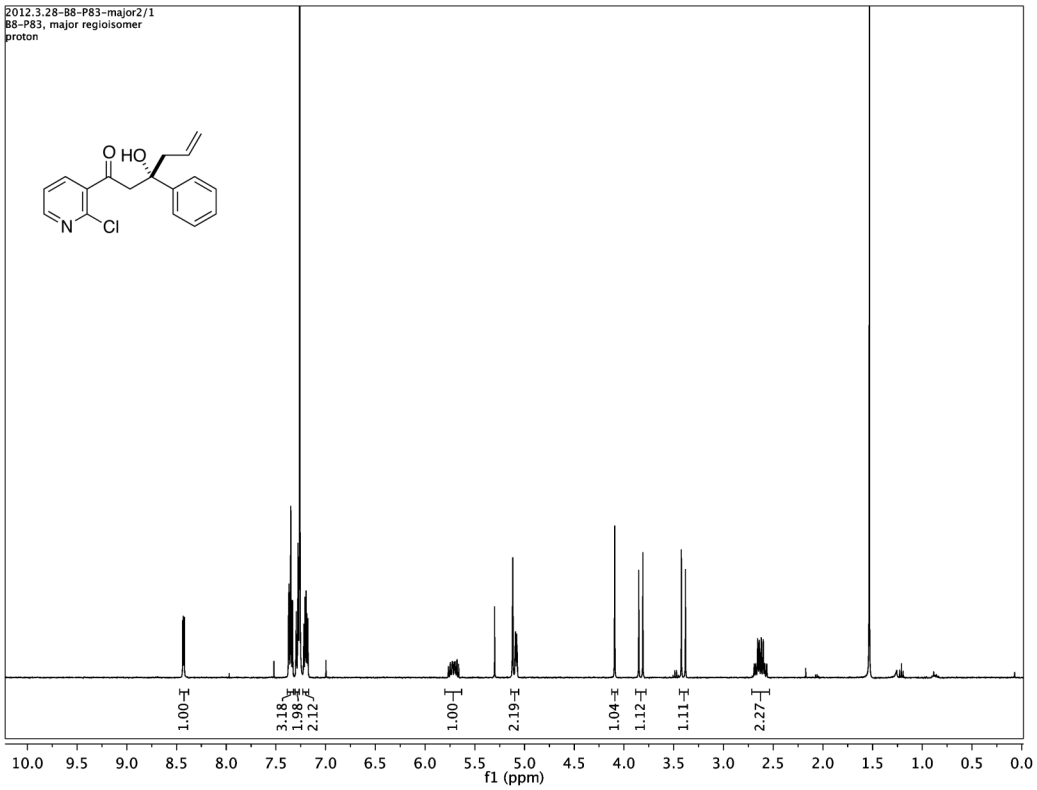

Supplementary Figure 63 | ^{1}H NMR spectrum of compound **19**.

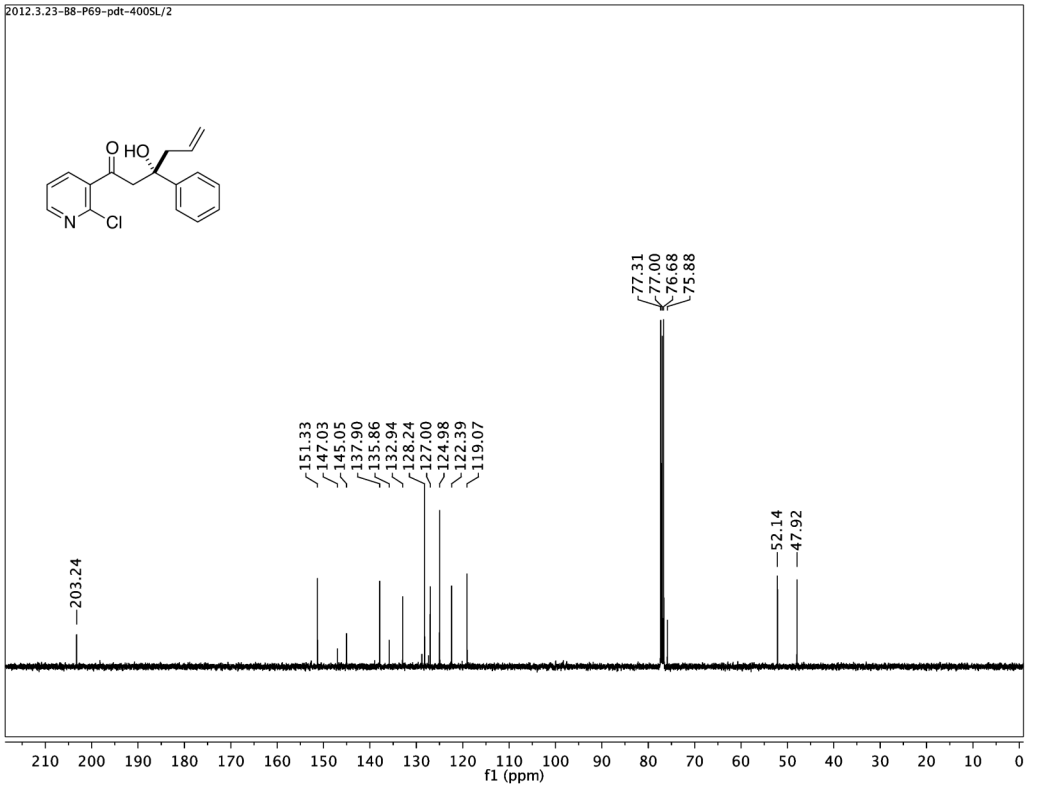

Supplementary Figure 64 | ^{13}C NMR spectrum of compound **19**.

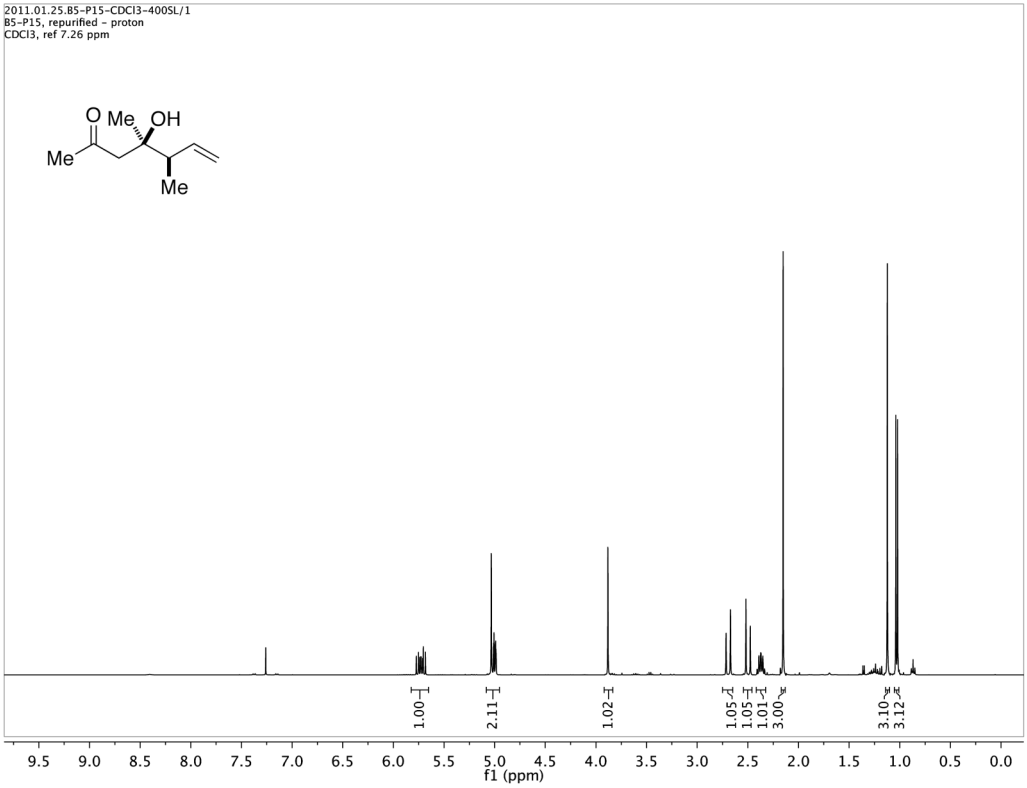

Supplementary Figure 65 | ^{1}H NMR spectrum of compound **22**.

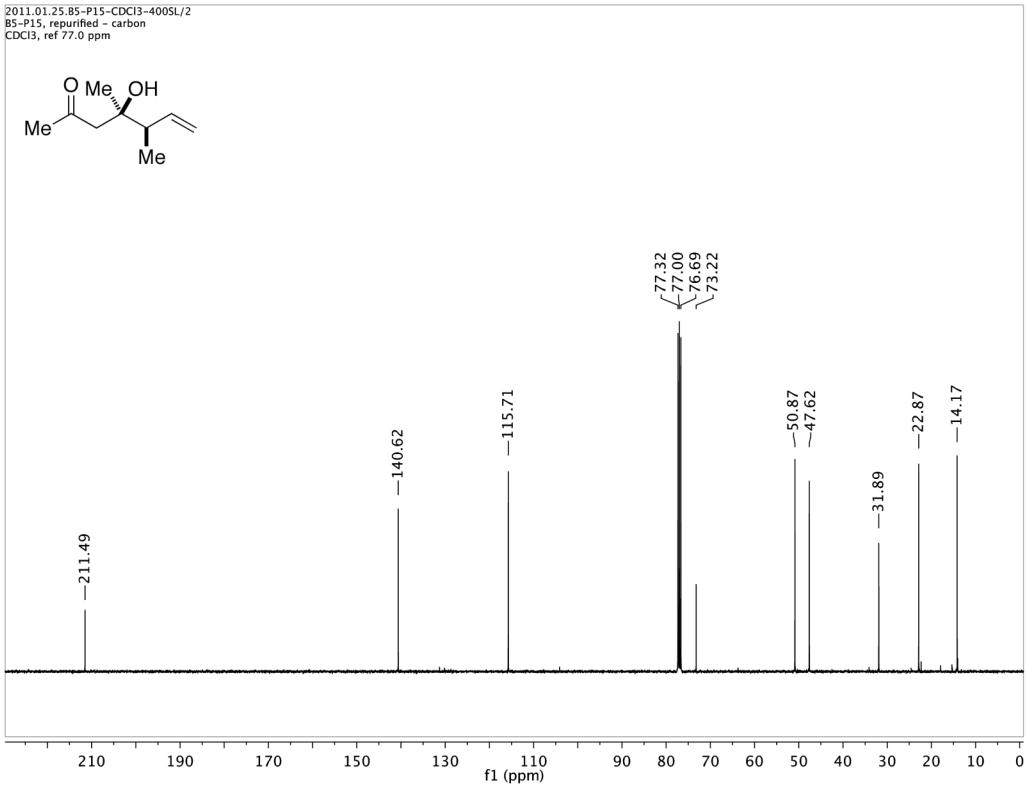

Supplementary Figure 66 | ^{13}C NMR spectrum of compound **22**.

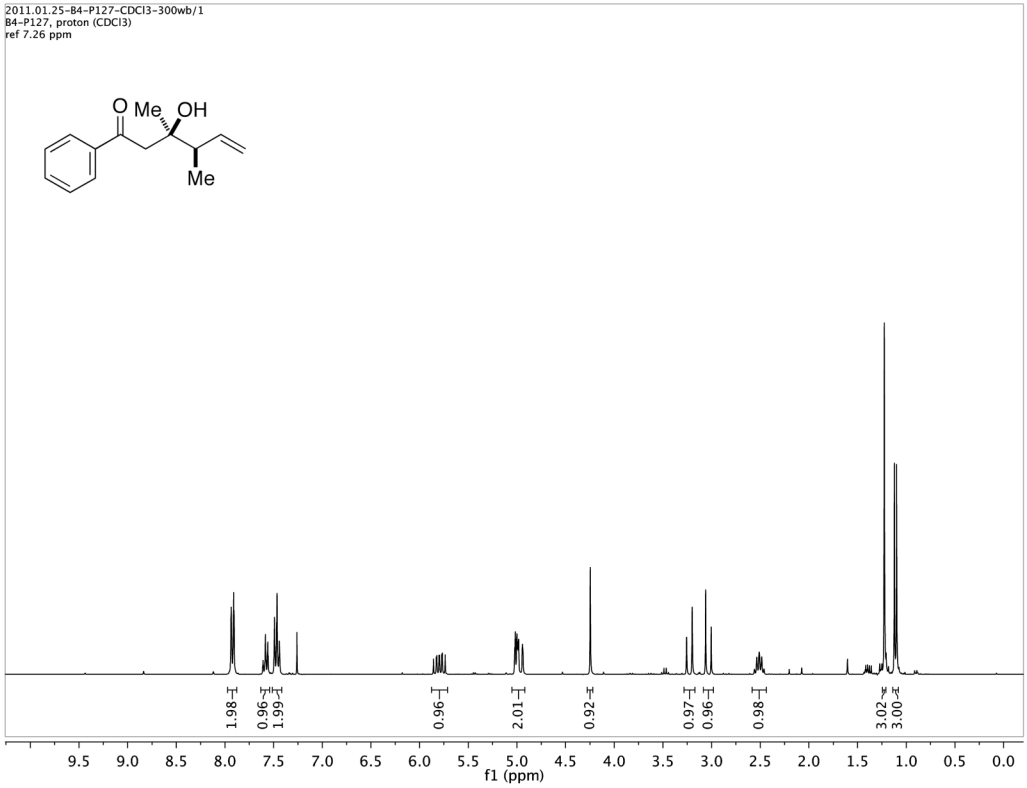

Supplementary Figure 67 | ^{1}H NMR spectrum of compound **23**.

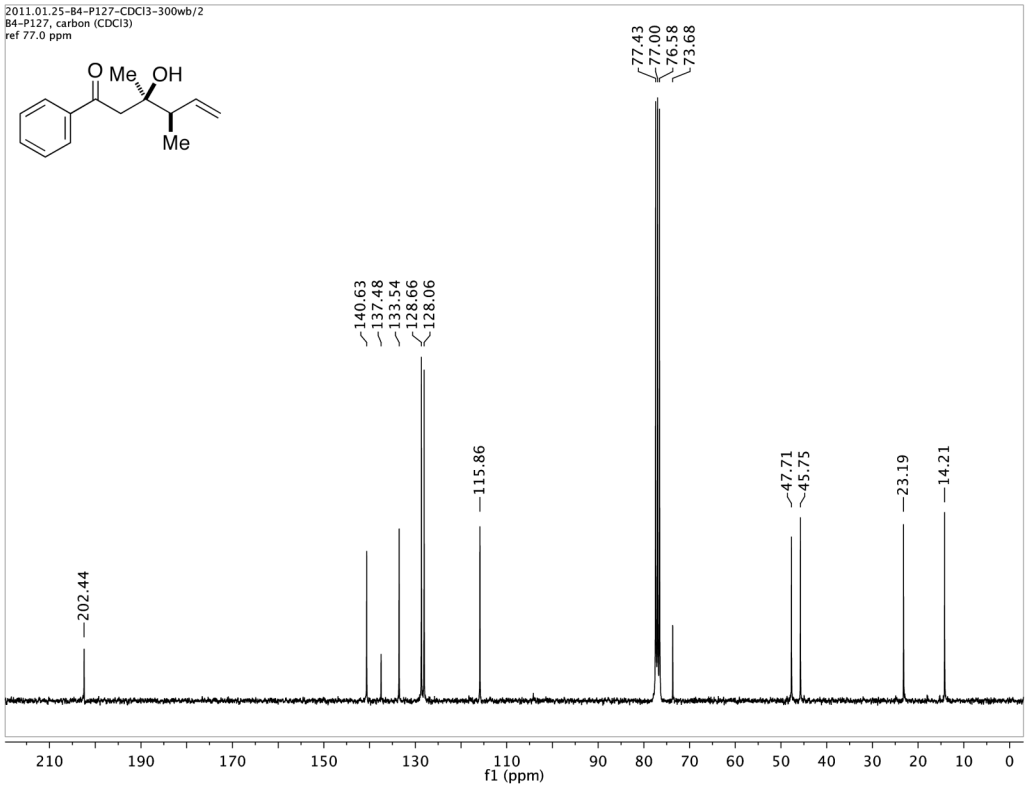

Supplementary Figure 68 | ^{13}C NMR spectrum of compound **23**.

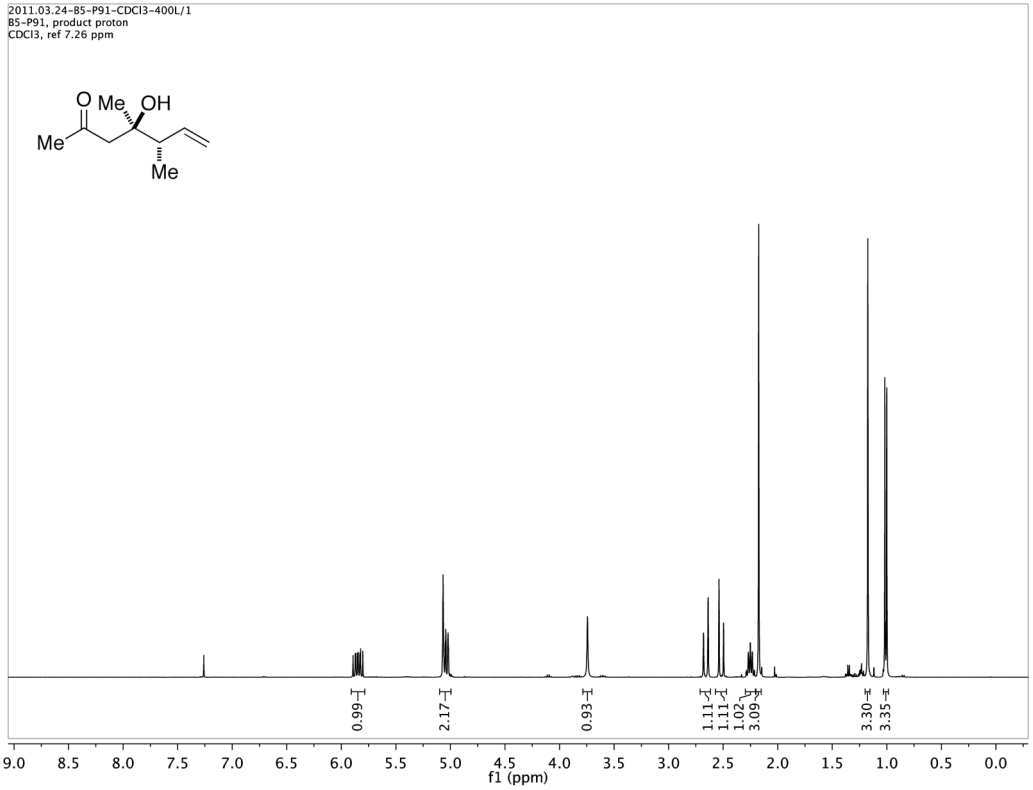

Supplementary Figure 69 | ^{1}H NMR spectrum of compound **25**.

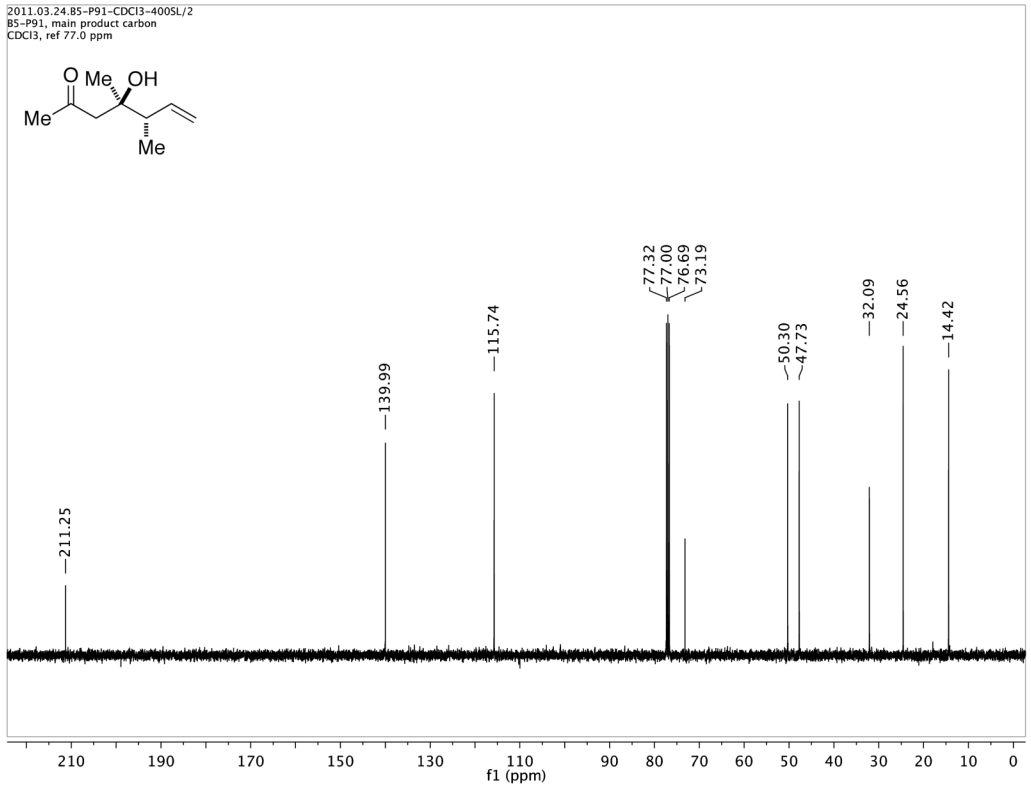

Supplementary Figure 70 | ^{13}C NMR spectrum of compound **25**.

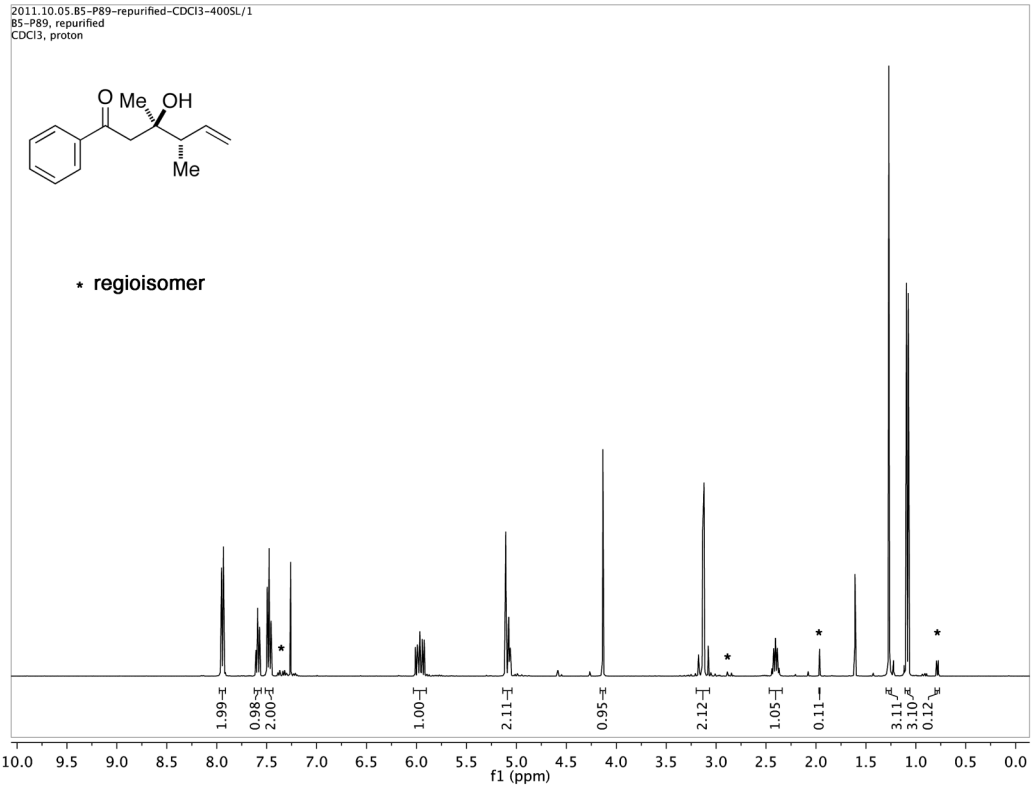

Supplementary Figure 71 | ^{1}H NMR spectrum of compound **26**.

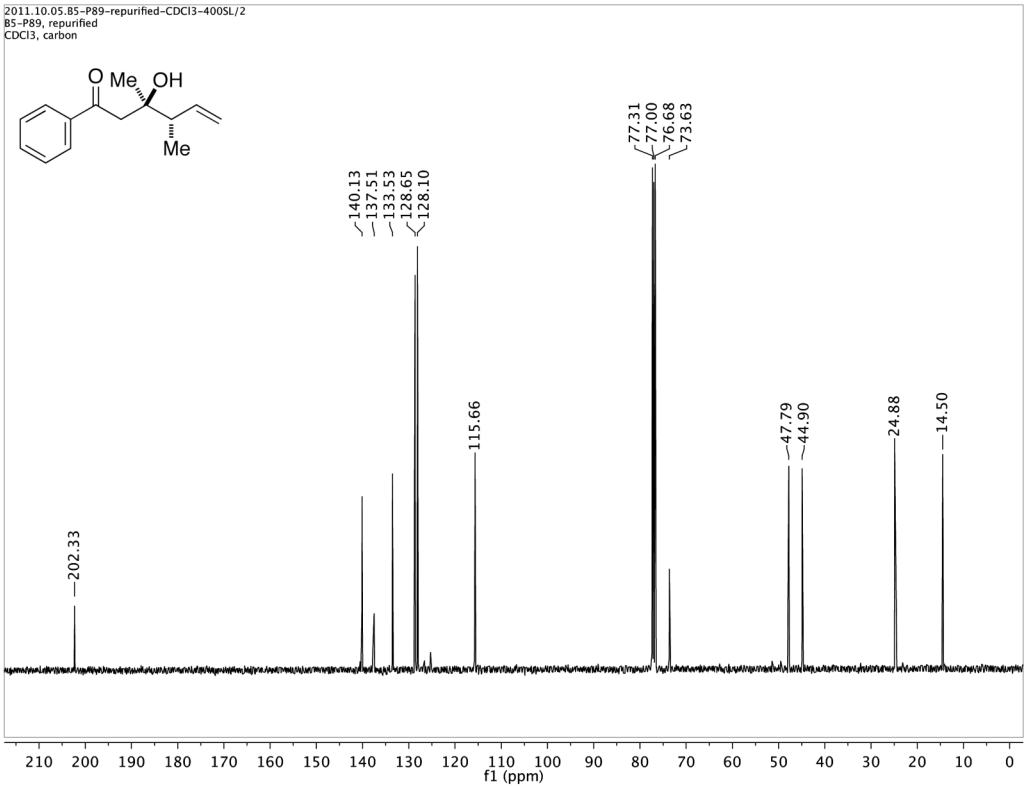

Supplementary Figure 72 | ^{13}C NMR spectrum of compound **26**.

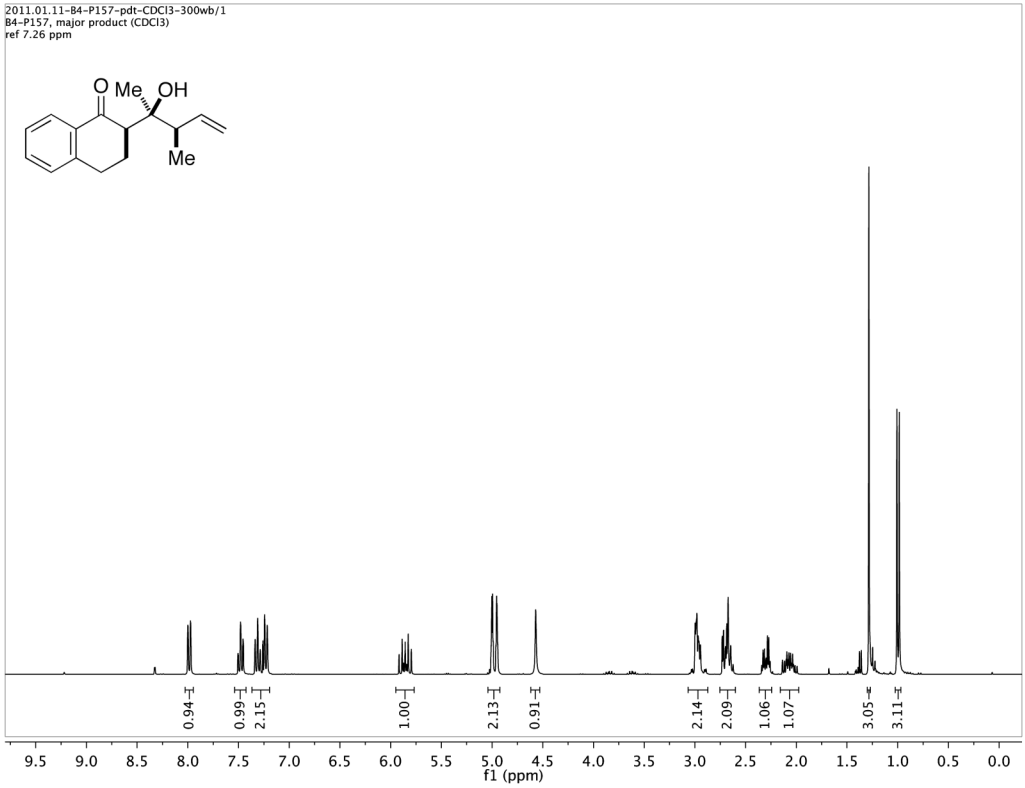

Supplementary Figure 73 | ^{1}H NMR spectrum of compound **29a**.

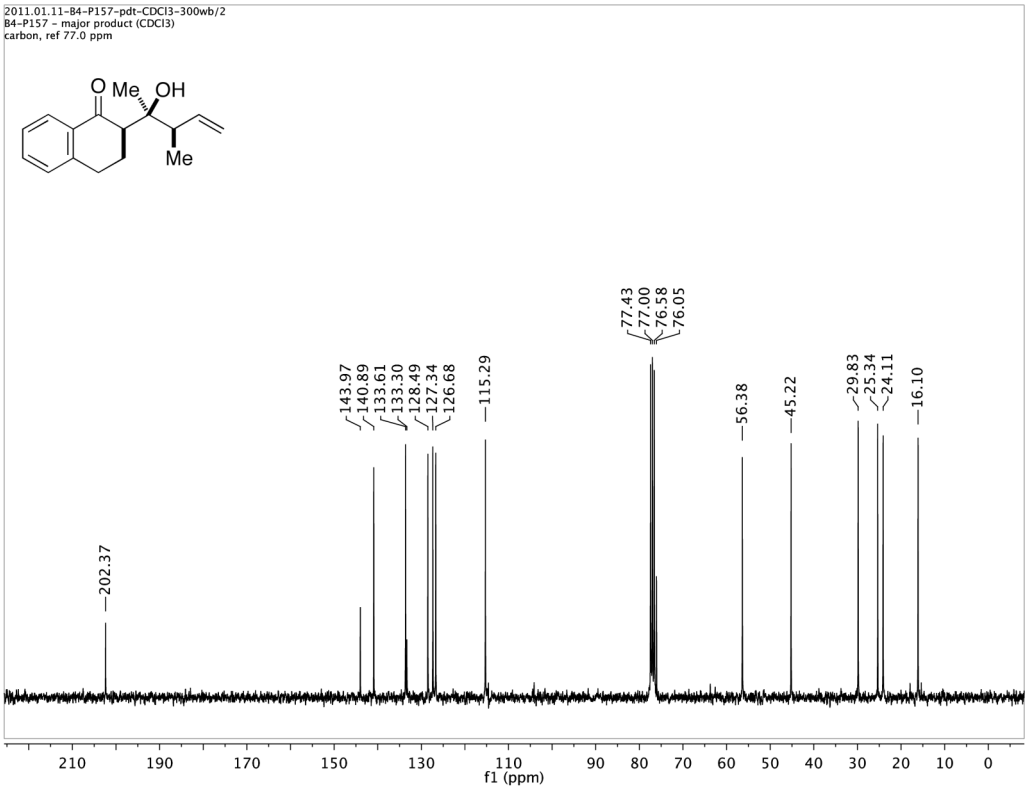

Supplementary Figure 74 | ^{13}C NMR spectrum of compound **29a**.

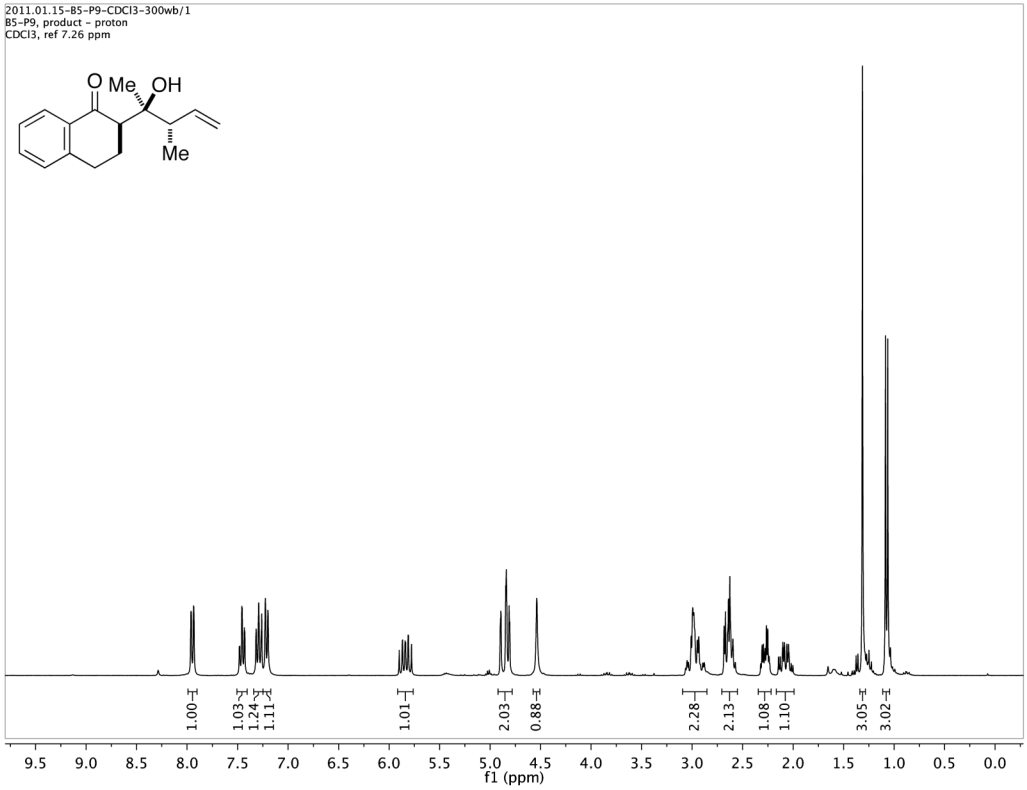

Supplementary Figure 75 | ^{1}H NMR spectrum of compound **30a**.

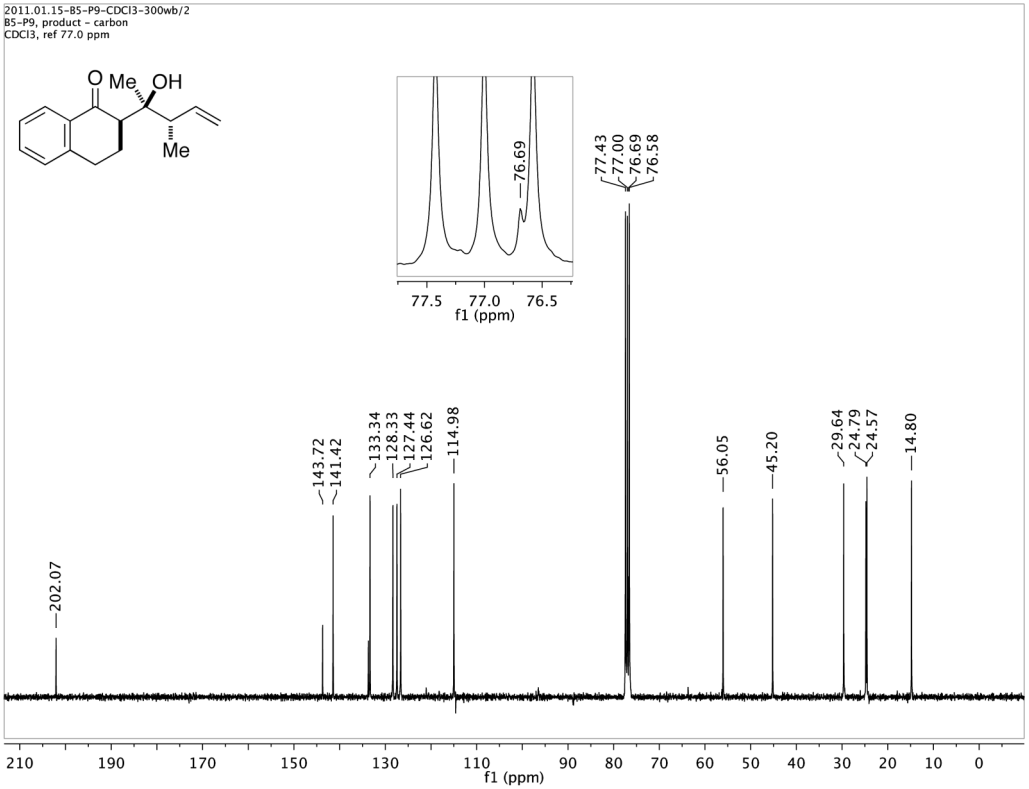

Supplementary Figure 76 | ^{13}C NMR spectrum of compound **30a**.

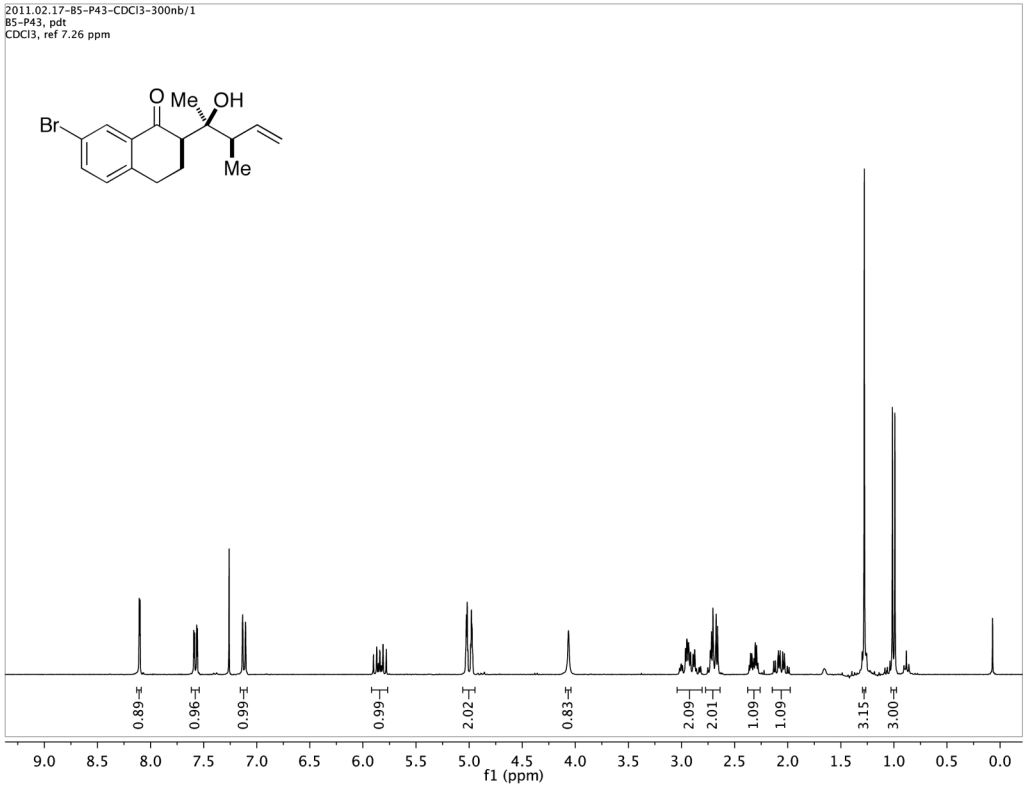

Supplementary Figure 77 | ^{1}H NMR spectrum of compound **S1**.

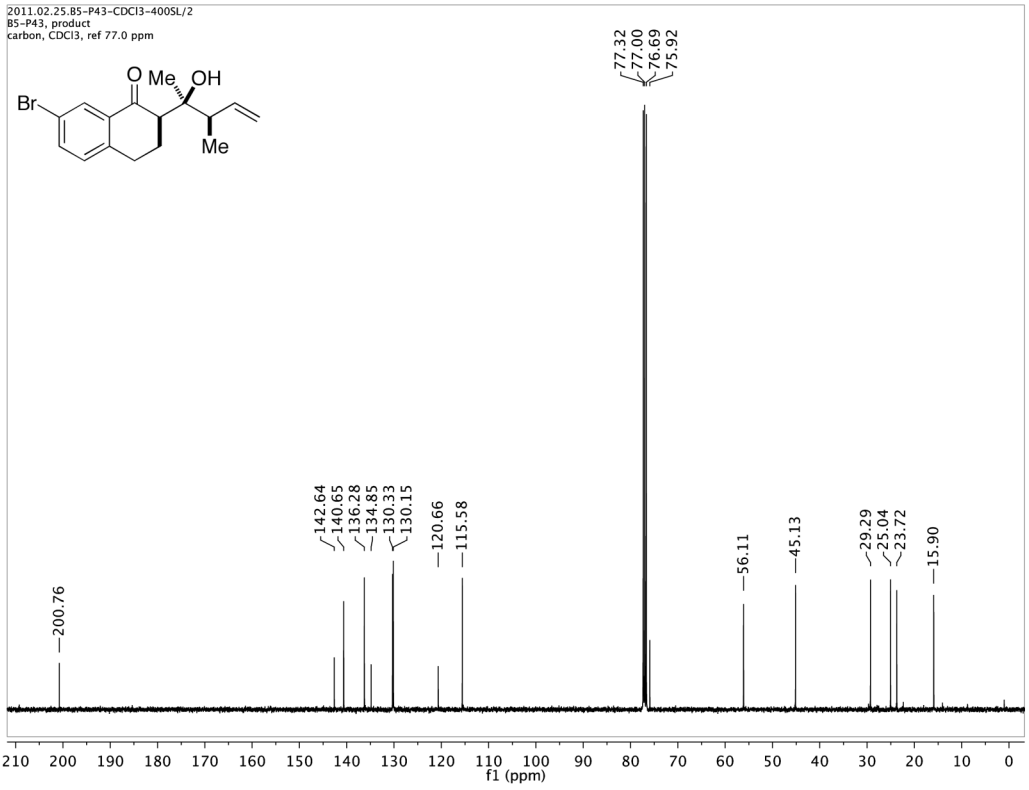

Supplementary Figure 78 | ^{13}C NMR spectrum of compound **S1**.

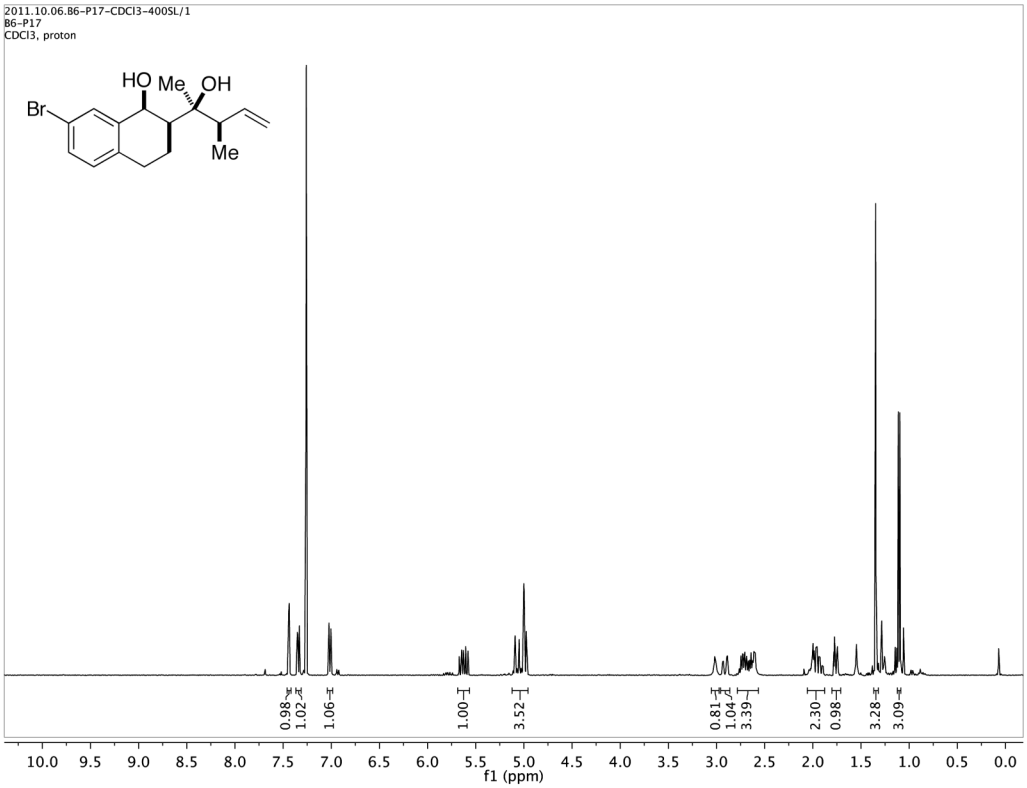

Supplementary Figure 79 | ^{1}H NMR spectrum of compound **S2**.

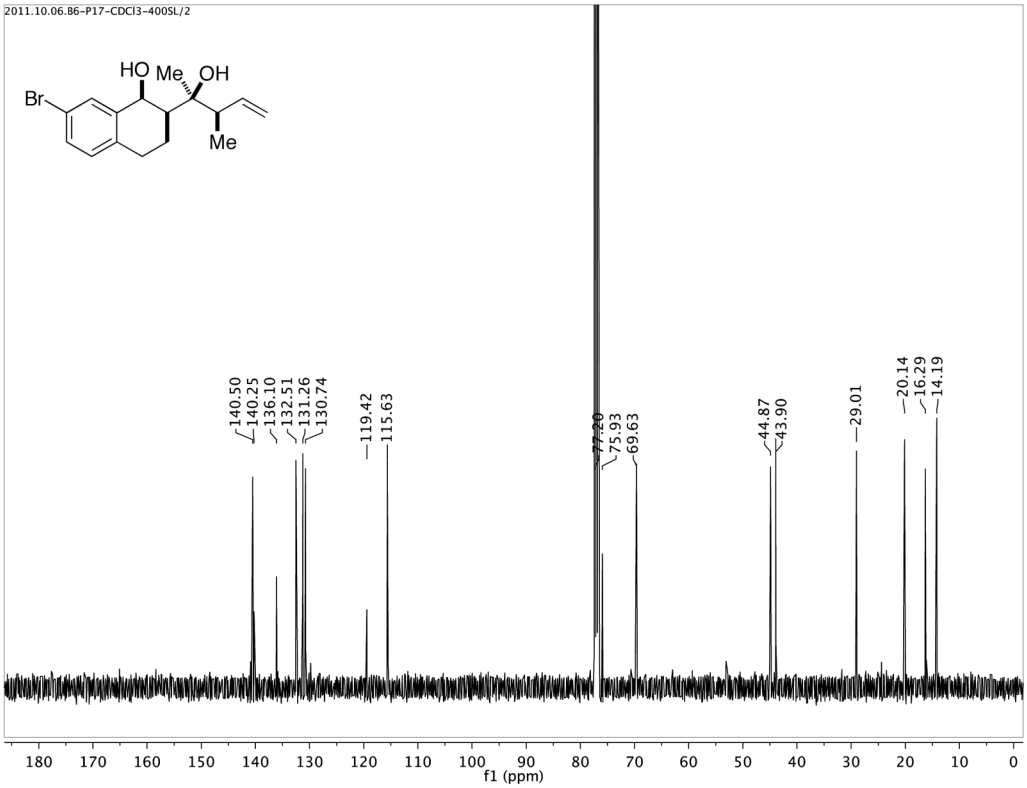

Supplementary Figure 80 | ^{13}C NMR spectrum of compound **S2**.